ANALYSIS OF THE RADIOSITY EQUATION

USING THE COLLOCATION METHOD

by

Jaehoon Seol

An Abstract

Of a thesis submitted in partial fulfillment of the
requirements for the Doctor of Philosophy
degree in Applied Mathematical and Computational Sciences
in the Graduate College of
The University of Iowa

December 2002

Thesis supervisor: Professor Kendall E. Atkinson

ABSTRACT

In this work, we consider solving the radiosity equation using the collocation method. We provide a physical setting for radiosity and derive the radiosity equation based on the explanation. We also provide the general framework of projection methods in Chapter 3.

In Chapter 4, we present a mathematical framework to analyze the concept of a visual event. Using the framework, we investigate the regularity of the radiosity solutions for basic geometric models which are most frequently encountered in three-dimensional computer graphics. We also discuss the rate of convergence of the collocation method solutions $u \in D^{r+1}(S)$. We show that interpolation error for $u \in D^{r+1}(S)$ converges at the same rate as for the functions $v \in C^{r+1}(S)$ even though $D^{r+1}u$ may not be continuous.

In Chapter 5 we develop analytic evaluation of the integrations which are needed to setup the linear system in solving the radiosity equation using the collocation method. These integrations are over triangular elements in R^3. We use affine transformations to convert integrations over elements in R^3 to integrations over elements in R^2. In Chapter 6 we define the function $H_{m,n,k}$ for $m, n, k \in N_0$, the set of all non-negative integers. The analytic evaluations of $H_{m,n,4}$ and other relevant integrations are given in detail for some values of m and n. The evaluation of these integrations is an essential part of the integrations discussed in Chapter 6.

In the final Chapter 7 we compare the performance of the analytic evaluation method of integration with that of other well-known numerical integration schemes. In order to provide numerical testing results for the centroid method, i.e., the piecewise constant collocation method, using the analytic evaluations, we use geometric models with given true solutions. The design decisions for the software package which has been used for the testing are summarized in the end. This package is quite general, both as regards the surface, subdivision scheme and the method of solution.

Abstract approved: ______________________

Thesis supervisor

____

Title and department

____

Date

ANALYSIS OF THE RADIOSITY EQUATION USING THE COLLOCATION METHOD

by

Jaehoon Seol

A thesis submitted in partial fulfillment of the
requirements for the Doctor of Philosophy
degree in Applied Mathematical and Computational Sciences
in the Graduate College of
The University of Iowa

December 2002

Thesis supervisor: Professor Kendall E. Atkinson

Graduate College
The University of Iowa
Iowa City, Iowa

CERTIFICATE OF APPROVAL

PH.D. THESIS

This is to certify that the Ph.D. thesis of

Jaehoon Seol

has been approved by the Examining Committee for the thesis requirement for the Doctor of Philosophy degree in Applied Mathematical and Computational Sciences at the December 2002 graduation.

Thesis Committee: ______________________
Kendall E. Atkinson, Thesis Supervisor

____
Juan Gatica

____
Kasturi Varadarajan

____
Keith Stroyan

____
Weimin Han

To my parents

ACKNOWLEDGEMENTS

I would like to thank my advisor, professor Kendall E. Atkinson for introducing me to this interesting subject of research, for his encouragement, and for his patience. Without his thoughtful advising and sound criticism, this work would not have been possible.

I would also like to thank professors at The University of Iowa for their kind concern. I am especially grateful to Prof. Paul S. Muhly, Prof. Juan A. Gatica, Prof. Keith D. Stroyan and Prof. Herbert W. Hethcote for their invaluable advice and constant attention.

I am very grateful to Brian Treadway for answering all my questions regarding LaTeX typesetting system. He showed impressive knowledge of that system and prevented me from getting lost in the maze of LaTeX.

Most of all, I wish to express sincere gratitude to my family. Seonho and Young showed great love, understanding and support while I was writing this thesis. Jinwook and Hyunjeong were always willing to share their busy time to encourage and motivate their brother.

ABSTRACT

In this work, we consider solving the radiosity equation using the collocation method. We provide a physical setting for radiosity and derive the radiosity equation based on the explanation. We also provide the general framework of projection methods in Chapter 3.

In Chapter 4, we present a mathematical framework to analyze the concept of a visual event. Using the framework, we investigate the regularity of the radiosity solutions for basic geometric models which are most frequently encountered in three-dimensional computer graphics. We also discuss the rate of convergence of the collocation method solutions $u \in D^{r+1}(S)$. We show that interpolation error for $u \in D^{r+1}(S)$ converges at the same rate as for the functions $v \in C^{r+1}(S)$ even though $D^{r+1}u$ may not be continuous.

In Chapter 5 we develop analytic evaluation of the integrations which are needed to setup the linear system in solving the radiosity equation using the collocation method. These integrations are over triangular elements in R^3. We use affine transformations to convert integrations over elements in R^3 to integrations over elements in R^2. In Chapter 6 we define the function $H_{m,n,k}$ for $m, n, k \in N_0$, the set of all non-negative integers. The analytic evaluations of $H_{m,n,4}$ and other relevant integrations are given in detail for some values of m and n. The evaluation of these integrations is an essential part of the integrations discussed in Chapter 6.

In the final Chapter 7 we compare the performance of the analytic evaluation

method of integration with that of other well-known numerical integration schemes. In order to provide numerical testing results for the centroid method, i.e., the piecewise constant collocation method, using the analytic evaluations, we use geometric models with given true solutions. The design decisions for the software package which has been used for the testing are summarized in the end. This package is quite general, both as regards the surface, subdivision scheme and the method of solution.

TABLE OF CONTENTS

LIST OF TABLES

Table Page

LIST OF FIGURES

CHAPTER 1
INTRODUCTION

1.1 Solving the Radiosity Equation

In this work, we consider some of the issues related to solving the radiosity equation using the collocation method. After summarizing the physics of the radiosity equation, we present the function space $D^{r+1}(S)$ as a mathematical framework to analyze the concept of a visual event. Using the framework, we investigate the regularity of the radiosity solutions for basic geometric models which are most frequently encountered in three-dimensional computer graphics. The rate of convergence of the collocation method solutions $u \in D^{r+1}(S)$ is discussed to show that interpolation error for $u \in D^{r+1}(S)$ converges at the same rate as for the functions $v \in C^{r+1}(S)$ even though $D^{r+1}u$ may not be continuous. Since $C^{r+1}(S) \subset D^{r+1}(S)$, this result is stronger than the standard results.

In Chapter 5 and 6 we develop analytic evaluation of the integrations which are needed to setup the linear system in solving the radiosity equation using the collocation method. These integrations are over triangular elements in R^3. We use affine transformations to convert integrations over elements in R^3 to integrations over standard integral domains in R^2. In the final Chapter 7 we compare the performance of the analytic evaluation method of integration with that of other well-known numerical integration schemes. In order to provide numerical testing results for the centroid method, i.e., the piecewise constant collocation method, using the analytic evaluations, we use geometric models with given true solutions.

The design decisions for the software package which has been used for the testing are summarized at the conclusion of Chapter 7. This package is quite general, both as regards the surface, subdivision scheme and the method of solution. In the following sections, we provide background information for the radiosity equation and computer graphics in general.

1.2 Illumination Models

Since the invention of the first general-purpose operational electronic computer, ENIAC, in 1946, computers have grown enormously in the number of users, application areas, and level of techniques being used. Needless to say, it is almost impossible to imagine the world without computers. Still, the first visual user interface device for the computer was a humble black-and-white cathode ray tube display. At the time, the color of each pixel was black-and-white and the work of graphics programming was much easier. All we needed to do was to decide which pixels to turn on or off.

With the introduction of raster graphics, we needed more elaborate rendering methods to decide the color of all the pixels. The first method of such kind was proposed by Bui Tuong Phong in 1975 [23]. His idea is based on a set of light properties ($L_d,\ L_s,\ L_a$) and surface properties ($k_d,\ k_d,\ k_a$) in the scene and on the following equation.

$$I_{color} = \frac{1}{(a+bd+cd^2)}(k_d L_d \overrightarrow{l} \cdot \overrightarrow{n} + k_d L_s \,(\overrightarrow{r} \cdot \overrightarrow{v})^{\alpha} + k_a L_a). \tag{1.1}$$

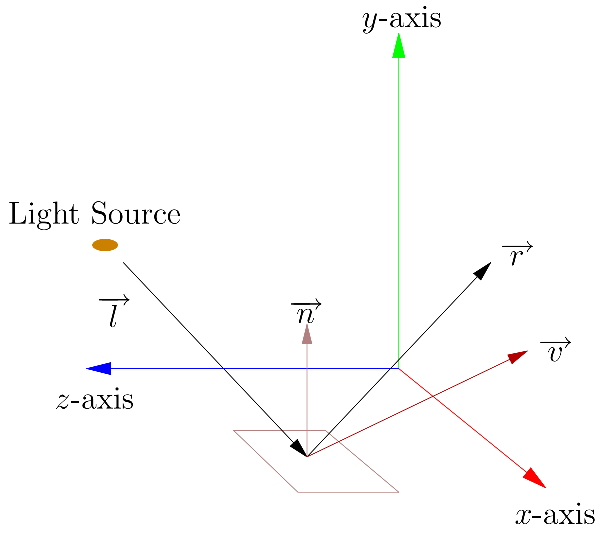

Figure 1.1: Illustration of vectors used in the local illumination model.

The vector $\overrightarrow{n}$ is the normal vector, $\overrightarrow{l}$ is the light vector, $\overrightarrow{r}$ is the reflection vector, and $\overrightarrow{v}$ is the view vector. The distance between the light source and the vertex on the surface is given by d. The meaning of the vectors used in this equation is illustrated in Figure 1.1. For further explanation of this equation and its use, refer to [12]. This equation works as a rule for the computation of the colors at each pixel. Phong calculated I_{red}, I_{green}, I_{blue} for each pixel and then used them as red, green and blue color components of the pixel. Since Phong's model considers only the direct interaction between the light sources and the surface points, this model is called a *local illumination model.*

Another rendering method to decide the color of each pixel was proposed by a group of researchers at Cornell University in 1984. Their idea is to simulate the actual underlying physical phenomena using the radiosity equation which had been developed in the radiative heat transfer community. The radiosity equation is given by

$$u(p) - \frac{\rho(p)}{\pi} \int_S V(p,q)G(p,q)u(q)dq = E(p) \text{ for } p \in S. \tag{1.2}$$

This equation is the result of applying the balance of energy to the radiosity under the assumption that all the surfaces are diffuse emitters, absorbers and reflectors in a nonparticipating medium. Mathematically, it is a Fredholm integral equation of the second kind and we need to use a numerical method to find an approximate solution of this equation. After solving (1.2) using various numerical methods, the value $u(p)$ is used to determine the color values for the pixel p on the surface S. This rendering method is called a *global illumination model* since it takes the interreflection between all the surfaces into consideration. We provide the derivation of this equation in Chapter 2 based on the definition of radiosity.

When two surfaces, one with red color and the other with white color, are placed in a close range, we can observe a reddish tint on the white surface. This is what is called the color bleeding effect. The radiosity equation has been successfully used to simulate the color bleeding effect. In addition to this, the rendering method using the radiosity equation is viewpoint independent. Thus, it is not necessary to repeat the computation of the color values even if the observer changes his/her position relative to the scene.

1.3 The Radiosity Equation

One of the most popular numerical solution methods of solving (1.2) in computer graphics is the *piecewise constant Galerkin method.* Applying the piecewise constant Galerkin method to the radiosity equation, we obtain the following linear system.

$$B_i = E_i + \rho_i \sum_{j=1}^{N} F_{ij} B_j, \tag{1.3}$$

where

$$F_{ij} = \alpha_{ij} \int_{x \in P_i} \int_{y \in P_j} \frac{\cos(\theta_i)\cos(\theta_j)}{\pi r^2} V(x,y)\,dy dx. \tag{1.4}$$

Here, B_i is the radiosity which we want to find and F_{ij} is called the *form factor* between two elements P_i and P_j. Most frequently, equation (1.3) is called the radiosity equation in the computer graphics community instead of (1.2).

The linear system (1.3) is a dense matrix and there are n^2 terms F_{ij}. Thus, it is important to find a fast and accurate method to evaluate F_{ij} in order to find a quality approximate solution of (1.3). Some of the special methods used to determine the form factors are the 'Monte Carlo method', 'crossed-strings method', 'unit sphere method', and 'inside sphere method'. These methods have been developed in the radiative heat transfer community and adapted by computer graphics. In particular, the implementation of the unit sphere method using rendering hardware has been studied in [10]. It is also called the 'hemi-cube method'.

In 1993, Peter Schröder presented a formula for F_{ij} between two general polygons. He derived the formula using repeated application of Stoke's theorem. For more information, refer to [33].

Another numerical solution method for solving (1.2) is the collocation method, and it is what is studied in this work. General solution methods for Fredholm integral equations of the second kind are given in [3]. In Chapter 3 and Chapter 4 of this work we present an analysis of the numerical solution of the radiosity equation using the collocation method. We also analyze the regularity of the radiosity solution in a mathematical framework instead of using the concept of visual events.

Applying the collocation method to the radiosity equation, (1.2) , we get the following linear system,

$$MB = E, \tag{1.5}$$

where

$$\begin{aligned} M_{ij} &= \delta_{ij} - \frac{\rho(t_i)}{\pi} \int_{A_j} G(t_i, q) dS_q, \\ B_i &= b_i, \\ E_i &= E(t_i). \end{aligned}$$

Again, the linear system (1.5) is a dense matrix with n^2 terms of integrations to evaluate. The analytic evaluation method of M_{ij} is considered in Chapter 5 and 6.

CHAPTER 2
PHYSICS OF THE RADIOSITY EQUATION

2.1 Radiative Intensity

In this section, we derive the following radiosity equation based on the physical concept of radiosity:

$$u(p) - \frac{\rho(p)}{\pi} \int_S V(p,q)G(p,q)u(q)dq = E(p) \text{ for } p \in S. \tag{2.1}$$

In this, S is a closed surface in R^3, $V(p,q)$ is the visibility function between two points $p, q \in S$ defined as

$$V(p,q) = \begin{cases} 1 & \text{if } \overleftrightarrow{pq} \cap S = \{p,q\}, \\ 0 & \text{otherwise.} \end{cases} \tag{2.2}$$

and $G(p,q)$ is the radiosity kernel function defined as

$$G(p,q) = \frac{\cos(\theta_p)\cos(\theta_q)}{\|p-q\|^2},$$

where θ_p and θ_q are the angle between the line $\overleftrightarrow{pq}$ and the normal vector n_p at $p \in S$ and the normal vector n_q at $q \in S$, respectively. See Figure 2.1.

For the derivation of equation (2.1), we start with the definition of *radiative intensity.*

Definition 2.1. The spectral radiative intensity $I_\lambda(p,v)$ at the position p in the direction of v is defined as the radiative energy flow rate at $p \in S$ per unit solid angle and unit area normal to the rays v, i.e.,

$$I_\lambda(p,v) = \frac{E}{dt\ da_p d\alpha d\lambda}$$

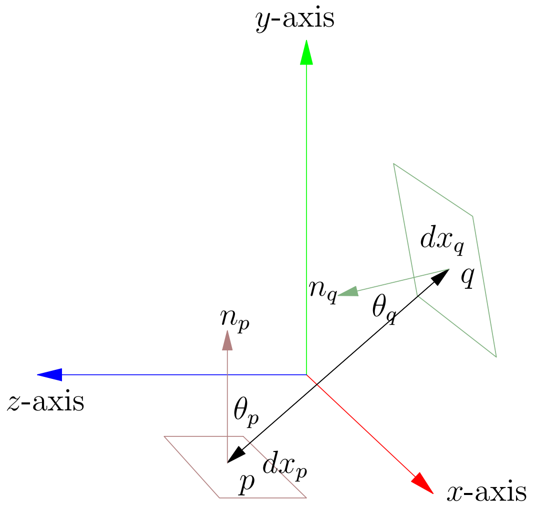

Figure 2.1: Radiative exchange between two surfaces.

In here,

$$\begin{aligned} E &= \text{energy flow between } dx_p \text{ and } d\alpha, \\ dt &= \text{differential time}, \\ da_p &= \text{differential area normal to } v,\ i.e.,\ dx_p \cos\theta, \\ d\alpha &= \text{differential solid angle in the direction of } v, \\ d\lambda &= \text{differential frequency spectrum.} \end{aligned}$$

For the illustration of this definition, refer to Figure 2.2.

Note that the energy flow E can be positive flow(coming out of the surface element dx_p) or negative flow(coming into the surface element dx_p). From this definition of the spectral radiative intensity $I_\lambda(p, v)$, it follows that *the total radiative*

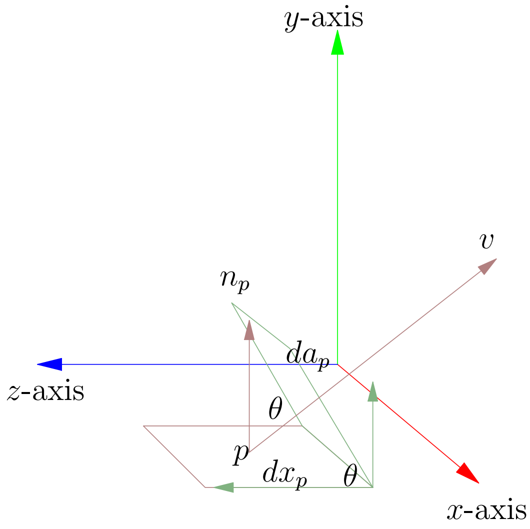

Figure 2.2: Relationship between emissive power and intensity.

intensity $I(p, v)$ is given by

$$\begin{aligned} I(p, v) &= \frac{E}{dt da_p d\alpha}, \\ &= \int_0^\infty I_\lambda(p, v) d\lambda. \end{aligned}$$

It is also clear from the definition of the radiative intensity that

$$I(p, v) da_p d\alpha = \frac{E}{dt}$$

means the energy flow between dx_p and $d\alpha$ in the direction of v per unit time.

Definition 2.2. We define the (radiative) heat flux q(p,v) of the differential surface element dx_p at p in the direction of v by

$$\begin{aligned} q(p, v) &= I(p, v) \cos\theta d\alpha, \\ &= \frac{E}{dt dx_p}. \end{aligned} \tag{2.3}$$

In here, θ is the angle between the normal of dx_p and the ray vector v.

This means the energy flows at the rate of $q(p, v)$ into the direction of the ray v per unit area around dx_p. Since $da_p = \cos\theta dx_p$ where θ is the angle between the normal of dx_p and s, the radiative heat flux $q(p, v)$ at the position p in the direction v becomes

$$q(p, v) = I(p, v)\cos\theta d\alpha, \tag{2.4}$$

$$= I(p, v)\ \cos\theta\ (\sin\theta d\theta d\phi), \tag{2.5}$$

$$= I(p, v)\cos\theta\sin\theta\ d\theta d\phi. \tag{2.6}$$

Based on equation (2.4), we can find the total incoming heat flux of the differential surface element dx_p located at p is

$$q_i(p) = \int_{\cos\theta_i < 0} I(p, v)\cos\theta_i d\alpha$$

and the total outgoing heat flux of the differential surface element dx_p located at p is

$$q_o(p) = \int_{\cos\theta_o > 0} I(p, v)\ \cos\theta_o\ d\alpha$$

In here, θ_i and θ_o are the angles between the normal of dx_p and direction vector v. See Figure 2.3. *The net heat flux* $q_n(p)$ of the differential surface element dx_p located at p is given by

$$q_n(p) = \ q_i(p) + q_o(p)$$

We can think of $q_o(p)$ as *the total energy emitted from a differential surface element* dx_p *at* p *per unit time and per unit area* and $q_i(p)$ as *the total energy absorbed into the differential surface element* dx_p *at* p *per unit time and per unit area.*

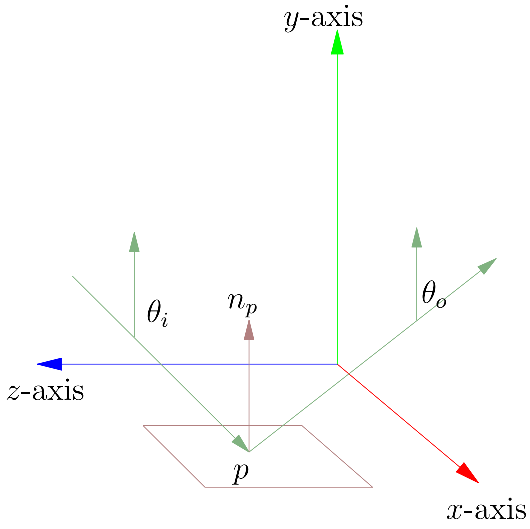

Figure 2.3: Incoming and outgoing heat flux.

Similarly, the total energy flowing out of dx_p is the integration of $q(p, v)$ over all upper hemisphere around dx_p at p, i.e.,

$$\begin{aligned} &\text{Total energy leaving } dx_p \\ &= \int_{2\pi} I(p, v) \cos\theta \sin\theta d\theta d\phi dx_p, \end{aligned} \tag{2.7}$$

by the definition of the heat flux $q(p, v)$.

Before the derivation of the radiosity equation (2.1) based on the *balance equation*, we need to make an assumption for the surfaces which we discuss in this dissertation. We assume that all the surfaces which we consider here are diffuse surfaces and we mean diffuse emitters and diffuse reflectors by that. Since the directional emissivity of nonmetals and metals varies, there can not exist physically perfect diffuse emitters. Still, our assumption makes some sense since the *grazing angle* for some materials are very close to 90°. Under this assumption of diffuse surfaces, we define the *(diffuse) configuration factor*.

Definition 2.3. The configuration factor $dF_{dx_p \to dx_q}$ from a differential surface element dx_p into another differential surface element dx_q as shown in the Figure 2.1 is defined as

$$dF_{dx_p \to dx_q} = \frac{\delta_{dx_p \,\to\, dx_q}}{\text{total energy leaving } dx_p}. \tag{2.8}$$

In here, $\delta_{dx_p \to dx_q}$ is the diffuse energy leaving dx_p directly toward and intercepted by dx_q. We define the configuration factors $F_{dx_p \to x_q}$, $dF_{x_p \to dx_q}$, $F_{x_p \to x_q}$ for finite surface elements x_p and x_q similarly, i.e.,

$$F_{dx_p \to x_q} = \frac{\delta_{dx_p \,\to\, x_q}}{\text{total energy leaving } dx_p}, \tag{2.9}$$

$$dF_{x_p \to dx_q} = \frac{\delta_{x_p \,\to\, dx_q}}{\text{total energy leaving } dx_p}, \tag{2.10}$$

$$F_{x_p \to x_q} = \frac{\delta_{x_p \,\to\, x_q}}{\text{total energy leaving } dx_p}. \tag{2.11}$$

In here, $\delta_{\alpha \to \beta}$ is the diffuse energy leaving α directly toward and intercepted by β.

The diffuse energy leaving dx_p directly toward and intercepted by dx_q is

$$q(dx_p, dx_q)dx = I(dx_p, dx_q) \cos\theta_p d\alpha_q dx,$$

by the definition of the flux, where $d\alpha_q$ is the solid angle covered by dx_q and θ_p is the angle between the surface normal at dx_p and the line connecting dx_p and dx_q. Thus, we have the diffuse energy leaving dx_p directly toward and intercepted by dx_q is

$$\begin{aligned} &q(dx_p, dx_q)dx_p \\ &= I(dx_p, dx_q) \cos\theta_p dx_p d\alpha_q, \\ &= \frac{I(dx_p, dx_q) \cos\theta_p \cos\theta_q dx_p dx_q}{r^2}. \end{aligned} \tag{2.12}$$

In this, the angle θ_q is the angle between dx_q and the line connecting dx_p and dx_q.

Moreover, the total diffuse energy leaving dx_p is given by

$$\begin{aligned}
&\int_{2\pi} I(dx_p, dx_q)\cos\theta_p dx_p d\alpha_q \\
&= dx_p\Big(\int_{2\pi} I(dx_p, dx_q)\cos\theta_p d\alpha_q\Big), \\
&= I(dx_p, dx_q)dx_p \int_{2\pi} \cos\theta_p d\alpha_q, \\
&= I(dx_p, dx_q)dx_p \int_{2\pi} \cos\theta_p \sin\theta_p d\theta_p d\phi_p, \\
&= \frac{I(dx_p, dx_q)dx_p}{2} \int_0^{2\pi} d\phi_p, \\
&= \pi I(dx_p, dx_q)dx_p. \qquad (2.13)
\end{aligned}$$

by equation (2.7) and the assumption of a diffuse surface. By equations (2.12), (2.13), and the definition of the configuration factor, we now have

$$\begin{aligned}
dF_{dx_p \to dx_q} &= \frac{\delta_{dx_p \to dx_q}}{\text{total energy leaving } dx_p}, \\
&= \frac{\cos\theta_p \cos\theta_q}{\pi r^2} dx_q. \qquad (2.14)
\end{aligned}$$

If you look at equation (2.14), you will see why $dF_{dx_p \to dx_q}$ which is defined physically is called the configuration factor. There are no physical concepts at all in the final simplification of the definition. So, in order to calculate the configuration factor, all we have to consider is the geometric configuration of the surfaces involved.

The law of reciprocity

$$\begin{aligned}
dF_{dx_p \to dx_q} dx_p &= \frac{\cos\theta_p \cos\theta_q}{\pi r^2} dx_q dx_p, \\
&= dF_{dx_q \to dx_p} dx_q,
\end{aligned}$$

follows from (2.14). Other form factors defined in (2.8) through (2.11) can be calculated using (2.14) and (2.13) .

2.2 Energy Balance for a Differential Surface

Let's consider an enclosure of arbitrary geometry S as shown in Figure 2.4 and make an energy balance for a differential surface element dx_p at p. Then, we have

$$u(p) = E(p) + \rho(p)H(p), \tag{2.15}$$

for *the radiosity u(p)* defined as the total flux leaving dx_p. In here, $E(p)$ is the total emitted energy per unit time per unit area at p, $\rho(p)$ is the reflectivity of the surface at p, and $H(p)$ is the total irradiation onto dx_p per unit time and per unit area. Since $u(q)dx_q$ is the total energy leaving from dx_q per unit time , the energy leaving from dx_q onto dx_p is $u(q)dx_q dF_{dx_q \to dx_p}$ by the definition of the form factor.

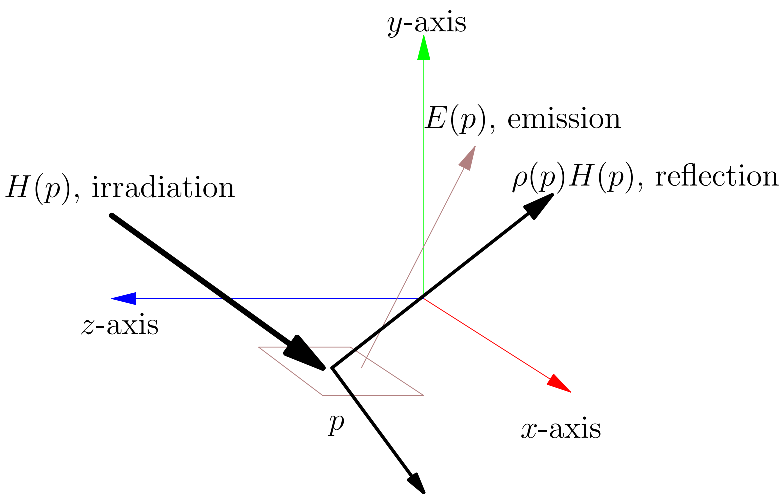

Figure 2.4: Definition of radiosity

Thus we have

$$H(p)dx_p = \int_S V(p,q)u(q)dx_q dF_{dx_q \to dx_p},$$
$$= \int_S V(p,q)u(q)dx_p dF_{dx_p \to dx_q},$$

by the law of reciprocity. This means that

$$H(p) = \int_S V(p,q)u(q)dF_{dx_p \to dx_q},$$
$$= \int_S V(p,q)u(q)\ \frac{\cos\theta_p \cos\theta_q}{\pi r^2} dx_q, \tag{2.16}$$

by equation (2.14).

By combining equations (2.15) and (2.16), we have

$$u(p) = E(p) + \frac{\rho(p)}{\pi}\int_S V(p,q)\frac{\cos\theta_p \cos\theta_q}{r^2} u(q)dx_q.$$

In here, $V(p,q)$ is the visibility function give in (2.2). By setting

$$G(p,q) = \ \frac{\cos\theta_p \cos\theta_q}{r^2},$$

we have

$$u(p) = E(p) + \frac{\rho(p)}{\pi}\int_S V(p,q)G(p,q)u(q)\ \ dx_q. \tag{2.17}$$

If we use the symbol dq instead of dx_q in (2.17), we have the equation (2.1). Note that the kernel function satisfies

$$V(p,q)G(p,q) \geq 0,\ \ p,q \in S.$$

The radiosity $u(p)$ is the one that was used by Goral et.al. [16] to render realistic synthetic images in 1984. We solve (2.17) three times for $u(p)$ with different choices of $E(p)$ to decide red, green, and blue colors in computer graphics. For a more detailed description of the material explained in this chapter, refer to [24].

CHAPTER 3
PROJECTION METHODS FOR THE RADIOSITY EQUATION

3.1 Introduction

If we put the integral equation (2.1) into operator form, we have

$$(I - \mathcal{K})u = E. \tag{3.1}$$

In here, $\mathcal{K}$ is an integral operator from a Banach space X to X defined as

$$\mathcal{K}u(p) = \frac{\rho(p)}{\pi} \int_S V(p,q)G(p,q)u(q)dq, \ \ p \in S. \tag{3.2}$$

Usually, $X = L^\infty(S)$ or $L^2(S)$. If the surface S is unoccluded, then we have $V(p,q) = 1$ for all p, $q \in S$ and the integral (3.2) simplifies into

$$\mathcal{K}u(p) = \frac{\rho(p)}{\pi} \int_S G(p,q)u(q)dq, \ \ p \in S. \tag{3.3}$$

In order to solve (3.1) approximately, we choose a sequence of finite-dimensional subspaces $X_n \subset X$ with $\dim(X_n) = d_n < \infty$ and try to find a function $\overline{u}_n \in X_n$ such that the *residual* defined by

$$r_n = E - (I - \mathcal{K})\overline{u}_n \tag{3.4}$$

is made small in some sense. *Projection methods* use projection operators $P_n : X \to X_n$ as a means to minimize the residual (3.4). For a given projection operator $P_n : X \to X_n$, our goal is to find $\overline{u}_n \in X_n$ such that

$$P_n r_n = P_n[E - (I - \mathcal{K})\overline{u}_n] = 0. \tag{3.5}$$

Different projection operators lead to different approximate solution methods. In the following sections we introduce *Galerkin's method* and *collocation methods*, the two most popular projection methods. After that, we develop an evaluation method for integrals which are related to collocation methods since collocation methods are the main subject of this work,.

3.2 Galerkin's Method

Suppose the Banach space X is an inner product space such as $L^2(S)$, then we can define a *projection operator* $P_n : X \to X_n$ by

$$P_n u = \sum_{j=1}^{d_n} \langle u, u_j \rangle \, u_j \tag{3.6}$$

for a finite dimensional subspace $X_n = \text{span}\{u_1, u_2, \dots, u_{d_n}\}$ of X with an orthonormal basis $\{u_1, u_2, \dots, u_{d_n}\}$. The operator P_n is called the *orthogonal projection operator*. Finding $\overline{u}_n \in X_n$ which satisfies (3.5) is called *Galerkin's method* for obtaining the approximate solution of (3.1).

For instance, suppose S is a polyhedral surface composed of planar polygons $\{S_j \subset R^3 \mid j = 1, .., N\}$ in R^3. We have

$$S = S_1 \cup S_2 \cup \ldots \cup S_N. \tag{3.7}$$

We assume that $S_j \cap S_k$ is (1) a line segment of S_j and S_k, (2) a vertex of S_j and S_k, or (3) $S_j \cap S_k = \emptyset$.

Let

$$T_n = \{\Delta_{n,k} \mid k = 1, 2, \dots, d_n\} \tag{3.8}$$

be a triangulation of S satisfying $S = \cup_{k=1}^{d_n} \Delta_{n,k}$ and $\Delta_{n,k} \subset S_i$ for some $i = 1, 2, \dots, N$. Take X_n as the space of all functions which are piecewise constant over the triangulation T_n. Then, we have

$$X_n = \text{span}\{u_j \mid j = 1, 2, \dots, d_n\},$$

where

$$u_j(q) = \begin{cases} \dfrac{1}{\sqrt{\text{area}(\Delta_{n,j})}}, & \text{if } q \in \Delta_{n,j}, \\ 0, & \text{otherwise.} \end{cases}$$

Since $\langle u_j, u_i \rangle = \delta_{i,j}$, the set $\{u_j \mid j = 1, 2, \dots, d_n\}$ is an orthonormal basis for X_n.

If we apply Galerkin's method to solve (3.1) approximately, we have

$$\begin{aligned} P_n[E - (I - \mathcal{K})\overline{u}_n] &= 0, \\ P_n[(I - \mathcal{K})\overline{u}_n] &= P_n(E), \\ \sum_{j=1}^{d_n} \langle (I - \mathcal{K})\overline{u}_n, u_j \rangle \, u_j &= \sum_{j=1}^{d_n} \langle E, u_j \rangle \, u_j, \end{aligned} \tag{3.9}$$

by the definition of P_n given in (3.6). Thus, we have

$$\sum_{j=1}^{d_n} \langle (I - \mathcal{K})\overline{u}_n, u_j \rangle \langle u_j, u_i \rangle = \sum_{j=1}^{d_n} \langle E, u_j \rangle \langle u_j, u_i \rangle, \tag{3.10}$$

for all $i = 1, 2, \dots, d_n$. Using $\langle u_j, u_i \rangle = \delta_{ij}$ for $i, j = 1, 2, \dots, d_n$, the system of equations (3.10) becomes

$$\langle (I - \mathcal{K})\overline{u}_n, u_i \rangle = \langle E, u_i \rangle, \tag{3.11}$$

for all $i = 1, 2, \dots, d_n$.

Since $\overline{u}_n \in X_n = \text{span}\{u_j \mid j = 1, 2, \ldots, d_n\}$, we can set

$$\overline{u}_n = \sum_{j=1}^{d_n} b_j u_j \tag{3.12}$$

for some $b_j \in R$, $i = 1, 2, \ldots, d_n$. Combining (3.11) and (3.12), we obtain the following linear system:

$$\sum_{j=1}^{d_n} b_j \langle (I - \mathcal{K})u_j, u_i \rangle = \langle E, u_i \rangle,$$

for all $i = 1, 2, \ldots, d_n$.

In matrix form, this is

$$MB = E, \tag{3.13}$$

with

$$M_{ij} = \delta_{ij} - \langle \mathcal{K}u_j, u_i \rangle,$$

$$B_i = b_i,$$

$$E_i = \langle E, u_i \rangle$$

for $i, j = 1, 2, \ldots, d_n$.

3.3 Collocation Methods

Let $X_n = \text{span}\{l_j \in X \mid j = 1, 2, \ldots, d_n\}$ be a subspace of X and let $t_1, t_2, \ldots, t_{d_n} \in S$ be fixed distinct points. Given $u \in X$, define $P_n u$ to be the element of X_n that interpolates u at the nodes $\{t_1, t_2, \ldots, t_{d_n}\}$. Thus, we can write

$$P_n u(t) = \sum_{j=1}^{d_n} b_j l_j(t), \tag{3.14}$$

with the coefficients $\{b_j \mid j = 1, 2, \ldots, d\}$ determined by solving the linear system

$$\sum_{j=1}^{d_n} b_j l_j(t_i) = u(t_i),\ i = 1, 2, \ldots, d_n.$$

This linear system has a unique solution if

$$\det[l_j(t_i)] \neq 0.$$

The projection operator P_n defined in (3.14) is called an *interpolatory projection operator*. Finding $\overline{u}_n \in X_n$ which satisfies (3.5) is called a *collocation method* for obtaining an approximate solution of (3.1).

For instance, suppose we are given the polyhedral surface S in R^3 and the triangulation T_n for S as given in (3.7) and (3.8), respectively. Let l_j be the characteristic function with support $\Delta_{n,j}$. Take $X_n = \text{span}\{l_j \mid j = 1, 2, \ldots, d_n\}$. For fixed distinct points $t_1, t_2, \ldots, t_{d_n} \in S$ satisfying $t_j \in \Delta_{n,j}$ we define a projection operator $P_n : X \to X_n$ by

$$P_n u(t) = \sum_{j=1}^{d_n} u(t_j) l_j(t)$$

Note that

$$P_n u(t_i) = u(t_i),\ \text{for } i = 1, 2, \ldots, d_n, \tag{3.15}$$

and

$$l_j(t_i) = \delta_{ij},\ \text{for } i = 1, 2, \ldots, d_n,$$

by the definition of P_n and l_j.

By using the collocation method to solve (3.1) approximately, we have

$$
\begin{aligned}
P_n[E-(I-\mathcal{K})\overline{u}_n] &= 0,\\
P_n[(I-\mathcal{K})\overline{u}_n] &= P_n(E),\\
(I-\mathcal{K})\overline{u}_n(t_i) &= E(t_i),
\end{aligned} \tag{3.16}
$$

for all $i = 1, 2, \dots, d_n$, by (3.15).

Since $\overline{u}_n \in X_n = \text{span}\{l_j \mid j = 1, 2, \dots, d_n\}$, we have

$$
\overline{u}_n = \sum_{j=1}^{d_n} b_j l_j. \tag{3.17}
$$

Combining (3.16) and (3.17), we get

$$
\begin{aligned}
\overline{u}_n(t_i) - \mathcal{K}\overline{u}_n(t_i) &= E(t_i)\\
\sum_{j=1}^{d_n} b_j \Big(l_j(t_i) - \frac{\rho(t_i)}{\pi} \int_{\Delta_{n,j}} V(t_i,q)G(t_i,q)l_j(q)dS_q\Big) &= E(t_i)
\end{aligned} \tag{3.18}
$$

for $i = 1, 2, \dots, d_n$. Since

$$
l_j(q) = \begin{cases} 1, & \text{if } q \in \Delta_{n,j},\\ 0, & \text{otherwise,} \end{cases}
$$

we have the following system of equations

$$
\sum_{j=1}^{d_n} b_j \Big(\delta_{ij} - \frac{\rho(t_i)}{\pi} \int_{\Delta_{n,j}} V(t_i,q)G(t_i,q)dS_q\Big) = E(t_i), \tag{3.19}
$$

for $i = 1, 2, \dots, d_n$, from equation (3.18).

In matrix form, (3.19) is

$$
MB = E,
$$

with

$$M_{ij} = \delta_{ij} - \frac{\rho(t_i)}{\pi} \int_{\Delta_{n,j}} V(t_i, q) G(t_i, q) dS_q,$$

$$B_i = b_i,$$

$$E_i = E(t_i),$$

for $i, j = 1, 2, \dots, d_n$. By solving this linear system for B, we can get the approximate solution $\overline{u}_n(t) = \sum_{j=1}^{d_n} b_j l_j(t) \in X_n$ of (3.1). We refer to this collocation method as the *centroid method* for obtaining the approximate solution of (3.1)

We can use higher degree piecewise polynomial functions over the triangulation $\{\Delta_{n,k} \mid k = 1, 2, \dots, d_n\}$ of S instead of using piecewise constant functions. In that case, we have to choose different node points depending on the degree of piecewise polynomial functions being used.

When we consider an interpolatory projection operator in $X = L^\infty(S)$, the evaluation of $u \in X$ at a point $p \in S$ is not well-defined. This issue and other relevant considerations of the collocation method in $L^\infty(S)$ has been considered and dealt with by Atkinson, Graham and Sloan in [2].

3.4 General Framework of the Projection Method

In this section we provide the analysis of the projection method for solving the radiosity equation. If we put the projection method for solving the radiosity equation in abstract framework, it can be written as

$$(I - P_n \mathcal{K}) u_n = P_n E.$$

In here, P_n is an interpolatory projection operator on a Banach space X. We usually take $X = L^\infty(S)$.

In order to prove

$$\|\mathcal{K}\| < 1,$$

we use the following result, proven in [5].

Lemma 3.1. *Assume S is a polyhedral surface and $p \in S^\circ$, the interior of a face of S. Then, we have*

$$\int_S V(p,q)G(p,q)dq \leq \pi. \tag{3.20}$$

The inequality (3.20) holds at all points $p \in S$ for which S is smooth in some neighborhood of p. Since we have

$$\text{measure}\,\{p \in S \mid p \text{ does not have a smooth neighborhood in } S\} = 0,$$

we can say the inequality (3.20) is true almost everywhere. With this lemma, we can obtain that

$$\frac{\rho(p)}{\pi}\int_S V(p,q)G(p,q)dq \leq \rho(p) \leq \|\rho\|_\infty\,,$$

for $p \in S$ almost everywhere. From this, we have

$$\begin{aligned}\|\mathcal{K}u\|_\infty &= \left\|\frac{\rho(p)}{\pi}\int_S V(p,q)G(p,q)u(q)dq\right\|_\infty \\ &\leq \|\rho\|_\infty \|u\|_\infty\,.\end{aligned}$$

This means

$$\|\mathcal{K}\| \leq \|\rho\|_\infty .$$

Thus, $\|\rho\|_\infty < 1$ implies that $(I - \mathcal{K})^{-1}$ exists as a bounded linear operator from $L^\infty(S)$ to $L^\infty(S)$ and

$$\left\|(I - \mathcal{K})^{-1}\right\| \leq \frac{1}{1 - \|\mathcal{K}\|},$$

by the use of the geometric series theorem.

Moreover, if we have

$$\sup_{n \geq 1} \|P_n\| \, \|\mathcal{K}\| < 1,$$

then

$$\|P_n \mathcal{K}\| < 1,$$

for all $n \geq 1$. Thus, $(I - P_n\mathcal{K})^{-1}$ exists as a bounded linear operator from $L^\infty(S)$ to $L^\infty(S)$ and

$$\left\|(I - P_n\mathcal{K})^{-1}\right\| \leq \frac{1}{1 - \alpha} \tag{3.21}$$

for $\alpha = \sup_n \|P_n\| \, \|\mathcal{K}\|$.

Note that u and u_n satisfy the following two identities.

$$(I - P_n\mathcal{K})\, u_n = P_n E,$$

$$(P_n - P_n\mathcal{K})\, u = P_n E.$$

By equating these identities, we have

$$
\begin{aligned}
(I - P_n\mathcal{K})\, u_n = &\ (P_n - P_n\mathcal{K})\, u, \\
&= (I - P_n\mathcal{K})\, u - (I - P_n)\, u.
\end{aligned}
$$

Thus, we have

$$(I - P_n\mathcal{K})\,(u - u_n) = (I - P_n)\, u.$$

That is,

$$(u - u_n) = (I - P_n\mathcal{K})^{-1}\,(I - P_n)\, u. \tag{3.22}$$

From (3.21) and (3.22), we obtain the following bounds

$$\frac{\|u - P_n u\|_\infty}{1+\alpha} \leq \|u - u_n\|_\infty \leq \frac{\|u - P_n u\|_\infty}{1-\alpha},$$

for all $n \geq 1$. Therefore, the speed of convergence of u_n to u is the same as the speed of convergence of $P_n u$ to u.

Note that we have the convergence of u_n to u if and only if $P_n u$ converges to u in $X = L^\infty(S)$, which is not true for some $u \in X$. However, if $u \in C(S)$, then u converges to $P_n u$ in X. In the following chapter, we give improved results for better behaved u on a piecewise planar surface S.

CHAPTER 4
PROPERTIES OF THE RADIOSITY EQUATION

4.1 Interpolation Error Analysis

We define a partition of S as a set $\{S_j \subset R^2 \mid j = 1,..,N\}$ of polygonal regions S_j which satisfies

$$S = S_1 \cup S_2 \cup \ldots \cup S_N$$

and $S_j \cap S_k$ is (1) a line segment of S_j and S_k, (2) a vertex of S_j and S_k, or (3) $S_j \cap S_k = \emptyset$. We say

$$T_n = \{\Delta_{n,k} \mid k = 1, 2, \ldots, N_n\}$$

is a triangulation of S if all the triangles $\Delta_{n,k} \subset S$ and $S = \cup_{k=1}^{N_n} \Delta_{n,k}$. We also say T_n *respects* a partition $\{S_j \subset R^2 \mid j = 1,..,N\}$ of S if for each $\Delta_{n,k} \in T_n$ there exists S_j such that $\Delta_{n,k} \subset S_j$. The mesh size h of this triangulation T_n is defined as

$$h = h_n = \max_{1 \le k \le N_n} diameter(\Delta_{n,k}).$$

If we follow the uniform meshing scheme explained in [3], we have the following relationship

$$|T_{n+1}| = 4\,|T_n|$$
$$|T_n| = |T_0|\, h_0^2 h^{-2}$$

where h_0 is the mesh size of T_0. If we use a uniform mesh, we will use the form of $O(h^p)$ as our error bound. If we use a graded mesh, we will use the formula $O(|T_n|^{-p})$

as our error bound. This is because the mesh size h does not have as much meaning for a graded mesh.

Notation 1. *Suppose that* $a = x_0 < x_1 < \ldots < x_n = b$ *is a partition of* $[a, b]$*. In the following, we denote the restriction of* u *onto* (x_j, x_{j+1}) *by* u_j*. That is,* $u_j = u_{|(x_j,x_{j+1})}$*.*

Definition 4.1. Suppose that $a = x_0 < x_1 < \ldots < x_n = b$ is a partition of $[a, b]$. For a function $u \in L^\infty[a, b]$ and $r \geq 0$, we say u is an element of $D^{r+1}[a, b]$ if and only if $u \in C^r[a, b]$ and there is a function $\overline{u}_j \in C^{r+1}[x_j, x_{j+1}]$ such that $\overline{u}_j(x) = u_j(x)$ on (x_j, x_{j+1}) for all $j = 0, 1, \ldots, n-1$.

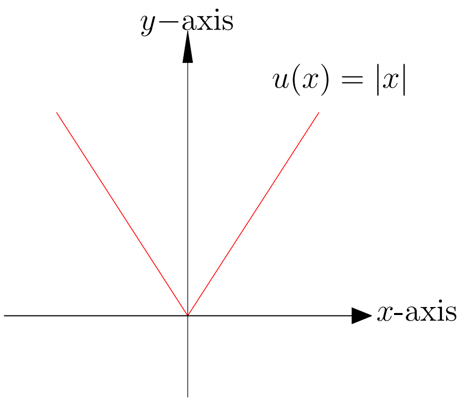

Figure 4.1: Graph of the function $u(x) = |x|$.

Definition 4.2. A function u is *absolutely continuous* on $[a, b]$ if and only if for all $\epsilon > 0$, there exists $\delta > 0$ such that

$$\sum_{i=0}^{k} |\alpha_i - \beta_i| < \delta$$

implies

$$\sum_{i=0}^{k} |u(\alpha_i) - u(\beta_i)| < \epsilon.$$

In here, $(\alpha_i,\ \beta_i)$, $i = 0, 1, \dots, k$, are disjoint subintervals of $[a, b]$.

Example 4.1. Let $u(x) = |x|$ on $[-1, 1]$. If we define $\overline{u}_0(x) = -x$ on $[-1, 0]$ and $\overline{u}_1(x) = x$ on $[0, 1]$, then $\overline{u}_0(x) \in C^1[-1, 0]$ and $\overline{u}_1(x) \in C^1[-1, 0]$. Since we have $u = \overline{u}_0$ on $(-1, 0)$, $u = \overline{u}_1$ on $(0, 1)$ and $u(x) \in C[-1, 1]$, we can say $u \in D^1[-1, 1]$ even if $u \notin C^1[-1, 1]$. See Figure 4.1.

Example 4.2. Let $u(x) = (x - 1)_+^{m+1}$, $m \geq 0$, which is defined as

$$(x-1)_+^{m+1} = \begin{cases} (x-1)^{m+1} & \text{if } x > 1, \\ 0 & \text{otherwise,} \end{cases}$$

We can prove $u(x) \in D^{m+1}[0, 2]$ in a similar way.

Lemma 4.1. *Suppose $u \in D^1[a, b]$. Then, u is absolutely continuous.*

Proof. In order to prove this lemma, we use the fact that $\overline{u_j} \in C^1\left[x_j, x_{j+1}\right]$ is absolutely continuous for $j = 0, 1, \dots, n-1$. Suppose $\epsilon > 0$ be given. Then, since $\overline{u_j} \in C^1\left[x_j, x_{j+1}\right]$ is absolutely continuous, there exits δ_j such that

$$\sum_{i=0}^{k_j} \left|\alpha_i^j - \beta_i^j\right| < \delta_j$$

implies

$$\sum_{i=0}^{k_j} \left|\overline{u_j}\left(\alpha_i^j\right) - \overline{u_j}\left(\beta_i^j\right)\right| < \frac{\epsilon}{n}.$$

In here, $\left(\alpha_i^j,\ \beta_i^j\right)$, $i = 0, 1, \dots, k_j$, are disjoint subintervals of $[x_j,\ x_{j+1}]$.

Suppose $(\alpha_i,\ \beta_i)$, $i = 0, 1, \ldots, k$, are disjoint intervals of $[a, b]$ such that

$$\alpha_i \leq \beta_{i+1},\ i = 0, .., k-1,$$

and

$$\sum_{i=0}^{k} |\alpha_i - \beta_i| < \min\{\delta_j \mid j = 0, 1, \ldots, n-1\}.$$

Let

$$(\alpha_i,\ \beta_i) \cap [x_j,\ x_{j+1}] \neq \emptyset \text{ for } i = i_j, i_j + 1, \ldots, i_{k_j}.$$

We construct a new set of subintervals $\left(\alpha_l^j,\ \beta_l^j\right)$, $l = 0, 1, \ldots, k_j$, of $[x_j,\ x_{j+1}]$ based on the following rules:

$$\alpha_l^j = \begin{cases} x_j & \text{if } x_j \in \left(\alpha_{i_j},\ \beta_{i_j}\right), \\ \alpha_{i_j+l} & \text{otherwise,} \end{cases}$$

and

$$\beta_l^j = \begin{cases} x_{j+1} & \text{if } x_{j+1} \in \left(\alpha_{i_{k_j}},\ \beta_{i_{k_j}}\right), \\ \beta_{i_j+l} & \text{otherwise.} \end{cases}$$

Then, we have

$$\begin{aligned} \sum_{i=0}^{k} |u(\alpha_i) - u(\beta_i)| &\leq \sum_{j=0}^{n-1} \sum_{l=0}^{k_j} \left|u\left(\alpha_l^j\right) - u\left(\beta_l^j\right)\right|, \\ &= \sum_{j=0}^{n-1} \sum_{l=0}^{k_j} \left|u_j\left(\alpha_l^j\right) - u_j\left(\beta_l^j\right)\right|, \\ &= \sum_{j=0}^{n-1} \sum_{l=0}^{k_j} \left|\overline{u}_j\left(\alpha_l^j\right) - \overline{u}_j\left(\beta_l^j\right)\right|, \\ &\leq \sum_{j=0}^{n-1} \frac{\epsilon}{n} = \epsilon. \end{aligned}$$

Therefore, u is absolutely continuous. $\square$

If $u \in D^{r+1}[a,b]$, then $D^r u \in D^1[a,b]$. Since $D^r u$ is absolutely continuous, $D^r u$ is differentiable almost everywhere and integrable on $[a,b]$. Moreover,

$$D^r u(b) - D^r u(a) = \int_a^b D^{r+1} u(t)\, dt.$$

Thus, we can prove the following generalized form of Peano's lemma.

In the following lemma, the symbol L denotes a composite linear functional

$$L : D^{r+1}[a,b] \to R$$

of the form

$$\begin{aligned} Lu &= \sum_{i=0}^{k} \int_a^b w_i(t) u^{(i)}(t) dt \\ &+ \sum_{i=0}^{l_0} \beta_{0,i} u(t_{0,i}) + \sum_{i=1}^{l_1} \beta_{1,i} u'(t_{1,i}) + \ldots \sum_{i=0}^{l_k} \beta_{k,i} u^{(k)}(t_{k,i}), \end{aligned}$$

for $k \leq r$.

Lemma 4.2. *Suppose that $u \in D^{r+1}[a,b]$ and $L(u) = 0$ for all $u \in P_r$. Then, we have*

$$Lu(s) = \frac{1}{r!} \int_a^b u^{(r+1)}(t) L[(s-t)_+^r] dt$$

In here, L is applied to $(s-t)_+^r$ with respect to s.

Proof. Suppose $u \in D^{r+1}[a,b]$. Then, we have

$$\begin{aligned} u(s) &= u(a) + u'(a)(s-a) + \ldots + \frac{1}{r!} u^{(r)}(a)(s-a)^r \\ &+ \frac{1}{r!} \int_a^b u^{(r+1)}(t)(s-t)_+^r dt \end{aligned} \tag{4.1}$$

for $s \in [a,b]$ by Taylor expansion. Thus,

$$Lu(s) = \frac{1}{r!}\int_a^b u^{(r+1)}(t)L\left[(s-t)_+^r\right]dt.$$

$\square$

Example 4.3. Let's define $u:[0,h]\to[0,h]$ by

$$u(s) = (s-\frac{h}{2})_+^2$$

and a linear operator $L: u\in D^2[0,h]\to R$ by

$$L[u] = u(x) - \frac{(h-x)u(0)+xu(h)}{h}$$

Then, we have $u\in D^2[0,h]$ and $L[u]=0$ for all $u\in P_1$. Since we have

$$L[(s-t)_+] = \begin{cases} -\dfrac{x(h-t)}{h}, & x\le t \\ (x-t)-\dfrac{x(h-t)}{h}, & x\ge t \end{cases} \tag{4.2}$$

Thus, by Lemma 4.2 and (4.2),

$$\begin{aligned} Lu(s) &= 2\int_{\frac{h}{2}}^{h} L[(s-t)_+^r]dt \\ &= 2[\int_{\frac{h}{2}}^{x} L[(s-t)_+^r]dt + \int_x^h L[(s-t)_+^r]dt] \\ &= 2[\int_{\frac{h}{2}}^{x}((x-t)-\frac{x(h-t)}{h})dt + \int_x^h(-\frac{x(h-t)}{h})dt] \\ &= (-1+\frac{x}{h})(x^2-\frac{h^2}{4}) - 2x(h-x) + \frac{x}{h}(h^2-x^2) \\ &= \frac{1}{4}(h^2+4x^2-5hx) \end{aligned} \tag{4.3}$$

Since x is taken from $[0,h]$, we get that $|L[u]| = O(h^2)$ from (4.3). This is stronger than standard results that require $u\in C^2\,[0,h]$.

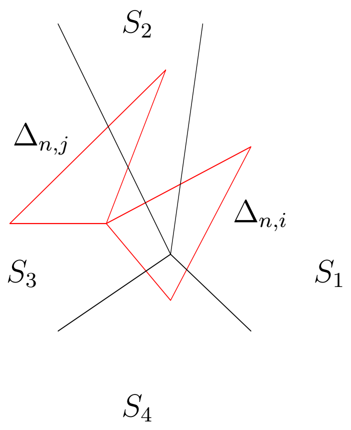

Figure 4.2: Triangulation which does not respect the given partition.

Notation 2. *Suppose that* $\{S_j \subset R^3 \mid j = 1, .., N\}$ *is a partition of* S. *For a function* u *defined on* S, *we use the notation* u_j *to denote the restriction of* u *onto* S_j°. *That is,* $u_j = u_{|S_j^\circ}$.

Definition 4.3. Suppose that $\{S_j \subset R^3 \mid j = 1, .., N\}$ is a fixed partition of S. For a function $u \in L^\infty(S)$ and $r \geq 0$, we say u is an element of $D^{r+1}(S)$ if and only if $u \in C^r(S)$ and there is a function $\overline{u_j} \in C^{r+1}(S_j)$ such that $\overline{u_j}(x) = u_j(x)$ on S_j^o for all $j = 1, \ldots, N$.

From the definition, it follows that $C^{r+1}(S) \subset D^{r+1}(S)$. The definition also implies that if $u \in D^{r+1}(S)$, then $D^r u$ is a continuous function, but $D^{r+1}u$ may be discontinuous across the edges joining adjacent polygonal faces of S. Thus, $D^{r+1}u$ may have a discontinuous line in the middle of $\Delta_{n,k} \in T_n$ if the triangulation T_n does not respect the partition $\{S_j \subset R^3 \mid j = 1, .., N\}$. See Figure 4.2. We call this discontinuous line a *discontinuous line of order* $r + 1$.

Definition 4.4. Let $r \geq 0$ be an integer. Given a triangulation $T_n = \{\Delta_{n,k} \mid k = 1, 2, \ldots, N_n\}$ of S, we define

$$X_{n,r} = \{u \in L^\infty(S) \mid u_{|\Delta^\circ_{n,k}} \in \mathcal{P}_r(\Delta^\circ_{n,k}) \text{ for all } \Delta_{n,k} \in T_n\}$$

where $\mathcal{P}_r(\Delta^\circ_{n,k})$ is the collection of all polynomials over $\Delta^\circ_{n,k}$ of degree less than or equal to r.

By the definition of $X_{n,r}$, we have that $X_{n,r}$ is the subspace of $D^{r+1}(S)$ for all n and $X_{n,0} \subset X_{n,1} \subset \ldots \subset X_{n,r} \subset \ldots$. In the following definition, we suppose σ denotes the unit simplex defined by $\{(x, y) \mid 0 \leq x, y, x + y \leq 1\}$.

Definition 4.5. Suppose $T_n = \{\Delta_{n,k} \mid k = 1, 2, \ldots, N_n\}$ is a triangulation of S and that each triangle $\Delta_{n,k}$ is determined by vertices $\{v_{k,1}, v_{k,2}, v_{k,3}\}$. Define a bijective map $T_k : \sigma \to \Delta_{n,k}$ by

$$T_k(s, t) = uv_{k,1} + sv_{k,2} + tv_{k,3}, \; u = 1 - s - t$$

and a projection operator $P_n : D^{r+1}(S) \to X_{n,r}$ by

$$P_n u(x, y) = \sum_{i=1}^{f_r} u(c_{k,i}) l_i(T_k^{-1}(x, y)) \text{ for all } (x, y) \in \Delta_{n,k} \tag{4.4}$$

where $c_{k,i} \in \Delta_{n,k}$ for $i = 1, 2, \ldots, f_r = \frac{(r+1)(r+2)}{2}$ are the collocation points determining the Lagrange interpolation functions l_i such that $l_i(c_{k,j}) = \delta_{i,j}$ for all $i, j = 1, 2, \ldots, f_r$.

The following theorem is well-known, but we give our proof of it since a similar argument will be used for the next theorem.

Theorem 4.3. *If $u \in C^{r+1}(S)$, then we have*

$$\max_{(x,y)\in\Delta_{n,k}} |u(x,y) - P_n u(x,y)| \le ch^{r+1} \max_{\substack{i,j\ge 0\\ i+j=r+1}} \max_{(x,y)\in\Delta_{n,k}} \left|D^i D^j u(x,y)\right|$$

no matter how we triangulate the partition $\{S_j \subset R^3 \mid j = 1,..,N\}$ of S.

Proof. Suppose that $u \in C^{r+1}(S)$ and $\Delta_{n,k}$ is a triangle of T_n. For $X = (x,y) \in \Delta_{n,k}$ and $X_0 = (x_0, y_0)$ belonging to $\Delta_{n,k}$, we define

$$\begin{aligned} v(s;x,y) &= u(X_0 + \frac{s}{h}(X - X_0)), \\ &= u(x_0 + \frac{s}{h}(x - x_0), y_0 + \frac{s}{h}(y - y_0)). \end{aligned}$$

Then, we have that $v(s;x,y) \in C^{(r+1)}[0,h]$ as a function of s for any $X = (x,y) \in \Delta_{n,k}$ since $u \in C^{r+1}(S)$. Applying Taylor expansion to $v(s;x,y)$ as a function of s to get

$$\begin{aligned} v(s;x,y) &= v(a) + v'(a)(s-a) + \ldots + \frac{1}{r!}v^{(r)}(a)(s-a)^r \\ &+ \frac{1}{r!}\int_0^h v^{(r+1)}(t)(s-t)_+^r dt, \\ &= A(s;x,y) + B(s;x,y). \end{aligned} \tag{4.5}$$

In here,

$$\begin{aligned} A(s;x,y) &= v(a) + v'(a)(s-a) + \ldots + \frac{1}{(r-1)!}v^{(r)}(a)(s-a)^r, \\ B(s;x,y) &= \frac{1}{r!}\int_0^h v^{(r+1)}(t)(s-t)_+^r dt. \end{aligned}$$

Let's define a linear functional $L : C^{r+1}(\Delta_{n,k}) \to R$ by

$$\begin{aligned} Lu(x,y) &= u(x,y) - P_n u(x,y) \\ &= u(x,y) - \sum_{i=1}^{f_r} u(c_{k,i}) l_i(T_k^{-1}(x,y)). \end{aligned}$$

In here, we are using the same projection P_n as in (4.4). Applying L to (4.5), we get

$$\begin{aligned}
L[v(s;x,y)] &= L[A(s;x,y)] + L[B(s;x,y)] \\
&= L[B(s;x,y)] \\
&= \frac{1}{r!}\int_0^h v^{(r+1)}(t) L[(s-t)_+^r]dt \qquad (4.6)\\
&= \frac{1}{h^{r+1}r!}\int_0^h [(X-X_0)\circ\nabla]^{r+1} \\
&\quad u(X_0+\frac{t}{h}(X-X_0))L[(s-t)_+^r]dt.
\end{aligned}$$

Using

$$\begin{aligned}
&[(X-X_0)\circ\nabla]^{r+1}u(x,y) \\
&= \sum_{j=0}^{r+1}\frac{(r+1)!}{j!(r+1-j)!}(x-x_0)^j(y-y_0)^{r+1-j}D_x^jD_y^{r+1-j}u(x,y),
\end{aligned}$$

equation (4.6) becomes

$$\begin{aligned}
L[v(s;x,y)] &= \frac{1}{h^{r+1}r!}\int_0^h \sum_{j=0}^{r+1}\frac{(r+1)!}{j!(r+1-j)!}(x-x_0)^j(y-y_0)^{r+1-j} \\
&\cdot D_x^jD_y^{r+1-j}u(X_0+\frac{t}{h}(X-X_0))L[(s-t)_+^r]dt, \\
&= \frac{1}{h^{r+1}r!}\int_0^h \sum_{j=0}^{r+1}\frac{(r+1)!}{j!(r+1-j)!}(x-x_0)^j(y-y_0)^{r+1-j} \qquad (4.7)\\
&\cdot D_x^jD_y^{r+1-j}u(X_0+\frac{t}{h}(X-X_0))\left(L[(s-t)_+^r]\right)dt.
\end{aligned}$$

Using

$$\sum_{i=1}^{f_r} l_i(T_k^{-1}(x,y)) = 1,$$

equation (4.7) becomes

$$L[v(s;x,y)] = \frac{1}{h^{r+1}r!}\sum_{j=0}^{r+1}\sum_{i=1}^{f_r}\frac{(r+1)!}{j!(r+1-j)!}l_i(T_k^{-1}(x,y)) \tag{4.8}$$

$$\int_0^h [(x-x_0)^j(y-y_0)^{r+1-j}$$

$$\cdot D_x^j D_y^{r+1-j}u(X_0+\frac{t}{h}(X-X_0))$$

$$-(x_{k,i}-x_0)^j(y_{k,i}-y_0)^{r+1-j}$$

$$\cdot D_x^j D_y^{r+1-j}u(X_0+\frac{t}{h}(c_{k,i}-X_0))](s-t)_+^r dt$$

Based on equation (4.8), we can easily derive the following estimate.

$$|L[v(s;x,y)]| \leq ch^{r+1}\max_{(x,y)\in\Delta_{n,k}}\left\|D_x^j D_y^{r+1-j}u(x,y)\right\|.$$

Therefore, we have

$$\max_{(x,y)\in\Delta_{n,k}}|u(x,y)-P_nu(x,y)| \leq ch^{r+1}\max_{\substack{i,j\geq 0\\ i+j=r+1}}\max_{(x,y)\in\Delta_{n,k}}\left|D^iD^ju(x,y)\right|.$$

$\square$

Theorem 4.4. *Suppose that $u \in D^{r+1}(S)$ and the uniform triangulation $T_n = \{\Delta_{n,k} \mid k = 1, 2, \ldots, N_n\}$ of S does not respect the partition $\{S_j \subset R^3 \mid j = 1, .., N\}$ of S and that the interpolation points $c_{k,i}$ of P_n are chosen in the interior of the triangle $\Delta_{n,k}$. Then we have*

$$\max_{(x,y)\in\Delta_{n,k}}|u(x,y)-P_nu(x,y)| \leq ch^{r+1}\max_{\substack{i,j\geq 0\\ i+j=r+1}}\sup_{(x,y)\in\Delta_{n,k}}\left|D^iD^ju(x,y)\right|$$

where $\Delta_{l,k}$ is an element of the uniform triangulation T_n.

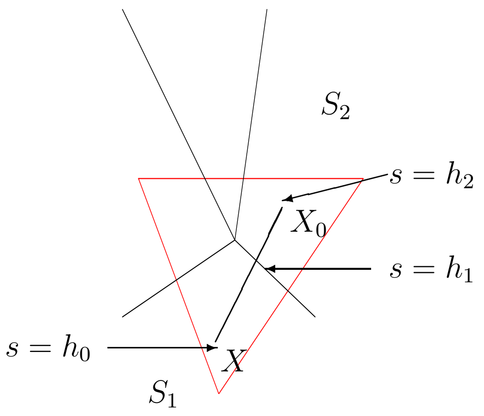

Figure 4.3: Path of $X_0 + \dfrac{s}{h}(X - X_0)$ as s varies from 0 to h.

Proof. It suffices to prove the theorem for $u \in D^{r+1}(S)\setminus C^{r+1}(S)$. Suppose that $u \in D^{r+1}(S)\setminus C^{r+1}(S)$ and $\Delta_{n,k}$ is a triangle of T_n. For fixed $X = (x, y)$ and $X_0 = (x_0, y_0)$ belonging to $\Delta_{n,k}$, we define

$$\begin{aligned} v(s; x, y) &= u(X_0 + \frac{s}{h}(X - X_0)) \\ &= u(x_0 + \frac{s}{h}(x - x_0), y_0 + \frac{s}{h}(y - y_0)). \end{aligned}$$

We prove that $v(s; x, y) \in D^{r+1}[0, h]$ as a function of s for any $(x, y) \in \Delta_{n,k}$. Since our triangulation T_n does not respect the partition $\{S_j | j = 1, 2, \ldots, N\}$, there are more than one planes S_l such that $\Delta_{n,k} \cap S_l \neq \emptyset$. Without loss of generality, we assume that

$$(1) \quad \Delta_{n,k} \cap S_l \neq \emptyset, \qquad l = 1, 2,$$

$$(2) \quad X_0 \in S_1,\ X \in S_2,$$

and $X_0 + \frac{s}{h}(X - X_0)$ crosses the edge between S_1 and S_2 as s varies from 0 to h. Then, we have a partition $0 = h_0 < h_1 < h_2 = h$ of $[0, h]$ satisfying the following property

$$X_0 + \frac{h_1}{h}(X - X_0) \in S_1 \cap S_2.$$

See Figure 4.3. Since $u \in D^{r+1}(S)$, there exits $\overline{u}_l(x, y) \in C^{r+1}(S_l)$ such that

$$\overline{u}_l(x, y) = u_l(x, y) \text{ for } (x, y) \in S_l^\circ,$$

for each $l = 1, 2$. Define $\overline{v}_l(s : x, y)$ by

$$\overline{v}_l(s; x, y) = \overline{u}_l(X_0 + \frac{s}{h}(X - X_0)),$$

for $s \in [h_l, h_{l+1}]$ and $l = 0, 1$. Then it is clear that

$$\overline{v}_l(s; x, y) \in C^{r+1}[h_l, h_{l+1}],$$

and

$$\overline{v}_l(s; x, y) = v_l(s; x, y) \text{ for } s \in (h_l, h_{l+1})\,.$$

Thus,

$$v(s; x, y) \in D^{r+1}[a, b].$$

Now we can apply Taylor expansion to $v(s; x, y)$ as a function of s to get

$$\begin{aligned} v(s; x, y) &= v(a) + v'(a)(s - a) + \ldots + \frac{1}{r!}v^{(r)}(a)(s - a)^r \\ &+ \frac{1}{r!}\int_0^h v^{(r+1)}(t)(s - t)_+^r dt \\ &= A(s; x, y) + B(s; x, y). \end{aligned} \tag{4.9}$$

In here,

$$A(s;x,y) = v(a) + v'(a)(s-a) + \ldots + \frac{1}{r!}v^{(r)}(a)(s-a)^r,$$
$$B(s;x,y) = \frac{1}{r!}\int_0^h v^{(r+1)}(t)(s-t)_+^r dt.$$

Let's define a linear functional $L : D^{r+1}(\Delta_{n,k}) \to R$ by

$$\begin{aligned} Lu(x,y) &= u(x,y) - P_n u(x,y) \\ &= u(x,y) - \sum_{i=1}^{f_r} u(c_{k,i}) l_i(T_k^{-1}(x,y)). \end{aligned}$$

In here, we are using the same projection P_n as in (4.4). Applying L to (4.9) with the property that $L[A(s;x,y)] = 0$ for $A(s;x,y) \in P_r(\Delta_{n,k})$, we get

$$\begin{aligned} Lv(s;x,y) &= L[A(s;x,y) + B(s;x,y)], \\ &= L[B(s;x,y)]. \end{aligned} \tag{4.10}$$

Let's consider $L[B(s;x,y)]$. Then, we have

$$\begin{aligned} L[B(s;x,y)] &= L[\frac{1}{r!}\int_0^h v^{(r+1)}(t)(s-t)_+^r dt], \\ &= \frac{1}{r!}\int_0^h L\left[v^{(r+1)}(t)\right](s-t)_+^r dt, \\ &= \frac{1}{r!}\sum_{l=0}^{1}\int_{h_l}^{h_{l+1}} L\left[v^{(r+1)}(t)\right](s-t)_+^r dt, \\ &= \frac{1}{h^{r+1}r!}\sum_{l=0}^{1}\int_{h_l}^{h_{l+1}} [[(X-X_0)\circ\nabla]^{r+1}\overline{u}_l(X_0 + \frac{t}{h}(X-X_0)) \\ &- \sum_{i=1}^{f_r} l_i(T_k^{-1}(x,y))[(c_{k,i}-X_0)\circ\nabla]^{r+1}\overline{u}_l(X_0 + \frac{t}{h}(c_{k,i}-X_0))](s-t)_+^r dt. \end{aligned}$$

Using

$$\sum_{i=1}^{f_r} l_i(T_k^{-1}(x,y)) = 1,$$

we have

$$L[B(s;x,y)] = \frac{1}{h^{r+1}r!}\sum_{l=0}^{1}\sum_{i=1}^{f_r}\int_{h_l}^{h_{l+1}} l_i(T_k^{-1}(x,y)) \tag{4.11}$$

$$\cdot\{[(X-X_0)\circ\nabla]^{r+1}\overline{u}_l(X_0+\frac{t}{h}(X-X_0))$$

$$-\ [(c_{k,i}-X_0)\circ\nabla]^{r+1}\overline{u}_l(X_0+\frac{t}{h}(c_{k,i}-X_0))\}(s-t)_+^r dt.$$

Using

$$[(X-X_0)\circ\nabla]^{r+1}u(x,y)$$

$$=\sum_{j=0}^{r+1}\frac{(r+1)!}{j!(r+1-j)!}(x-x_0)^j(y-y_0)^{r+1-j}D_x^jD_y^{r+1-j}u(x,y),$$

and

$$c_{k,i}=(x_{k,i},y_{k,i}),$$

equation (4.11) becomes

$$L[B(s;x,y)] = \frac{1}{h^{r+1}r!}\sum_{l=0}^{1}\sum_{i=1}^{f_r}\int_{h_l}^{h_{l+1}} l_i(T_k^{-1}(x,y))$$

$$\cdot\{\sum_{j=0}^{r+1}\frac{(r+1)!}{j!(r+1-j)!}(x-x_0)^j(y-y_0)^{r+1-j}$$

$$D_x^jD_y^{r+1-j}\overline{u}_l(X_0+\frac{t}{h}(X-X_0))$$

$$-\sum_{j=0}^{r+1}\frac{(r+1)!}{j!(r+1-j)!}(x_{k,i}-x_0)^j(y_{k,i}-y_0)^{r+1-j}$$

$$D_x^jD_y^{r+1-j}\overline{u}_l(X_0+\frac{t}{h}(c_{k,i}-X_0))\}(s-t)_+^r dt,$$

$$=\frac{1}{h^{r+1}r!}\sum_{l=0}^{1}\sum_{i=1}^{f_r}\sum_{j=0}^{r+1}\frac{(r+1)!}{j!(r+1-j)!}\int_{h_l}^{h_{l+1}} l_i(T_k^{-1}(x,y))$$

$$\cdot\{(x-x_0)^j(y-y_0)^{r+1-j}D_x^jD_y^{r+1-j}\overline{u}_l(X_0+\frac{t}{h}(X-X_0))$$

$$-(x_{k,i}-x_0)^j(y_{k,i}-y_0)^{r+1-j}D_x^jD_y^{r+1-j}\overline{u}_l(X_0+\frac{t}{h}(c_{k,i}-X_0))\}(s-t)_+^r dt.$$

Thus, we can say that

$$L[B(s;x,y)] = \frac{1}{h^{r+1}r!}\sum_{l=0}^{1}\sum_{i=1}^{f_r}\sum_{j=0}^{r+1}\frac{(r+1)!}{j!(r+1-j)!}\int_{h_l}^{h_{l+1}} l_i(T_k^{-1}(x,y)) \tag{4.12}$$

$$\cdot\{(x-x_0)^j(y-y_0)^{r+1-j}D_x^jD_y^{r+1-j}u_l(X_0+\frac{t}{h}(X-X_0))$$

$$-(x_{k,i}-x_0)^j(y_{k,i}-y_0)^{r+1-j}D_x^jD_y^{r+1-j}u_l(X_0+\frac{t}{h}(c_{k,i}-X_0))\}(s-t)_+^r dt.$$

Based on equation (4.12), we can easily derive the following estimate.

$$|L[v(s;x,y)]| \le ch^{r+1}\max_{(x,y)\in\Delta_{n,k}}\left\|D_x^jD_y^{r+1-j}u(x,y)\right\|.$$

Therefore, we have

$$\max_{(x,y)\in\Delta_{n,k}}|u(x,y)-P_nu(x,y)| \le ch^{r+1}\max_{\substack{i,j\ge 0\\ i+j=r+1}}\max_{(x,y)\in\Delta_{n,k}}\left|D^iD^ju(x,y)\right|.$$

$\square$

As a special case of the above theorem, we have the following corollary. If the triangulation $T_n = \{\Delta_{n,k} \mid k = 1, 2, \ldots, N_n\}$ respects the partition $\{S_j \subset R^3 \mid j = 1, .., N\}$ of S, then we have only one plane S_l such that $\Delta_{n,k} \cap S_l \ne \emptyset$. Thus, we can follow exactly the same path to prove the following theorem.

Corollary 1. *Suppose that $u \in D^{r+1}(S)\setminus C^{r+1}(S)$ and the uniform triangulation $T_n = \{\Delta_{n,k} \mid k = 1, 2, \ldots, N_n\}$ of S respects the partition $\{S_j \subset R^3 \mid j = 1, .., N\}$ of S and the interpolation points $c_{k,i}$ of P_n are chosen in the interior of the triangle $\Delta_{n,k}$, then we have*

$$\sup_{(x,y)\in\Delta_{n,k}}|u(x,y)-P_nu(x,y)| \le ch^{r+1}\max_{\substack{i,j\ge 0\\ i+j=r+1}}\sup_{(x,y)\in\Delta_{n,k}}\left|D^iD^ju(x,y)\right|$$

where $\Delta_{n,k}$ is an element of the uniform triangulation T_n.

4.2 Regularity Analysis Using D^{r+1}

The regularity of the solution of the radiosity equation has been understood using the concept of *visual events* in computer graphics. Visual events happen when there is a change of visibility. For more detailed description of the visual events based on aspect graphs, refer to [14] and [15]. The two most typical visual events are *edge-vertex* (*EV*) *events* or *edge-edge-edge* (*EEE*) *events*. They are used to classify the regularity of the radiosity solution.

In this section, we provide a mathematical framework which can be used to understand the regularity of the radiosity solution using $D^{r+1}(S)$ function space. We show this by analyzing the regularity of the radiosity solution for the following four basic models which are most frequently used in computer graphics. We can use the same mathematical framework to analyze models of other event types including EEE events, but providing the complete catalog of the analysis of all possible visible events is left for future works.

Model 1. As our first model, let's consider the configuration S given in Figure 4.4. That is,

$$S = S_1 \cup S_2 \cup S_3 \cup S_4 \cup S_5 \cup S_6,$$

where

$$S_1 = \{(x, 0, z) \; |0 \leq x \leq 1, 0 \leq z \leq 2\},$$

$$S_2 = \{(x, y, 0) \; |0 \leq x \leq 1, 0 \leq y \leq 1\},$$

$$S_3 = \{(x, 1, z) \; |0 \leq x \leq 1, 0 \leq z \leq 1\},$$

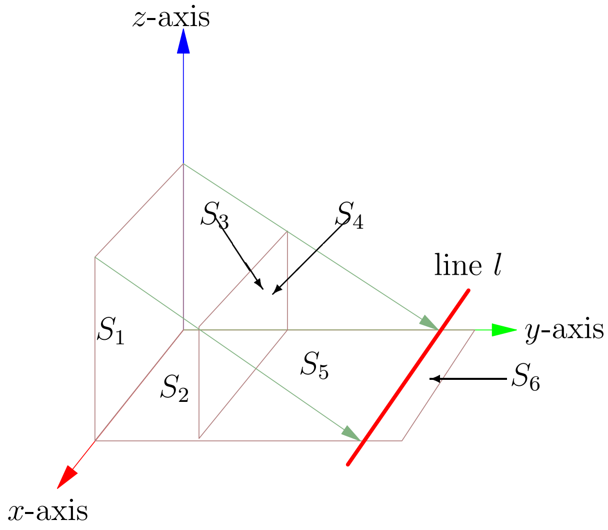

Figure 4.4: Model type 1.

and

$$S_4 = \{(x, 1, z) \ |0 \leq x \leq 1, 0 \leq z \leq 1\},$$

$$S_5 = \{(x, y, 0) \ |0 \leq x \leq 1, 1 \leq y \leq 2\},$$

$$S_6 = \{(x, y, 0) \ |0 \leq x \leq 1, 2 \leq y \leq 4\}.$$

In here, the surfaces S_3 and S_4 are two different sides of the same plane. Even though they share the same geometric position, their normal vectors point to the opposite directions. There is an *edge-edge*(EE) event happening as we cross the line in l along y-axis. We investigate the regularity of the radiosity solution $u(p)$ around l for this model. For any $p \in S$, the radiosity solution $u(p)$ is given by

$$u(p) = E(p) + \int_S K(p, q)V(p, q)u(q)dq. \tag{4.13}$$

Because of the effect of the visibility function $V(p,q)$, equation (4.13) becomes

$$u(p) = \begin{cases} E(p) + \int_{S_4} K(p,q)u(q)dq & \text{if } p \in S_5 \\ E(p) + \int_{S_4} K(p,q)u(q)dq & \text{if } p \in S_6 \\ + \int_T K(p,q)u(q)dq \end{cases} \tag{4.14}$$

where $T = \{(x,0,z) \mid 0 \leq x \leq 1, \frac{y_p}{y_p-1} \leq y \leq 2\}$ for $p = (x_p, y_p, 0) \in S_6$. Thus, it is clear that $u(p)$ is continuous on S by (4.14) as $\lim_{y_p \to 2} T = \emptyset$.

Next, let's consider the first derivative of $u(p)$ on $S_5 \cup S_6$ under the assumption that $E(p)$ is equal to a constant on S. For all $p = (x_p, y_p) \in S_5^o$, we have

$$\begin{aligned} \frac{\partial u(p)}{\partial y_p} &= \frac{\partial}{\partial y_p} \int_{S_4} K(x_p, y_p, q)u(q)dq \\ &= \int_{S_4} \frac{\partial}{\partial y_p} K(x_p, y_p, q)u(q)dq \end{aligned} \tag{4.15}$$

Similarly, for all $p = (x_p, y_p) \in S_6^o$, we have

$$\begin{aligned} \frac{\partial u(p)}{\partial y_p} &= \frac{\partial}{\partial y_p} \int_{S_4} K(x_p, y_p, q)u(q)dq \\ &+ \frac{\partial}{\partial y_p} \int_{\frac{y_p}{y_p-1}}^{2} \int_0^1 K(x_p, y_p, x_q, z_q)u(x_q, z_q)dx_q dz_q \\ &= \int_{S_4} \frac{\partial}{\partial y_p} K(x_p, y_p, q)u(q)dq \\ &+ \int_{\frac{y_p}{y_p-1}}^{2} \int_0^1 \frac{\partial}{\partial y_p} K(x_p, y_p, x_q, z_q)u(x_q, z_q)dx_q dz_q \\ &+ \int_0^1 K(x_p, y_p, x_q, \frac{y_p}{y_p-1})u(x_q, \frac{y_p}{y_p-1})dx_q (\frac{1}{y_p-1})^2 \end{aligned} \tag{4.16}$$

By equations (4.15) and (4.16), we can say that in general

$$\lim_{y_p \to 2-} \frac{\partial u(p)}{\partial y_p} \neq \lim_{y_p \to 2+} \frac{\partial u(p)}{\partial y_p} < \infty$$

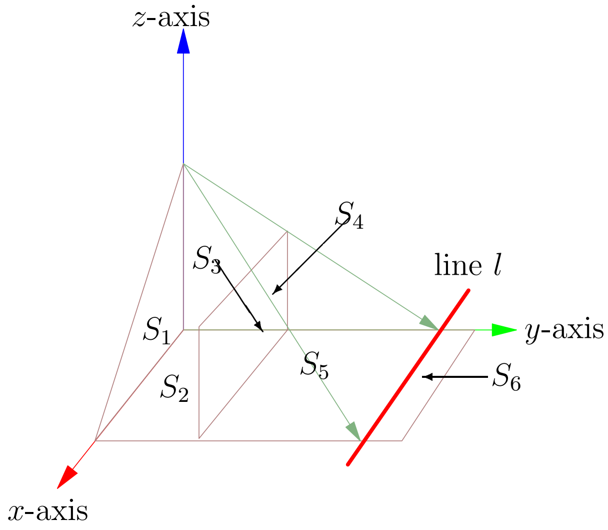

Figure 4.5: Model type 2.

since

$$\lim_{y_p \to 2} \int_{\frac{y_p}{y_p-1}}^{2} \int_0^1 \frac{\partial}{\partial y_p} K(x_p, y_p, x_q, z_q) u(x_q, z_q) dx_q dz_q = 0$$

but generally

$$\lim_{y_p \to 2} \int_0^1 K(x_p, y_p, x_q, z_q) u(x_q, \frac{y_p}{y_p - 1}) dx_q (\frac{1}{y_p - 1})^2 \neq 0$$

Therefore we have $u(p) \in D^1(S)$.

Model 2. As our second model, we consider the geometric configuration S given in Figure 4.5. That is,

$$S = S_1 \cup S_2 \cup S_3 \cup S_4 \cup S_5 \cup S_6,$$

where

$$S_1 = \{(x, 0, z) \ |0 \le x \le 1, 0 \le z \le 2x + 2\},$$

$$S_2 = \{(x, y, 0) \ |0 \le x \le 1, 0 \le y \le 1\},$$

$$S_3 = \{(x, 1, z) \ |0 \le x \le 1, 0 \le z \le 1\},$$

$$S_4 = \{(x, 1, z) \ |0 \le x \le 1, 0 \le z \le 1\},$$

$$S_5 = \{(x, y, 0) \ |0 \le x \le 1, 1 \le y \le 2\},$$

$$S_6 = \{(x, y, 0) \ |0 \le x \le 1, 2 \le y \le 4\}.$$

In here we assume that surfaces S_3 and S_4 are two different sides of the same plane. There happens a typical EV event as we cross the line l. We will check the regularity of the radiosity solution $u(p)$ of the equation (4.17) around this line l.

$$u(p) = E(p) + \int_S K(p, q)V(p, q)u(q)dq. \tag{4.17}$$

Because of the effect of the visibility function $V(p, q)$, equation (4.17) becomes

$$u(p) = \begin{cases} E(p) + \int_{S_4} K(p, q)u(q)dq & \text{if } p \in S_5, \\ E(p) + \int_{S_4} K(p, q)u(q)dq & \\ + \int_T K(p, q)u(q)dq & \text{if } p \in S_6, \end{cases}$$

where $T = \{(x, 0, z) \mid 0 \le x \le \frac{y_p - 2}{2(y_p - 1)}, \frac{y_p}{y_p - 1} \le z \le 2\}$ for $p = (x_p, y_p, 0) \in S_6$. Thus, it is clear that $u(p)$ is continuous on S by examination of (4.14) as $\lim_{y_p \to 2} T = \emptyset$.

Next, let's consider the first derivative of $u(p)$ on $S_5 \cup S_6$ under the assumption that $E(p)$ is equal to a constant on S. For all $p=(x_p,y_p)\in S_5^o$, we have

$$
\begin{aligned}
\frac{\partial u(p)}{\partial y_p} &= \frac{\partial}{\partial y_p}\int_{S_4} K(x_p,y_p,q)u(q)dq \\
&= \int_{S_4}\frac{\partial}{\partial y_p}K(x_p,y_p,q)u(q)dq
\end{aligned} \tag{4.18}
$$

Similarly, for all $p=(x_p,y_p)\in S_6^o$, we have

$$
\begin{aligned}
\frac{\partial u(p)}{\partial y_p} &= \frac{\partial}{\partial y_p}\int_{S_4} K(x_p,y_p,q)u(q)dq \\
&+ \frac{\partial}{\partial y_p}\int_{\frac{y_p}{y_p-1}}^{2}\int_0^{\frac{y_p-2}{2(y_p-1)}} K(x_p,y_p,x_q,z_q)u(x_q,z_q)dx_q dz_q \\
&= \int_{S_4}\frac{\partial}{\partial y_p}K(x_p,y_p,q)u(q)dq \\
&+ \int_{\frac{y_p}{y_p-1}}^{2}\frac{\partial}{\partial y_p}[\int_0^{\frac{y_p-2}{2(y_p-1)}} K(x_p,y_p,x_q,z_q)u(x_q,z_q)dx_q]dz_q \\
&+ \int_0^{\frac{y_p-2}{2(y_p-1)}} K(x_p,y_p,x_q,\frac{y_p}{y_p-1})u(x_q,\frac{y_p}{y_p-1})dx_q\frac{1}{(y_p-1)^2} \\
&= \int_{S_4}\frac{\partial}{\partial y_p}K(x_p,y_p,q)u(q)dq \qquad\qquad (4.19)\\
&+ \int_{\frac{y_p}{y_p-1}}^{2}\int_0^{\frac{y_p-2}{2(y_p-1)}} \frac{\partial}{\partial y_p}K(x_p,y_p,x_q,z_q)u(x_q,z_q)dx_q dz_q \\
&+ \frac{1}{2\,(y_p-1)^2}\int_{\frac{y_p}{y_p-1}}^{2} K(x_p,y_p,\frac{y_p-2}{2(y_p-1)},z_p)u(\frac{y_p-2}{2(y_p-1)},z_p)dz_q \\
&+ \frac{1}{(y_p-1)^2}\int_0^{\frac{y_p-2}{2(y_p-1)}} K(x_p,y_p,x_q,\frac{y_p}{y_p-1})u(x_q,\frac{y_p}{y_p-1})dx_q
\end{aligned}
$$

By examination of (4.18) and (4.19), we can say that

$$
\begin{aligned}
\lim_{y_p\to 2-}\frac{\partial u(p)}{\partial y_p} &= \lim_{y_p\to 2+}\frac{\partial u(p)}{\partial y_p}, \\
&= \int_{S_4}\frac{\partial}{\partial y_p}K(x_p,y_p,q)u(q)dq,
\end{aligned}
$$

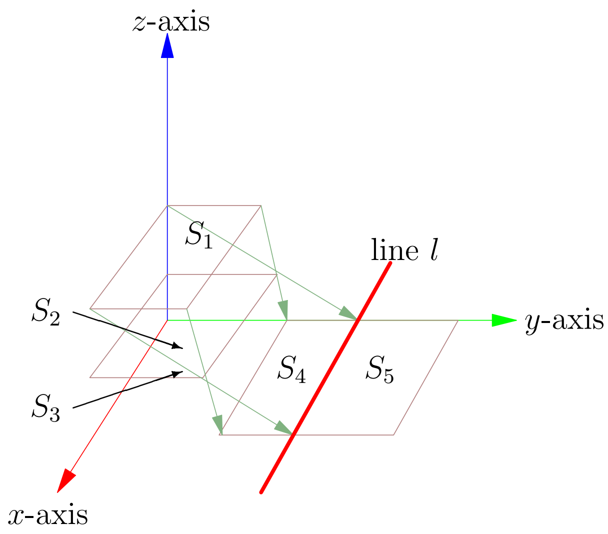

Figure 4.6: Model type 3.

since

$$\lim_{y_p \to 2} \int_{\frac{y_p}{y_p-1}}^{2} \int_{0}^{\frac{y_p-2}{2(y_p-1)}} \frac{\partial}{\partial y_p} K(x_p, y_p, x_q, z_q) u(x_q, z_q) dx_q dz_q = 0,$$

$$\lim_{y_p \to 2} \int_{\frac{y_p}{y_p-1}}^{2} K(x_p, y_p, \frac{y_p-2}{2(y_p-1)}, z_p) u(\frac{y_p-2}{2(y_p-1)}, z_p) dz_q = 0,$$

and

$$\lim_{y_p \to 2} \int_{0}^{\frac{y_p-2}{2(y_p-1)}} K(x_p, y_p, x_q, \frac{y_p}{y_p-1}) u(x_q, \frac{y_p}{y_p-1}) dx_q = 0.$$

Similarly, we can check that

$$\lim_{y_p \to 2-} \frac{\partial u(p)}{\partial y_p} \neq \lim_{y_p \to 2+} \frac{\partial u(p)}{\partial y_p} < \infty.$$

Thus, we can claim that $u(p) \in D^2(S)$.

Models 3 and 4. As our third and fourth models, we consider the geometric configurations given in Figure 4.6 and Figure 4.7. It can be shown that $u(p) \in D^1(S)$

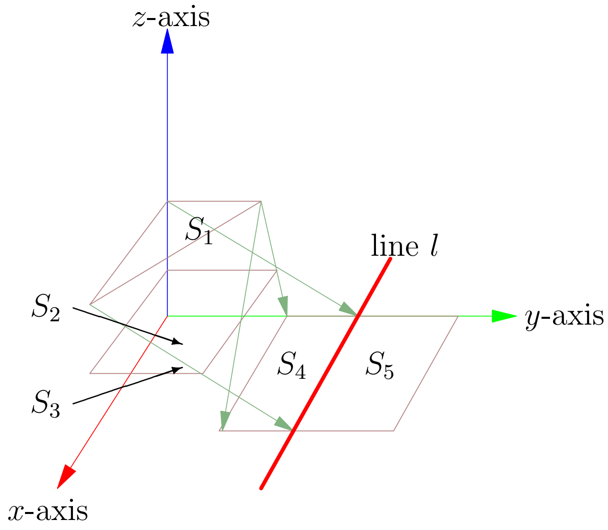

Figure 4.7: Model type 4.

for Figure 4.6 and $u(p) \in D^2(S)$ for Figure 4.7 using the same analysis used for the first and second models.

CHAPTER 5
CALCULATION OF THE COLLOCATION INTEGRALS

5.1 Transformation from R^3 into R^2

In order to solve the linear system (3.19), we are required to evaluate the following integral

$$\int_{\Delta_{n,j}} G(t_i, q) dS_q. \tag{5.1}$$

where $\Delta_{n,j}$ is an arbitrary triangle in R^3. For that, we have to convert the integral (5.1) into the following form of integral

$$\int_{\sigma} f(t_i, q) dS_q,$$

over the triangle $\sigma = \{ \ (s, t, 0) \mid 0 \leq s \leq a, \text{ and } 0 \leq t \ \leq \frac{b}{a}s \ \}$. See Figure 5.1. We call this type of triangle a *standard integral domain.* In this section, we show how to use an affine transformation to transform integrals over triangles in R^3 into integrals over triangles in R^2. In the next section we use another affine transformation to transform integrals over triangles in R^2 into integrals over the standard integral domain.

Definition 5.1. Let S be a n-polygon in R^3 defined by the vertices $v_0, v_1, \ldots, v_{n-1}$ with v_0 satisfying

$$\|v_0\| = \min\{\|v_i\| \ \mid i = 0, 1, \ldots, n-1\}$$

For S having the normal vector n_S which is equal to

$$(1, \theta, \phi)$$

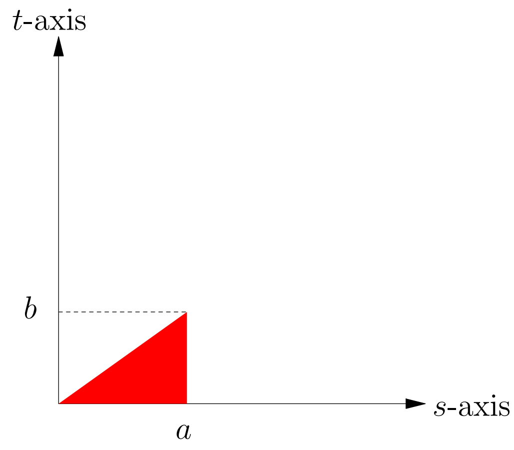

Figure 5.1: Standard integral domain

in spherical coordinates, or

$$(n_x, n_y, n_z)^T$$
$$= (\sin(\phi)\cos(\theta), \sin(\phi)\sin(\theta), \cos(\phi))^T$$

in rectangular coordinates, we define affine transformations A_S, $B_S : R^3 \to R^3$ by

$$A_S q = U(q - v_0),\ \ q \in R^3, \tag{5.2}$$

and

$$B_S r = v_0 + U^T r,\ \ r \in R^3, \tag{5.3}$$

where U is an unitary transformation defined by

$$U = \begin{pmatrix} \cos(\theta)\cos(\phi) & \cos(\phi)\sin(\theta) & -\sin(\phi) \\ -\sin(\theta) & \cos(\theta) & 0 \\ \cos(\theta)\sin(\phi) & \sin(\theta)\sin(\phi) & \cos(\phi) \end{pmatrix}.$$

See Figure 5.2.

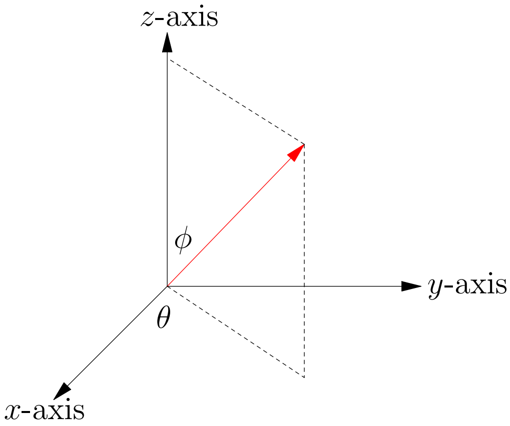

Figure 5.2: Normal vector of the plane S in spherical coordinate.

Note that

$$Un_S = (0, 0, 1)^T.$$

It is because the unitary transformation U rotates n_S with respect to z-axis by $-\theta$ degree first, and then it rotates the vector with respect to y-axis by ϕ degree. Since U is an unitary matrix, it is clear that

$$\begin{aligned} A_S B_S p &= U(B_S p - v_0) \\ &= U(v_0 + U^T p - v_0) \\ &= p, \end{aligned}$$

for all $p \in R^3$ and it follows also that

$$\begin{aligned} A_S B_S r &= A_S \left(v_0 + U^T r\right) \\ &= U \left(v_0 + U^T r - v_0\right) \\ &= r, \end{aligned}$$

for all $r \in R^3$. By definition, $A_S(S) \subset \{(s,t,0) \mid s,\, t \in R\}$. That is, the affine transformation A_S puts n-polygon S into the xy-plane with the property that $A_S(v_0) = 0$.

Given $p \in R^3$, the normal n_p at p and n-polygon $S \subset R^3$, we consider the following integration.

$$\begin{aligned} & \mathcal{K}_1 u(p) \\ &= \int_S G(p,q)u(q)dS_q \\ &= \int_S \frac{\langle p-q, n_q\rangle \langle q-p, n_p\rangle}{\|p-q\|^4} u(q)dS_q \\ &= \int_S \frac{\langle p-q, n_q\rangle \langle q-p, n_p\rangle}{\|p-q\|^4} u(q)dS_q \ . \end{aligned} \tag{5.4}$$

If we use the change of variable $q = B_S r$, then (5.4) becomes

$$\mathcal{K}_1 u(p) = \int_{A_S(S)} \frac{\langle p - B_S r, B_S(0,0,1)\rangle \langle B_S r - p, n_p\rangle}{\|p - B_S r\|^4} u(B_S r) \left| \frac{\partial B_S(r)}{\partial r} \right| dS_r.$$

Using,

$$\left| \frac{\partial B_S(r)}{\partial r} \right| = |\det(U)| = 1,$$

we have

$$\mathcal{K}_1 u(p) = \int_{A_S(S)} \frac{\langle p - B_S r, B_S(0,0,1)\rangle \langle B_S r - p, n_p\rangle}{\|p - B_S r\|^4} u(B_S r) dS_r.$$

Thus,

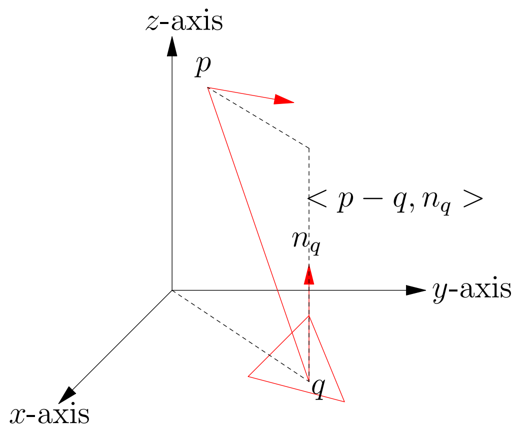

Figure 5.3: Geometric meaning of $< p - q, n_q >$.

$$
\begin{aligned}
&\mathcal{K}_1 u(p) \\
&= \mathcal{K}_1 u(B_S A_S p) \\
&= \int_{A_S(S)} \frac{\langle p - B_S r, B_S(0,0,1)\rangle \langle B_S r - p, n_p\rangle}{\|B_S A_S p - B_S r\|^4} u(B_S r) dS_r \\
&= \int_{A_S(S)} \frac{\langle p - B_S r, B_S(0,0,1)\rangle \langle B_S r - p, n_p\rangle}{\|A_S p - r\|^4} u(B_S r) dS_r. \qquad (5.5)
\end{aligned}
$$

Since

$$
\begin{aligned}
\langle p - B_S r, B_S(0,0,1)\rangle &= \langle p - q, n_q\rangle \\
&= \|p - q\| \cos(\theta)
\end{aligned}
$$

is constant for any $r \in A_S(S)$ as shown in Figure 5.3, the integration (5.5) becomes

$$
\begin{aligned}
&\mathcal{K}_1 u(p) \\
&= \langle p - B_S r, B_S(0,0,1)\rangle \int_{A_S(S)} \frac{\langle B_S r - p, n_p\rangle}{\|A_S p - r\|^4} u(B_S r) dS_r \\
&= \ \langle p - B_S r, B_S(0,0,1)\rangle \int_{A_S(S)} \frac{\langle B_S r, n_p\rangle}{\|A_S p - r\|^4} u(B_S r) dS_r && (5.6)\\
&- \langle p - B_S r, B_S(0,0,1)\rangle \int_{A_S(S)} \frac{\langle p, n_p\rangle}{\|A_S p - r\|^4} u(B_S r) dS_r. && (5.7)
\end{aligned}
$$

Since an arbitrary n-polygon S can always be divided into triangles, it suffices to consider the integration (5.6) and (5.7) for a triangular region S in R^3.

5.2 Transformation into a Standard Integral Domain

The affine transformation A_S maps triangles in R^3 into triangles in R^2. Now, we use the affine transformation defined in the following to transform triangles in R^2 into standard triangles of standard integral domain as shown in Figure 5.1.

Definition 5.2. Let S be a triangle in R^2 defined by the vertices $v_0 = 0, v_1, v_2 \in R^1$ counterclockwise and $\psi \in [0, 2\pi)$ be the angle between the x-axis and vertex v_1, then we can define the rotation, $R_S : R^3 \longrightarrow R^3$, by

$$p \mapsto R_S p, \ p \in R^3,$$

$$R_S = \begin{pmatrix} \cos(\psi) & \sin(\psi) & 0 \\ -\sin(\psi) & \cos(\psi) & 0 \\ 0 & 0 & 1 \end{pmatrix}.$$

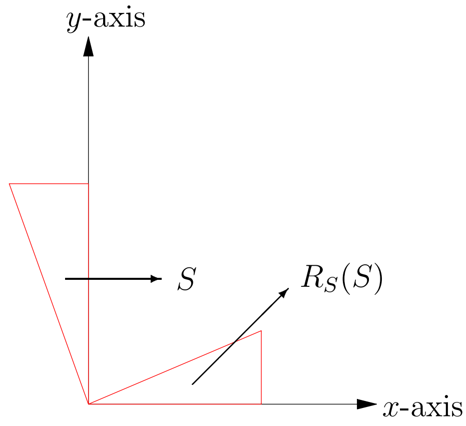

Figure 5.4: Rotation R_S

By definition, the vertex $R_S(v_0) = 0$ and the vertex $R_S(v_1)$ is on the x-axis. See Figure 5.4.

Using the rotation R_S, the integration in (5.6) becomes

$$\int_{A_S(S)} \frac{\langle B_S r, n_p \rangle}{\|A_S p - r\|^4} u(B_S r) dS_r \tag{5.8}$$

$$= \int_{R_{A_s(S)} A_S(S)} \frac{\left\langle B_S R^{-1}_{A_s(S)} s, n_p \right\rangle}{\left\| A_S p - R^{-1}_{A_s(S)} s \right\|^4} u(B_S R^{-1}_{A_s(S)} s) dS_s$$

$$= \int_{R_{A_s(S)} A_S(S)} \frac{\left\langle B_S R^{-1}_{A_s(S)} s, n_p \right\rangle}{\left\| R_{A_s(S)} A_S p - s \right\|^4} u(B_S R^{-1}_{A_s(S)} s) dS_s. \tag{5.9}$$

Using

$$B_S R^{-1}_{A_s(S)} s = v_0 + U^T R^{-1}_{A_s(S)} s, \tag{5.10}$$

equation (5.9) becomes

$$\int_{R_{A_s(S)}A_S(S)} \frac{\left\langle v_0 + U^T R_{A_s(S)}^{-1} s, n_p \right\rangle}{\left\| R_{A_s(S)} A_S p - s \right\|^4} u(B_S R_{A_s(S)}^{-1} s) dS_s$$
$$= \langle v_0, n_p \rangle \int_{R_{A_s(S)}A_S(S)} \frac{1}{\left\| R_{A_s(S)} A_S p - s \right\|^4} u(B_S R_{A_s(S)}^{-1} s) dS_s$$
$$+ \int_{R_{A_s(S)}A_S(S)} \frac{\left\langle U^T R_{A_s(S)}^{-1} s, n_p \right\rangle}{\left\| R_{A_s(S)} A_S p - s \right\|^4} u(B_S R_{A_s(S)}^{-1} s) dS_s. \tag{5.11}$$

In here, the vertex v_0 is the vertex described in (5.2) and (5.3) . By (5.9) and (5.11), we have

$$\int_{A_S(S)} \frac{\langle B_S r, n_p \rangle}{\| A_S p - r \|^4} u(B_S r) dS_r$$
$$= \langle v_0, n_p \rangle \int_{R_{A_s(S)}A_S(S)} \frac{1}{\left\| R_{A_s(S)} A_S p - s \right\|^4} u(B_S R_{A_s(S)}^{-1} s) dS_s \tag{5.12}$$
$$+ \int_{R_{A_s(S)}A_S(S)} \frac{\left\langle U^T R_{A_s(S)}^{-1} s, n_p \right\rangle}{\left\| R_{A_s(S)} A_S p - s \right\|^4} u(B_S R_{A_s(S)}^{-1} s) dS_s.$$

Similarly, the integration in (5.7) becomes

$$\int_{A_S(S)} \frac{\langle p, n_p \rangle}{\| A_S p - r \|^4} u(B_S r) dS_r$$
$$= \langle p, n_p \rangle \int_{R_{A_s(S)}A_S(S)} \frac{1}{\left\| A_S p - R_{A_s(S)}^{-1} s \right\|^4} u(B_S R_{A_s(S)}^{-1} s) dS_s$$
$$= \langle p, n_p \rangle \int_{R_{A_s(S)}A_S(S)} \frac{1}{\left\| R_{A_s(S)} A_S p - s \right\|^4} u(B_S R_{A_s(S)}^{-1} s) dS_s. \tag{5.13}$$

Combining (5.12) with (5.13), we get

$$\mathcal{K}_1 u(p) = c_1 \int_{R_{A_s(S)}A_S(S)} \frac{1}{\left\| R_{A_s(S)} A_S p - s \right\|^4} u(B_S R_{A_s(S)}^{-1} s) dS_s \tag{5.14}$$
$$+ c_2 \int_{R_{A_s(S)}A_S(S)} \frac{\left\langle U^T R_{A_s(S)}^{-1} s, n_p \right\rangle}{\left\| R_{A_s(S)} A_S p - s \right\|^4} u(B_S R_{A_s(S)}^{-1} s) dS_s. \tag{5.15}$$

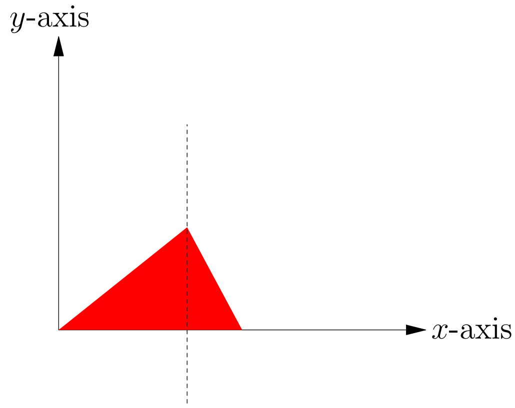

Figure 5.5: Type A triangle

In here,

$$c_1 = \langle p - B_S r, B_S(0,0,1) \rangle \langle v_0 - p, n_p \rangle ,$$

$$c_2 = \langle p - B_S r, B_S(0,0,1) \rangle ,$$

and

$$\begin{aligned} & R_{A_s(S)} A_S p \\ & = R_{A_s(S)} U(p - v_0) \\ & = R_{A_s(S)} U p + R_{A_s(S)} U v_0. \end{aligned}$$

First, let's consider the evaluation of the integration (5.14) for various types of triangles in R^3. Suppose S is a triangle in R^3, then $R_{A_s(S)} A_S(S)$ becomes a triangle of type A, type B, type C, or type D in R^2. Suppose $R_{A_s(S)} A_S(S)$ is the triangle with vertices $v_0 = (0,0)$, $v_1 = (x_1, 0)$, and $v_2 = (x_2, y_2)$.Then the type of the triangle $R_{A_s(S)} A_S(S)$ is determined by x_2. If $0 < x_2 < x_1$, then the triangle becomes a triangle

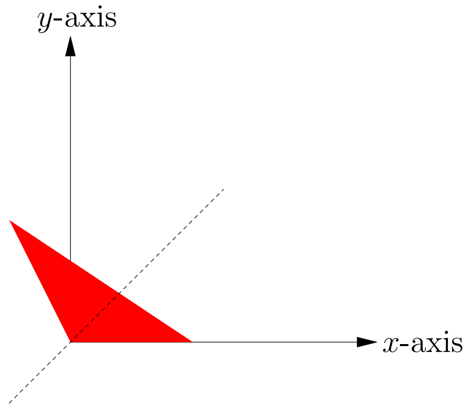

Figure 5.6: Type B triangle

of type A. See Figure 5.5. If $x_2 \leq 0$, then the triangle becomes a triangle of type B. See Figure 5.6. If $x_2 > x_1$, then the triangle becomes a triangle of type C. See Figure 5.7.If $x_2 = x_1$, then the triangle becomes a triangle of type D. See Figure 5.8. The triangles of type A, type B, and type C can be split into two triangles of type D along the dotted line as shown in Figure 5.5, 5.6, and 5.7. The divided parts of the triangle can be affine transformed to a triangle of type D.

For instance, if the triangle $R_{A_s(S)}A_S(S)$ is the triangle of type A, it can be split into two subtriangles T_1 and T_2 as shown in Figure 5.9 and 5.10. Then, we have

$$\int_{R_{A_s(S)}A_S(S)} \frac{1}{\left\|R_{A_s(S)}A_S p - s\right\|^4} u(B_S R^{-1}_{A_s(S)} s) dS_s$$

$$= \int_{T_1} \frac{1}{\left\|R_{A_s(S)}A_S p - s\right\|^4} u(B_S R^{-1}_{A_s(S)} s) dS_s \tag{5.16}$$

$$+ \int_{T_2} \frac{1}{\left\|R_{A_s(S)}A_S p - s\right\|^4} u(B_S R^{-1}_{A_s(S)} s) dS_s. \tag{5.17}$$

Note that triangle T_1 in (5.16) is already a triangle of type D. In order to transform the triangle T_2 into a triangle of type D, we use the following affine transformation.

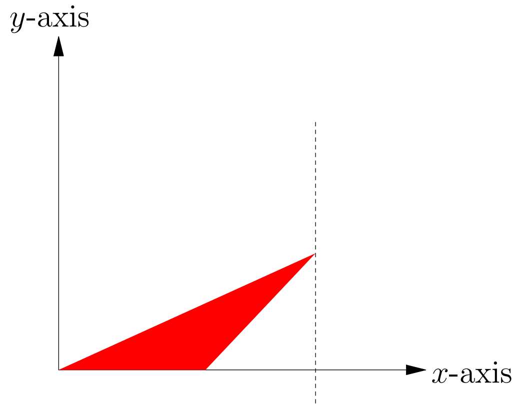

Figure 5.7: Type C triangle

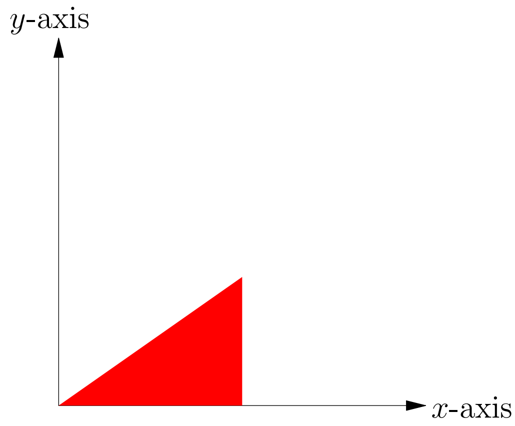

Figure 5.8: Type D triangle

Definition 5.3. For a triangle T in R^2 with vertices $v_0 = 0$, v_1, and v_2, we define $M_{i,T} : R^2 \longrightarrow R^2$ by

$$s \mapsto M_{i,T}s,\ \ s \in R^2,$$

$$M_{i,T}\ (s) = R_{T-v_i}(s - v_i), \tag{5.18}$$

where the triangle $T - v_i$ is the triangle T translated by $-v_i$.

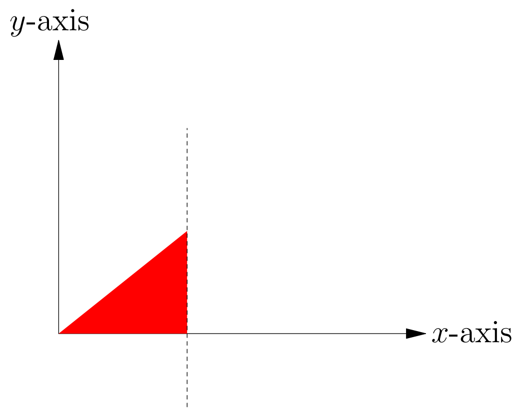

Figure 5.9: Subtriangle T_1

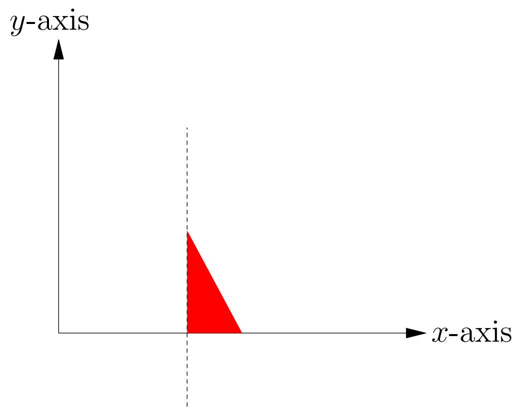

Figure 5.10: Subtriangle T_2

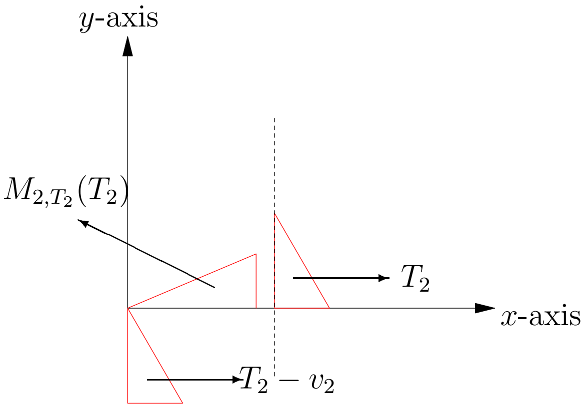

Figure 5.11: Affine transform M_{2,T_2}.

For example, the affine transform $M_{2,T_2}\ (T_2)$ of T_2 is given in Figure 5.11. In matrix form, M_{2,T_2} is

$$
\begin{aligned}
& M_{2,T_2} s \\
&= \begin{pmatrix} \cos(\frac{2\pi}{3}) & \sin(\frac{2\pi}{3}) & 0 \\ -\sin(\frac{2\pi}{3}) & \cos(\frac{2\pi}{3}) & 0 \\ 0 & 0 & 1 \end{pmatrix} (s - v_2) \\
&= \begin{pmatrix} 0 & -1 & 0 \\ 1 & 0 & 0 \\ 0 & 0 & 1 \end{pmatrix} (s - v_2),
\end{aligned}
\tag{5.19}
$$

since $\psi = \frac{2\pi}{3}$ if $R_{A_s(S)} A_S(S)$ is a triangle of type A and T_2 is the triangle as given in Figure 5.10. The inverse M_{2,T_2}^{-1} of M_{2,T_2} is given by

$$
\begin{aligned}
&M_{2,T_2}^{-1}t \\
&= v_2 + R_{T_2-v_2}^{-1}t \\
&= v_2 + \begin{pmatrix} 0 & -1 & 0 \\ 1 & 0 & 0 \\ 0 & 0 & 1 \end{pmatrix}^{-1} t \\
&= v_2 + \begin{pmatrix} 0 & 1 & 0 \\ -1 & 0 & 0 \\ 0 & 0 & 1 \end{pmatrix} t,
\end{aligned} \tag{5.20}
$$

in matrix form.

Using the change of variable $s = M_{2,T_2}^{-1}(t)$, the integration (5.17) becomes

$$
\begin{aligned}
&\int_{T_2} \frac{1}{\left\|R_{A_s(S)}A_S p - s\right\|^4} u(B_S R_{A_s(S)}^{-1} s) dS_s \\
&= \int_{M_{2,T_2}(T_2)} \frac{1}{\left\|R_{A_s(S)}A_S p - M_{2,T_2}^{-1}t\right\|^4} u(B_S R_{A_s(S)}^{-1} M_{2,T_2}^{-1}t) \left|\frac{\partial M_{2,T_2}^{-1}(t)}{\partial t}\right| dS_t.
\end{aligned} \tag{5.21}
$$

Since

$$
M_{2,T_2}^{-1}(t) = R_{T_2-v_2}^{-1}t + v_2,
$$

we have

$$
\begin{aligned}
\left|\frac{\partial M_{2,T_2}^{-1}(t)}{\partial t}\right| &= \left|\det(R_{T_2-v_2}^{-1})\right| \\
&= 1.
\end{aligned} \tag{5.22}
$$

Thus, by (5.21) and (5.22) , the equation (5.17) becomes

$$\begin{aligned}
&\int_{T_2} \frac{1}{\left\|R_{A_s(S)}A_Sp - s\right\|^4} u(B_S R^{-1}_{A_s(S)} s) dS_s \\
&= \int_{M_{2,T_2}(T_2)} \frac{1}{\left\|R_{A_s(S)}A_Sp - M^{-1}_{2,T_2} t\right\|^4} u(B_S R^{-1}_{A_s(S)} M^{-1}_{2,T_2} t) dS_t \\
&= \int_{M_{2,T_2}(T_2)} \frac{1}{\left\|R_{A_s(S)}A_Sp - R^{-1}_{T_2-v_2} t - v_2\right\|^4} u(B_S R^{-1}_{A_s(S)} M^{-1}_{2,T_2} t) dS_t \\
&= \int_{M_{2,T_2}(T_2)} \frac{1}{\left\|R_{A_s(S)}A_Sp - v_2 - R^{-1}_{T_2-v_2} t\right\|^4} u(B_S R^{-1}_{A_s(S)} M^{-1}_{2,T_2} t) dS_t \\
&= \int_{M_{2,T_2}(T_2)} \frac{1}{\left\|R_{T_2-v_2}(R_{A_s(S)}A_Sp - v_2) - t\right\|^4} u(B_S R^{-1}_{A_s(S)} M^{-1}_{2,T_2} t) dS_t \\
&= \int_{M_{2,T_2}(T_2)} \frac{1}{\left\|M_{2,T_2} R_{A_s(S)}A_Sp - \ t\right\|^4} u(B_S R^{-1}_{A_s(S)} M^{-1}_{2,T_2} t) dS_t .
\end{aligned}$$

By the definition of M_{2,T_2}, the triangle $M_{2,T_2}(T_2)$ is of type D.

If the domain D is the triangle $R_{A_s(S)}A_S(S)$ of type B, we first affine transform the triangle into a triangle of type A using $M_{1,D}$. Since

$$M_{1,D}(D) = M_{1,R_{A_s(S)}A_S(S)}(R_{A_s(S)}A_S(S))$$

is a triangle of type A, we have

$$\begin{aligned}
&\int_{R_{A_s(S)}A_S(S)} \frac{1}{\left\|R_{A_s(S)}A_Sp - s\right\|^4} u(B_S R^{-1}_{A_s(S)} s) dS_s \\
&= \int_{D} \frac{1}{\left\|R_{A_s(S)}A_Sp - s\right\|^4} u(B_S R^{-1}_{A_s(S)} s) dS_s \\
&= \int_{M_{1,D}(D)} \frac{1}{\left\|R_{A_s(S)}A_Sp - M^{-1}_{1,D}(t)\right\|^4} u(B_S R^{-1}_{A_s(S)} M^{-1}_{1,D}(t)) dS_s \\
&= \int_{M_{1,D}(D)} \frac{1}{\left\|M_{1,D} R_{A_s(S)}A_Sp - (t)\right\|^4} u(B_S R^{-1}_{A_s(S)} M^{-1}_{1,D}(t)) dS_s . \qquad (5.23)
\end{aligned}$$

using the change of variable $t = M_{1,D}(s)$. See Figure 5.12. Once we have the

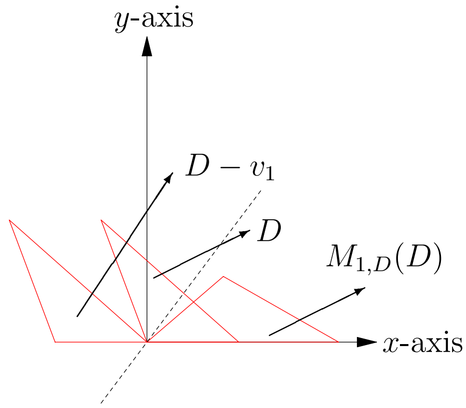

Figure 5.12: Transforming type B triangle into type A.

integration(5.23) over $M_{1,D}(D)$, a triangle of type A, we can follow the same algorithm which is described in the above to handle the triangle of type A.

Similarly, if the domain D is the triangle $R_{A_s(S)}A_S(S)$ of type C, we first affine transform the triangle into a triangle of type A using $M_{2,D}$. Since

$$M_{2,D}(D) = M_{2,R_{A_s(S)}A_S(S)}(R_{A_s(S)}A_S(S))$$

is a triangle of type A, we have

$$\begin{aligned}
&\int_{R_{A_s(S)}A_S(S)} \frac{1}{\left\|R_{A_s(S)}A_S p - s\right\|^4} u(B_S R^{-1}_{A_s(S)} s) dS_s \\
&= \int_D \frac{1}{\left\|R_{A_s(S)}A_S p - s\right\|^4} u(B_S R^{-1}_{A_s(S)} s) dS_s \\
&= \int_{M_{2,D}(D)} \frac{1}{\left\|R_{A_s(S)}A_S p - M^{-1}_{2,D}(t)\right\|^4} u(B_S R^{-1}_{A_s(S)} M^{-1}_{2,D}(t)) dS_t \\
&= \int_{M_{2,D}(D)} \frac{1}{\left\|M_{2,D} R_{A_s(S)}A_S p - (t)\right\|^4} u(B_S R^{-1}_{A_s(S)} M^{-1}_{2,D}(t)) dS_t. \qquad (5.24)
\end{aligned}$$

using the change of variable $t = M_{2,D}(s)$. See Figure 5.13. Once we have the

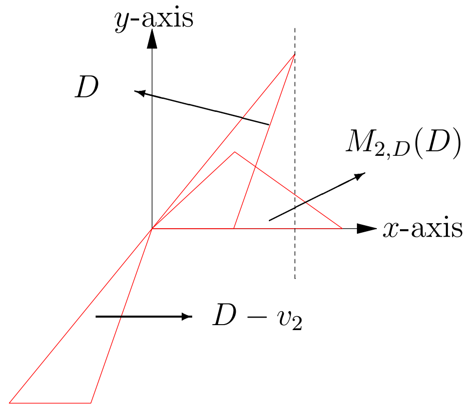

Figure 5.13: Transforming type C triangle into type A.

integration(5.24) over $M_{2,D}(D)$, a triangle of type A, we can follow the same algorithm which is described in the above to handle the triangle of type A.

Next, let's consider the integration (5.15). In order to evaluate integration (5.15), we need to evaluate $U^T R^{-1}_{A_s(S)}$. By the definition of U and $R^{-1}_{A_s(S)}$, we have

$$U^T R^{-1}_{A_s(S)} = \begin{pmatrix} c_{11} & c_{12} & \cos(\theta)\sin(\phi) \\ c_{21} & c_{22} & \sin(\theta)\sin(\phi) \\ -\cos(\psi)\sin(\phi) & \sin(\phi)\sin(\psi) & \cos(\phi) \end{pmatrix}, \tag{5.25}$$

and

$$R_{A_s(S)}U = \begin{pmatrix} c_{11} & c_{21} & -\cos(\psi)\sin(\phi) \\ c_{12} & c_{22} & \sin(\phi)\sin(\psi) \\ \cos(\theta)\sin(\phi) & \sin(\theta)\sin(\phi) & \cos(\phi) \end{pmatrix}.$$

In here,

$$c_{11} = \cos(\theta)\cos(\phi)\cos(\psi) - \sin(\theta)\sin(\psi),$$

$$c_{12} = -\cos(\psi)\sin(\theta) - \cos(\theta)\cos(\phi)\sin(\psi),$$

$$c_{21} = \cos(\phi)\cos(\psi)\sin(\theta) + \cos(\theta)\sin(\psi),$$

$$c_{22} = \cos(\theta)\cos(\psi) - \cos(\phi)\sin(\theta)\sin(\psi).$$

Since,

$$\begin{aligned}
&U^T R^{-1}_{A_s(S)} s \\
&= U^T R^{-1}_{A_s(S)} (s_1 e_1 + s_2 e_2) \\
&= s_1 U^T R^{-1}_{A_s(S)} e_1 + s_2 U^T R^{-1}_{A_s(S)} e_2 \\
&= s_1 \begin{pmatrix} c_{11} \\ c_{21} \\ -\cos(\psi)\sin(\phi) \end{pmatrix} + s_2 \begin{pmatrix} c_{12} \\ c_{22} \\ \sin(\phi)\sin(\psi) \end{pmatrix},
\end{aligned}$$

we have

$$\left\langle U^T R^{-1}_{A_s(S)} s, n_p \right\rangle = s_1 d_1 + s_2 d_2,$$

where

$$d_1 = \left\langle \begin{pmatrix} c_{11} \\ c_{21} \\ -\cos(\psi)\sin(\phi) \end{pmatrix}, n_p \right\rangle, \tag{5.26}$$

and

$$d_2 = \left\langle \begin{pmatrix} c_{12} \\ c_{22} \\ \sin(\phi)\sin(\psi) \end{pmatrix}, n_p \right\rangle. \tag{5.27}$$

Using this, the integration in (5.15) becomes

$$\int_{R_{A_s(S)}A_S(S)} \frac{\left\langle U^T R^{-1}_{A_s(S)} s, n_p \right\rangle}{\left\| R_{A_s(S)} A_S p - s \right\|^4} u(B_S R^{-1}_{A_s(S)} s) dS_s$$

$$= d_1 \int_{R_{A_s(S)}A_S(S)} \frac{s_1}{\left\| R_{A_s(S)} A_S p - s \right\|^4} u(B_S R^{-1}_{A_s(S)} s) dS_s \tag{5.28}$$

$$+ d_2 \int_{R_{A_s(S)}A_S(S)} \frac{s_2}{\left\| R_{A_s(S)} A_S p - s \right\|^4} u(B_S R^{-1}_{A_s(S)} s) dS_s. \tag{5.29}$$

First, if the domain $R_{A_s(S)}A_S(S)$ of the integration (5.15) is a triangle of type A, then we have

$$\int_{R_{A_s(S)}A_S(S)} \frac{\left\langle U^T R^{-1}_{A_s(S)} s, n_p \right\rangle}{\left\| R_{A_s(S)} A_S p - s \right\|^4} u(B_S R^{-1}_{A_s(S)} s) dS_s$$

$$= \int_{T_1} \frac{\left\langle U^T R^{-1}_{A_s(S)} s, n_p \right\rangle}{\left\| R_{A_s(S)} A_S p - s \right\|^4} u(B_S R^{-1}_{A_s(S)} s) dS_s \tag{5.30}$$

$$+ \int_{T_2} \frac{\left\langle U^T R^{-1}_{A_s(S)} s, n_p \right\rangle}{\left\| R_{A_s(S)} A_S p - s \right\|^4} u(B_S R^{-1}_{A_s(S)} s) dS_s. \tag{5.31}$$

The integration (5.30) can be evaluated in the same manner as given in (5.28) and (5.29) since the integration domain T_1 is a triangle of type D. Next, in order to evaluate (5.31), we use the affine transform M_{2,T_2} defined in (5.18) to transform T_2

into a triangle of type D.

$$\begin{aligned}
&\int_{T_2} \frac{\left\langle U^T R_{A_s(S)}^{-1} s, n_p \right\rangle}{\left\| R_{A_s(S)} A_S p - s \right\|^4} u(B_S R_{A_s(S)}^{-1} s) dS_s \\
= &\int_{M_{2,T_2}(T_2)} \frac{\left\langle U^T R_{A_s(S)}^{-1} M_{2,T_2}^{-1} t, n_p \right\rangle}{\left\| R_{A_s(S)} A_S p - M_{2,T_2}^{-1} t \right\|^4} u(B_S R_{A_s(S)}^{-1} M_{2,T_2}^{-1} t) \left| \frac{\partial M_{2,T_2}^{-1}(t)}{\partial t} \right| dS_t \\
= &\int_{M_{2,T_2}(T_2)} \frac{\left\langle U^T R_{A_s(S)}^{-1} M_{2,T_2}^{-1} t, n_p \right\rangle}{\left\| M_{2,T_2} R_{A_s(S)} A_S p - t \right\|^4} u(B_S R_{A_s(S)}^{-1} M_{2,T_2}^{-1} t) dS_t. \qquad (5.32)
\end{aligned}$$

If we evaluate $U^T R_{A_s(S)}^{-1} M_{2,T_2}^{-1}$ using (5.20) , we have

$$\begin{aligned}
&U^T R_{A_s(S)}^{-1} M_{2,T_2}^{-1} t \\
&= U^T R_{A_s(S)}^{-1} (v_2 + R_{T_2-v_2}^{-1} t) \\
&= U^T R_{A_s(S)}^{-1} v_2 + U^T R_{A_s(S)}^{-1} R_{T_2-v_2}^{-1} (t_1 e_1 + t_2 e_2) \\
&= U^T R_{A_s(S)}^{-1} v_2 + t_1 U^T R_{A_s(S)}^{-1} R_{T_2-v_2}^{-1} e_1 + t_2 U^T R_{A_s(S)}^{-1} R_{T_2-v_2}^{-1} e_2 \\
&= U^T R_{A_s(S)}^{-1} v_2 + t_1 U^T R_{A_s(S)}^{-1} m_1 + t_2 U^T R_{A_s(S)}^{-1} m_2, \qquad (5.33)
\end{aligned}$$

where

$$m_1 = R_{T_2-v_2}^{-1} e_1 = \begin{pmatrix} 0 \\ -1 \\ 0 \end{pmatrix}, \qquad (5.34)$$

and

$$m_2 = R_{T_2-v_2}^{-1} e_2 = \begin{pmatrix} 1 \\ 0 \\ 0 \end{pmatrix}. \qquad (5.35)$$

Now, we can evaluate (5.31) using (5.32) and (5.33).

$$
\begin{aligned}
&\int_{T_2} \frac{\left\langle U^T R_{A_s(S)}^{-1} s, n_p \right\rangle}{\left\| R_{A_s(S)} A_S p - s \right\|^4} u(B_S R_{A_s(S)}^{-1} s) dS_s \\
&= \int_{M_{2,T_2}(T_2)} \frac{\left\langle U^T R_{A_s(S)}^{-1} M_{2,T_2}^{-1} t, n_p \right\rangle}{\left\| M_{2,T_2} R_{A_s(S)} A_S p - t \right\|^4} u(B_S R_{A_s(S)}^{-1} M_{2,T_2}^{-1} t) dS_t \\
&= d_3 \int_{M_{2,T_2}(T_2)} \frac{t_1}{\left\| M_{2,T_2} R_{A_s(S)} A_S p - t \right\|^4} u(B_S R_{A_s(S)}^{-1} M_{2,T_2}^{-1} t) dS_t \\
&+ d_4 \int_{M_{2,T_2}(T_2)} \frac{t_2}{\left\| M_{2,T_2} R_{A_s(S)} A_S p - t \right\|^4} u(B_S R_{A_s(S)}^{-1} M_{2,T_2}^{-1} t) dS_t \\
&+ d_5 \int_{M_{2,T_2}(T_2)} \frac{1}{\left\| M_{2,T_2} R_{A_s(S)} A_S p - t \right\|^4} u(B_S R_{A_s(S)}^{-1} M_{2,T_2}^{-1} t) dS_t,
\end{aligned}
\tag{5.36}
$$

where

$$
d_3 = \left\langle U^T R_{A_s(S)}^{-1} m_1 \ , n_p \right\rangle, \tag{5.37}
$$

$$
d_4 = \left\langle U^T R_{A_s(S)}^{-1} m_2 \ , n_p \right\rangle, \tag{5.38}
$$

$$
d_5 = \left\langle U^T R_{A_s(S)}^{-1} v_2 \ , n_p \right\rangle. \tag{5.39}
$$

Thus, by (5.30), (5.31), (5.32), and (5.36), we have

$$
\begin{aligned}
&\int_{R_{A_s(S)} A_S(S)} \frac{\left\langle U^T R_{A_s(S)}^{-1} s, n_p \right\rangle}{\left\| R_{A_s(S)} A_S p - s \right\|^4} u(B_S R_{A_s(S)}^{-1} s) dS_s \\
&= d_1 \int_{T_1} \frac{s_1}{\left\| R_{A_s(S)} A_S p - s \right\|^4} u(B_S R_{A_s(S)}^{-1} s) dS_s \\
&+ d_2 \int_{T_1} \frac{s_2}{\left\| R_{A_s(S)} A_S p - s \right\|^4} u(B_S R_{A_s(S)}^{-1} s) dS_s. \\
&+ d_3 \int_{M_{2,T_2}(T_2)} \frac{t_1}{\left\| M_{2,T_2} R_{A_s(S)} A_S p - t \right\|^4} u(B_S R_{A_s(S)}^{-1} M_{2,T_2}^{-1} t) dS_t \\
&+ d_4 \int_{M_{2,T_2}(T_2)} \frac{t_2}{\left\| M_{2,T_2} R_{A_s(S)} A_S p - t \right\|^4} u(B_S R_{A_s(S)}^{-1} M_{2,T_2}^{-1} t) dS_t \\
&+ d_5 \int_{M_{2,T_2}(T_2)} \frac{1}{\left\| M_{2,T_2} R_{A_s(S)} A_S p - t \right\|^4} u(B_S R_{A_s(S)}^{-1} M_{2,T_2}^{-1} t) dS_t,
\end{aligned}
$$

where the definitions of d_1, d_2, d_3, d_4, and d_5 are given in (5.26), (5.27), (5.37), (5.38), and (5.39) respectively. Note that both T_1 and $M_2, T_2(T_2)$ are triangles of type D.

If the domain $D = R_{A_s(S)}A_S(S)$ of the integration (5.15) is a triangle of type B, we first transform the domain triangle D into the triangle of type A using $M_{1,D}$. Since

$$M_{1,D}(D) = M_{1,R_{A_s(S)}A_S(S)}(R_{A_s(S)}A_S(S))$$

is a triangle of type A, we have

$$\begin{aligned}
&\int_{R_{A_s(S)}A_S(S)} \frac{\left\langle U^T R^{-1}_{A_s(S)} s, n_p \right\rangle}{\left\| R_{A_s(S)}A_S p - s \right\|^4} u(B_S R^{-1}_{A_s(S)} s) dS_s \\
&= \int_D \frac{\left\langle U^T R^{-1}_{A_s(S)} s, n_p \right\rangle}{\left\| R_{A_s(S)}A_S p - s \right\|^4} u(B_S R^{-1}_{A_s(S)} s) dS_s \\
&= \int_{M_{1,D}(D)} \frac{\left\langle U^T R^{-1}_{A_s(S)} M^{-1}_{1,D} t, n_p \right\rangle}{\left\| R_{A_s(S)}A_S p - M^{-1}_{1,D} t \right\|^4} u(B_S R^{-1}_{A_s(S)} M^{-1}_{1,D} t) dS_t \\
&= \int_{M_{1,D}(D)} \frac{\left\langle U^T R^{-1}_{A_s(S)} M^{-1}_{1,D} t, n_p \right\rangle}{\left\| M_{1,D} R_{A_s(S)}A_S p - t \right\|^4} u(B_S R^{-1}_{A_s(S)} M^{-1}_{1,D} t) dS_t,
\end{aligned}$$

using the change of variable $t = M_{1,D}(s)$. Since $M_{1,D}(D)$ is a triangle of type A, we can split into two parts as we did before. That is,

$$\int_{M_{1,D}(D)} \frac{\left\langle U^T R^{-1}_{A_s(S)} M^{-1}_{1,D} t, n_p \right\rangle}{\left\| M_{1,D} R_{A_s(S)}A_S p - t \right\|^4} u(B_S R^{-1}_{A_s(S)} M^{-1}_{1,D} t) dS_t \tag{5.40}$$

$$= \int_{T_1} \frac{\left\langle U^T R^{-1}_{A_s(S)} M^{-1}_{1,D} t, n_p \right\rangle}{\left\| M_{1,D} R_{A_s(S)}A_S p - t \right\|^4} u(B_S R^{-1}_{A_s(S)} M^{-1}_{1,D} t) dS_t \tag{5.41}$$

$$+ \int_{T_2} \frac{\left\langle U^T R^{-1}_{A_s(S)} M^{-1}_{1,D} t, n_p \right\rangle}{\left\| M_{1,D} R_{A_s(S)}A_S p - t \right\|^4} u(B_S R^{-1}_{A_s(S)} M^{-1}_{1,D} t) dS_t. \tag{5.42}$$

In order to evaluate (5.41) , we need to evaluate $\left\langle U^T R^{-1}_{A_s(S)} M^{-1}_{2,D} t, n_p \right\rangle$. Since

$$
\begin{aligned}
& U^T R^{-1}_{A_s(S)} M^{-1}_{1,D} t \\
&= U^T R^{-1}_{A_s(S)} \left(R^{-1}_{D-v_1} t + v_1 \right) \\
&= U^T R^{-1}_{A_s(S)} R^{-1}_{D-v_1} t + U^T R^{-1}_{A_s(S)} v_1 \\
&= U^T R^{-1}_{A_s(S)} R^{-1}_{D-v_1} \left(t_1 e_1 + t_2 e_2 \right) + U^T R^{-1}_{A_s(S)} v_1 \\
&= t_1 U^T R^{-1}_{A_s(S)} R^{-1}_{D-v_1} e_1 + t_2 U^T R^{-1}_{A_s(S)} R^{-1}_{D-v_1} e_2 + U^T R^{-1}_{A_s(S)} v_1,
\end{aligned}
$$

we have

$$
\begin{aligned}
& \left\langle U^T R^{-1}_{A_s(S)} M^{-1}_{1,D} t, n_p \right\rangle \\
&= t_1 \left\langle U^T R^{-1}_{A_s(S)} R^{-1}_{D-v_1} e_1, n_p \right\rangle \\
&+ t_2 \left\langle U^T R^{-1}_{A_s(S)} R^{-1}_{D-v_1} e_2, n_p \right\rangle \\
&+ \left\langle U^T R^{-1}_{A_s(S)} v_1, n_p \right\rangle .
\end{aligned}
$$

Thus, the integration (5.41) becomes

$$
\begin{aligned}
& \int_{T_1} \frac{\left\langle U^T R^{-1}_{A_s(S)} M^{-1}_{1,D} t, n_p \right\rangle}{\left\| M_{1,D} R_{A_s(S)} A_S p - t \right\|^4} u(B_S R^{-1}_{A_s(S)} M^{-1}_{1,D} t) dS_t \\
&= f_1 \int_{T_1} \frac{t_1}{\left\| M_{1,D} R_{A_s(S)} A_S p - t \right\|^4} u(B_S R^{-1}_{A_s(S)} M^{-1}_{1,D} t) dS_t \\
&+ f_2 \int_{T_1} \frac{t_2}{\left\| M_{1,D} R_{A_s(S)} A_S p - t \right\|^4} u(B_S R^{-1}_{A_s(S)} M^{-1}_{1,D} t) dS_t \\
&+ f_3 \int_{T_1} \frac{1}{\left\| M_{1,D} R_{A_s(S)} A_S p - t \right\|^4} u(B_S R^{-1}_{A_s(S)} M^{-1}_{1,D} t) dS_t,
\end{aligned} \tag{5.43}
$$

where

$$f_1 = \left\langle U^T R_{A_s(S)}^{-1} R_{D-v_1}^{-1} e_1, n_p \right\rangle, \tag{5.44}$$

$$f_2 = \left\langle U^T R_{A_s(S)}^{-1} R_{D-v_1}^{-1} e_2, n_p \right\rangle, \tag{5.45}$$

$$f_3 = \left\langle U^T R_{A_s(S)}^{-1} v_1, n_p \right\rangle, \tag{5.46}$$

and v_1 is the first vertex of the triangle $D = R_{A_s(S)} A_S(S)$.

Next, let's consider (5.42). To transform T_2 into the triangle of type D, we use the affine transform M_{2,T_2} since $M_{2,T_2}(T_2)$ is the triangle of type D. Then, by the change of variable $\tau = M_{2,T_2}(t)$, we have

$$\begin{aligned}
&\int_{T_2} \frac{\left\langle U^T R_{A_s(S)}^{-1} M_{1,D}^{-1} t, n_p \right\rangle}{\left\| M_{1,D} R_{A_s(S)} A_S p - t \right\|^4} u(B_S R_{A_s(S)}^{-1} M_{1,D}^{-1} t) dS_t \\
&= \int_{M_{2,T_2}(T_2)} \frac{\left\langle U^T R_{A_s(S)}^{-1} M_{1,D}^{-1} M_{2,T_2}^{-1} \tau, n_p \right\rangle}{\left\| M_{1,D} R_{A_s(S)} A_S p - M_{2,T_2}^{-1} \tau \right\|^4} u(E_1 \tau) dS_\tau \\
&= \int_{M_{2,T_2}(T_2)} \frac{\left\langle U^T R_{A_s(S)}^{-1} M_{1,D}^{-1} M_{2,T_2}^{-1} \tau, n_p \right\rangle}{\left\| M_{2,T_2} M_{1,D} R_{A_s(S)} A_S p - \tau \right\|^4} u(E_1 \tau) dS_\tau,
\end{aligned} \tag{5.47}$$

where

$$E_1 = B_S R_{A_s(S)}^{-1} M_{1,D}^{-1} M_{2,T_2}^{-1}.$$

Since

$$\begin{aligned}
&U^T R_{A_s(S)}^{-1} M_{1,D}^{-1} M_{2,T_2}^{-1} \tau \\
&= U^T R_{A_s(S)}^{-1} M_{1,D}^{-1} \left(R_{T_2-v_2}^{-1} \tau + v_2 \right) \\
&= U^T R_{A_s(S)}^{-1} \left(R_{D-v_1}^{-1} \left(R_{T_2-v_2}^{-1} \tau + v_2 \right) + v_1 \right) \\
&= U^T R_{A_s(S)}^{-1} \left(R_{D-v_1}^{-1} R_{T_2-v_2}^{-1} \tau + R_{D-v_1}^{-1} v_2 + v_1 \right) \\
&= U^T R_{A_s(S)}^{-1} R_{D-v_1}^{-1} R_{T_2-v_2}^{-1} \tau + U^T R_{A_s(S)}^{-1} R_{D-v_1}^{-1} v_2 + U^T R_{A_s(S)}^{-1} v_1,
\end{aligned}$$

we have

$$\begin{aligned}
&\left\langle U^T R_{A_s(S)}^{-1} M_{1,D}^{-1} M_{2,T_2}^{-1} \tau, n_p \right\rangle \\
&= \left\langle U^T R_{A_s(S)}^{-1} R_{D-v_1}^{-1} R_{T_2-v_2}^{-1} \tau, n_p \right\rangle \\
&+ \left\langle U^T R_{A_s(S)}^{-1} R_{D-v_1}^{-1} v_2, n_p \right\rangle \\
&+ \left\langle U^T R_{A_s(S)}^{-1} v_1, n_p \right\rangle \\
&= \tau_1 \left\langle U^T R_{A_s(S)}^{-1} R_{D-v_1}^{-1} R_{T_2-v_2}^{-1} e_1, n_p \right\rangle \\
&+ \tau_2 \left\langle U^T R_{A_s(S)}^{-1} R_{D-v_1}^{-1} R_{T_2-v_2}^{-1} e_2, n_p \right\rangle \\
&+ \left\langle U^T R_{A_s(S)}^{-1} R_{D-v_1}^{-1} v_2, n_p \right\rangle + \left\langle U^T R_{A_s(S)}^{-1} v_1, n_p \right\rangle .
\end{aligned} \tag{5.48}$$

By (5.48) and (5.47), we get

$$\begin{aligned}
&\int_{T_2} \frac{\left\langle U^T R_{A_s(S)}^{-1} M_{1,D}^{-1} t, n_p \right\rangle}{\left\| M_{1,D} R_{A_s(S)} A_S p - t \right\|^4} u(B_S R_{A_s(S)}^{-1} M_{1,D}^{-1} t) dS_t \\
&= f_4 \int_{M_{2,T_2}(T_2)} \frac{\tau_1}{\left\| M_{2,T_2} M_{1,D} R_{A_s(S)} A_S p - \tau \right\|^4} u(E_1 \tau) dS_\tau \\
&+ f_5 \int_{M_{2,T_2}(T_2)} \frac{\tau_2}{\left\| M_{2,T_2} M_{1,D} R_{A_s(S)} A_S p - \tau \right\|^4} u(E_1 \tau) dS_\tau \\
&+ f_6 \int_{M_{2,T_2}(T_2)} \frac{1}{\left\| M_{2,T_2} M_{1,D} R_{A_s(S)} A_S p - \tau \right\|^4} u(E_1 \tau) dS_\tau \\
&+ f_7 \int_{M_{2,T_2}(T_2)} \frac{1}{\left\| M_{2,T_2} M_{1,D} R_{A_s(S)} A_S p - \tau \right\|^4} u(E_1 \tau) dS_\tau ,
\end{aligned} \tag{5.49}$$

where

$$f_4 = \left\langle U^T R_{A_s(S)}^{-1} R_{D-v_1}^{-1} R_{T_2-v_2}^{-1} e_1, n_p \right\rangle \tag{5.50}$$
$$= \left\langle U^T R_{A_s(S)}^{-1} R_{D-v_1}^{-1} m_1, n_p \right\rangle,$$
$$f_5 = \left\langle U^T R_{A_s(S)}^{-1} R_{D-v_1}^{-1} R_{T_2-v_2}^{-1} e_2, n_p \right\rangle \tag{5.51}$$
$$= \left\langle U^T R_{A_s(S)}^{-1} R_{D-v_1}^{-1} m_2, n_p \right\rangle,$$
$$f_6 = \left\langle U^T R_{A_s(S)}^{-1} R_{D-v_1}^{-1} v_2, n_p \right\rangle, \tag{5.52}$$
$$f_7 = \left\langle U^T R_{A_s(S)}^{-1} v_1, n_p \right\rangle, \tag{5.53}$$
$$E_1 = B_S R_{A_s(S)}^{-1} M_{1,D}^{-1} M_{2,T_2}^{-1}.$$

Therefore, by (5.15) , (5.28) , (5.29) , (5.43) , and (5.49) , we have

$$\int_{R_{A_s(S)}A_S(S)} \frac{\left\langle U^T R_{A_s(S)}^{-1} s, n_p \right\rangle}{\left\| R_{A_s(S)} A_S p - s \right\|^4} u(B_S R_{A_s(S)}^{-1} s) dS_s$$
$$= f_1 \int_{T_1} \frac{t_1}{\left\| M_{1,D} R_{A_s(S)} A_S p - t \right\|^4} u(B_S R_{A_s(S)}^{-1} M_{1,D}^{-1} t) dS_t$$
$$+ f_2 \int_{T_1} \frac{t_2}{\left\| M_{1,D} R_{A_s(S)} A_S p - t \right\|^4} u(B_S R_{A_s(S)}^{-1} M_{1,D}^{-1} t) dS_t$$
$$+ f_3 \int_{T_1} \frac{1}{\left\| M_{1,D} R_{A_s(S)} A_S p - t \right\|^4} u(B_S R_{A_s(S)}^{-1} M_{1,D}^{-1} t) dS_t$$
$$+ f_4 \int_{M_{2,T_2}(T_2)} \frac{\tau_1}{\left\| M_{2,T_2} M_{1,D} R_{A_s(S)} A_S p - \tau \right\|^4} u(E_1 \tau) dS_\tau$$
$$+ f_5 \int_{M_{2,T_2}(T_2)} \frac{\tau_2}{\left\| M_{2,T_2} M_{1,D} R_{A_s(S)} A_S p - \tau \right\|^4} u(E_1 \tau) dS_\tau$$
$$+ f_6 \int_{M_{2,T_2}(T_2)} \frac{1}{\left\| M_{2,T_2} M_{1,D} R_{A_s(S)} A_S p - \tau \right\|^4} u(E_1 \tau) dS_\tau$$
$$+ f_7 \int_{M_{2,T_2}(T_2)} \frac{1}{\left\| M_{2,T_2} M_{1,D} R_{A_s(S)} A_S p - \tau \right\|^4} u(E_1 \tau) dS_\tau.$$

In here, the definitions of f_1, f_2, f_3, f_4, f_5, f_6, and f_7 are given by (5.44) , (5.45) , (5.46) , (5.50) , (5.51) , (5.52) , and (5.53) , respectively.

Similarly, if the domain $D = R_{A_s(S)}A_S(S)$ of the integration (5.15) is a triangle of type C, we first transform the domain triangle into the triangle of type A using $M_{2,D}$. Then, we have

$$\begin{aligned}
&\int_{R_{A_s(S)}A_S(S)} \frac{\left\langle U^T R_{A_s(S)}^{-1} s, n_p \right\rangle}{\left\| R_{A_s(S)}A_S p - s \right\|^4} u(B_S R_{A_s(S)}^{-1} s) dS_s \\
&= \int_D \frac{\left\langle U^T R_{A_s(S)}^{-1} s, n_p \right\rangle}{\left\| R_{A_s(S)}A_S p - s \right\|^4} u(B_S R_{A_s(S)}^{-1} s) dS_s \\
&= \int_{M_{2,D}(D)} \frac{\left\langle U^T R_{A_s(S)}^{-1} M_{2,D}^{-1} t, n_p \right\rangle}{\left\| R_{A_s(S)}A_S p - M_{2,D}^{-1} t \right\|^4} u(B_S R_{A_s(S)}^{-1} M_{2,D}^{-1} t) dS_s \\
&= \int_{M_{2,D}(D)} \frac{\left\langle U^T R_{A_s(S)}^{-1} M_{2,D}^{-1} t, n_p \right\rangle}{\left\| M_{2,D} R_{A_s(S)}A_S p - t \right\|^4} u(B_S R_{A_s(S)}^{-1} M_{2,D}^{-1} t) dS_s
\end{aligned}$$

using the change of variable $t = M_{2,D}(s)$. Since $M_{2,D}(D)$ is a triangle of type A, we can split into two parts as we did before. That is,

$$\int_{M_{2,D}(D)} \frac{\left\langle U^T R_{A_s(S)}^{-1} M_{2,D}^{-1} t, n_p \right\rangle}{\left\| M_{2,D} R_{A_s(S)}A_S p - t \right\|^4} u(B_S R_{A_s(S)}^{-1} M_{2,D}^{-1} t) dS_s \tag{5.54}$$

$$= \int_{T_1} \frac{\left\langle U^T R_{A_s(S)}^{-1} M_{2,D}^{-1} t, n_p \right\rangle}{\left\| M_{2,D} R_{A_s(S)}A_S p - t \right\|^4} u(B_S R_{A_s(S)}^{-1} M_{2,D}^{-1} t) dS_s \tag{5.55}$$

$$+ \int_{T_2} \frac{\left\langle U^T R_{A_s(S)}^{-1} M_{2,D}^{-1} t, n_p \right\rangle}{\left\| M_{2,D} R_{A_s(S)}A_S p - t \right\|^4} u(B_S R_{A_s(S)}^{-1} M_{2,D}^{-1} t) dS_s. \tag{5.56}$$

In order to evaluate (5.55) , we need to evaluate $\left\langle U^T R^{-1}_{A_s(S)} M^{-1}_{2,D} t, n_p \right\rangle$ first. Since

$$
\begin{aligned}
& U^T R^{-1}_{A_s(S)} M^{-1}_{2,D} t \\
& = U^T R^{-1}_{A_s(S)} \left(R^{-1}_{D-v_2} t + v_2 \right) \\
& = U^T R^{-1}_{A_s(S)} R^{-1}_{D-v_2} t + U^T R^{-1}_{A_s(S)} v_2 \\
& = U^T R^{-1}_{A_s(S)} R^{-1}_{D-v_2} \left(t_1 e_1 + t_2 e_2 \right) + U^T R^{-1}_{A_s(S)} v_2 \\
& = t_1 U^T R^{-1}_{A_s(S)} R^{-1}_{D-v_2} e_1 + t_2 U^T R^{-1}_{A_s(S)} R^{-1}_{D-v_2} e_2 + U^T R^{-1}_{A_s(S)} v_2,
\end{aligned}
$$

we have

$$
\begin{aligned}
& \left\langle U^T R^{-1}_{A_s(S)} M^{-1}_{2,D} t, n_p \right\rangle \\
& = t_1 \left\langle U^T R^{-1}_{A_s(S)} R^{-1}_{D-v_2} e_1, n_p \right\rangle \\
& + t_2 \left\langle U^T R^{-1}_{A_s(S)} R^{-1}_{D-v_2} e_2, n_p \right\rangle \\
& + \left\langle U^T R^{-1}_{A_s(S)} v_2, n_p \right\rangle .
\end{aligned}
$$

Thus, the integration (5.55) becomes

$$
\begin{aligned}
& \int_{T_1} \frac{\left\langle U^T R^{-1}_{A_s(S)} M^{-1}_{2,D} t, n_p \right\rangle}{\left\| M_{2,D} R_{A_s(S)} A_S p - t \right\|^4} u(B_S R^{-1}_{A_s(S)} M^{-1}_{2,D} t) dS_s \\
= \;& g_1 \int_{T_1} \frac{t_1}{\left\| M_{2,D} R_{A_s(S)} A_S p - t \right\|^4} u(B_S R^{-1}_{A_s(S)} M^{-1}_{2,D} t) dS_s \qquad (5.57) \\
+ \;& g_2 \int_{T_1} \frac{t_2}{\left\| M_{2,D} R_{A_s(S)} A_S p - t \right\|^4} u(B_S R^{-1}_{A_s(S)} M^{-1}_{2,D} t) dS_s \\
+ \;& g_3 \int_{T_1} \frac{1}{\left\| M_{2,D} R_{A_s(S)} A_S p - t \right\|^4} u(B_S R^{-1}_{A_s(S)} M^{-1}_{2,D} t) dS_s,
\end{aligned}
$$

where

$$g_1 = \left\langle U^T R^{-1}_{A_s(S)} R^{-1}_{D-v_2} e_1, n_p \right\rangle, \tag{5.58}$$

$$g_2 = \left\langle U^T R^{-1}_{A_s(S)} R^{-1}_{D-v_2} e_2, n_p \right\rangle, \tag{5.59}$$

$$g_3 = \left\langle U^T R^{-1}_{A_s(S)} v_2, n_p \right\rangle, \tag{5.60}$$

and v_2 is the second vertex of the triangle $D = R_{A_s(S)} A_S(S)$. Next, let's consider (5.56). To transform T_2 into the triangle of type D, we use the affine transform M_{2,T_2} since $M_{2,T_2}(T_2)$ is the triangle of type D. Then, by the change of variable $\tau = M_{2,T_2}(t)$, we have

$$\begin{aligned}
&\int_{T_2} \frac{\left\langle U^T R^{-1}_{A_s(S)} M^{-1}_{2,D} t, n_p \right\rangle}{\left\| M_{2,D} R_{A_s(S)} A_S p - t \right\|^4} u(B_S R^{-1}_{A_s(S)} M^{-1}_{2,D} t) dS_s \\
&= \int_{M_{2,T_2}(T_2)} \frac{\left\langle U^T R^{-1}_{A_s(S)} M^{-1}_{2,D} M^{-1}_{2,T_2}(\tau), n_p \right\rangle}{\left\| M_{2,D} R_{A_s(S)} A_S p - M^{-1}_{2,T_2}(\tau) \right\|^4} u(E_2(\tau)) dS_\tau \\
&= \int_{M_{2,T_2}(T_2)} \frac{\left\langle U^T R^{-1}_{A_s(S)} M^{-1}_{2,D} M^{-1}_{2,T_2}(\tau), n_p \right\rangle}{\left\| M_{2,T_2} M_{2,D} R_{A_s(S)} A_S p - (\tau) \right\|^4} u(E_2(\tau)) dS_\tau,
\end{aligned} \tag{5.61}$$

where

$$E_2 = B_S R^{-1}_{A_s(S)} M^{-1}_{2,D} M^{-1}_{2,T_2}.$$

Since

$$
\begin{aligned}
& U^T R_{A_s(S)}^{-1} M_{2,D}^{-1} M_{2,T_2}^{-1} \tau \\
& = \; U^T R_{A_s(S)}^{-1} M_{2,D}^{-1} \left(R_{T_2 - \overline{v_2}}^{-1} \tau + \overline{v_2} \right) \\
& = \; U^T R_{A_s(S)}^{-1} \left(R_{D-v_2}^{-1} \left(R_{T_2 - \overline{v_2}}^{-1} \tau + \overline{v_2} \right) + v_2 \right) \\
& = U^T R_{A_s(S)}^{-1} \left(R_{D-v_2}^{-1} R_{T_2 - \overline{v_2}}^{-1} \tau + R_{D-v_2}^{-1} \overline{v_2} + v_2 \right) \\
& = U^T R_{A_s(S)}^{-1} R_{D-v_2}^{-1} R_{T_2 - \overline{v_2}}^{-1} \tau \\
& + U^T R_{A_s(S)}^{-1} R_{D-v_2}^{-1} \overline{v_2} + U^T R_{A_s(S)}^{-1} v_2,
\end{aligned}
$$

we have

$$
\begin{aligned}
& \left\langle U^T R_{A_s(S)}^{-1} M_{2,D}^{-1} M_{2,T_2}^{-1} \tau, n_p \right\rangle \\
& = \left\langle U^T R_{A_s(S)}^{-1} R_{D-v_2}^{-1} R_{T_2 - \overline{v_2}}^{-1} \tau, n_p \right\rangle \\
& + \left\langle U^T R_{A_s(S)}^{-1} R_{D-v_2}^{-1} \overline{v_2}, n_p \right\rangle \\
& + \left\langle U^T R_{A_s(S)}^{-1} v_2, n_p \right\rangle \\
& = \tau_1 \left\langle U^T R_{A_s(S)}^{-1} R_{D-v_2}^{-1} R_{T_2 - \overline{v_2}}^{-1} e_1, n_p \right\rangle \qquad (5.62) \\
& + \tau_2 \left\langle U^T R_{A_s(S)}^{-1} R_{D-v_2}^{-1} R_{T_2 - \overline{v_2}}^{-1} e_2, n_p \right\rangle \\
& + \left\langle U^T R_{A_s(S)}^{-1} R_{D-v_2}^{-1} \overline{v_2}, n_p \right\rangle + \left\langle U^T R_{A_s(S)}^{-1} v_2, n_p \right\rangle .
\end{aligned}
$$

By (5.61) , and (5.62) , we have

$$\int_{T_2} \frac{\left\langle U^T R_{A_s(S)}^{-1} M_{2,D}^{-1} t, n_p \right\rangle}{\left\| M_{2,D} R_{A_s(S)} A_S p - t \right\|^4} u(B_S R_{A_s(S)}^{-1} M_{2,D}^{-1} t) dS_s$$

$$= g_4 \int_{M_{2,T_2}(T_2)} \frac{\tau_1}{\left\| M_{2,T_2} M_{2,D} R_{A_s(S)} A_S p - \tau \right\|^4} u(E_2(\tau)) dS_\tau \tag{5.63}$$

$$+ g_5 \int_{M_{2,T_2}(T_2)} \frac{\tau_2}{\left\| M_{2,T_2} M_{2,D} R_{A_s(S)} A_S p - \tau \right\|^4} u(E_2(\tau)) dS_\tau$$

$$+ g_6 \int_{M_{2,T_2}(T_2)} \frac{1}{\left\| M_{2,T_2} M_{2,D} R_{A_s(S)} A_S p - \tau \right\|^4} u(E_2(\tau)) dS_\tau$$

$$+ g_7 \int_{M_{2,T_2}(T_2)} \frac{1}{\left\| M_{2,T_2} M_{2,D} R_{A_s(S)} A_S p - \tau \right\|^4} u(E_2(\tau)) dS_\tau .$$

In here,

$$g_4 = \left\langle U^T R_{A_s(S)}^{-1} R_{D-v_2}^{-1} R_{T_2-\overline{v_2}}^{-1} e_1, n_p \right\rangle \tag{5.64}$$

$$= \left\langle U^T R_{A_s(S)}^{-1} R_{D-v_2}^{-1} m_1, n_p \right\rangle ,$$

$$g_5 = \left\langle U^T R_{A_s(S)}^{-1} R_{D-v_2}^{-1} R_{T_2-\overline{v_2}}^{-1} e_2, n_p \right\rangle \tag{5.65}$$

$$= \left\langle U^T R_{A_s(S)}^{-1} R_{D-v_2}^{-1} m_2, n_p \right\rangle$$

$$g_6 = \left\langle U^T R_{A_s(S)}^{-1} R_{D-v_2}^{-1} \overline{v_2}, n_p \right\rangle , \tag{5.66}$$

$$g_7 = \left\langle U^T R_{A_s(S)}^{-1} v_2, n_p \right\rangle , \tag{5.67}$$

and $\overline{v_2}$ is the second vertex of the triangle T_2 and v_2 is the second vertex of the triangle

D. Therefore, by $(5.54), (5.55), (5.56), (5.57)$, and (5.63), we have

$$\int_{R_{A_s(S)}A_S(S)} \frac{\left\langle U^T R_{A_s(S)}^{-1} s, n_p \right\rangle}{\left\| R_{A_s(S)} A_S p - s \right\|^4} u(B_S R_{A_s(S)}^{-1} s) dS_s$$
$$= g_1 \int_{T_1} \frac{t_1}{\left\| M_{2,D} R_{A_s(S)} A_S p - t \right\|^4} u(B_S R_{A_s(S)}^{-1} M_{2,D}^{-1} t) dS_s$$
$$+ g_2 \int_{T_1} \frac{t_2}{\left\| M_{2,D} R_{A_s(S)} A_S p - t \right\|^4} u(B_S R_{A_s(S)}^{-1} M_{2,D}^{-1} t) dS_s$$
$$+ g_3 \int_{T_1} \frac{1}{\left\| M_{2,D} R_{A_s(S)} A_S p - t \right\|^4} u(B_S R_{A_s(S)}^{-1} M_{2,D}^{-1} t) dS_s$$
$$+ g_4 \int_{M_{2,T_2}(T_2)} \frac{\tau_1}{\left\| M_{2,T_2} M_{2,D} R_{A_s(S)} A_S p - \tau \right\|^4} u(E_2(\tau)) dS_\tau$$
$$+ g_5 \int_{M_{2,T_2}(T_2)} \frac{\tau_2}{\left\| M_{2,T_2} M_{2,D} R_{A_s(S)} A_S p - \tau \right\|^4} u(E_2(\tau)) dS_\tau$$
$$+ g_6 \int_{M_{2,T_2}(T_2)} \frac{1}{\left\| M_{2,T_2} M_{2,D} R_{A_s(S)} A_S p - \tau \right\|^4} u(E_2(\tau)) dS_\tau$$
$$+ g_7 \int_{M_{2,T_2}(T_2)} \frac{1}{\left\| M_{2,T_2} M_{2,D} R_{A_s(S)} A_S p - \tau \right\|^4} u(E_2(\tau)) dS_\tau.$$

In here, the definitions of g_1, g_2, g_3, g_4, g_5, g_6, and g_7 are given by (5.58), (5.59), $(5.60), (5.64)$, (5.65), (5.66), and (5.67), respectively.

CHAPTER 6
ANALYTIC EVALUATION OF $H_{M,N,P}$

6.1 Introduction

In this chapter, we study an analytic evaluation of the integrations which are needed for the setup of collocation methods for the radiosity equation.

Definition 6.1. For the set R of real numbers, we define a function

$$H_{m,n,p} : R^3 \to R$$

by

$$(x, y, z) \mapsto H_{m,n,p}(x, y, z),$$

$$H_{m,n,p}(x, y, z) = \int\int_{\Delta} \frac{\xi^m \eta^n}{((x-\xi)^2 + (y-\eta)^2 + z^2)^{\frac{p}{2}}} d\sigma(\xi, \eta). \tag{6.1}$$

In here, the region Δ is a triangular region bounded by $\xi = a, \eta = 0$, and $\eta = \frac{b}{a}\xi$ as given in Figure 5.1.

The analytic evaluation of this function when p is an odd number is given in [20]. In this section, we consider the analytic evaluation of $H_{m,n,4}(x, y, z)$ given in (6.1) for various m and n since they are what we need in order to evaluate exactly the integrals needed in implementing piecewise polynomial collocation methods. For piecewise polynomial collocation of degree $r \geq 0$, we need to evaluate $H_{m,n,4}(x, y, z)$ for $m, n \leq r + 1$.

If $p = 4$, then we will use the notation $H_{m,n}$ instead of $H_{m,n,4}$.

In most cases, we are interested in evaluating the integration $H_{m,n}(x,y,z)$ for $z \neq 0$, but we allow the use of very small $z > 0$. If the value of z is large enough, then the integrand (6.2)

$$k(x,y,z,\xi,\eta) = \frac{\xi^m \eta^n}{((x-\xi)^2 + (y-\eta)^2 + z^2)^2} \tag{6.2}$$

is well-behaved and the integral (6.1) is not hard to evaluate numerically. However, if the value of z is very small, then the denominator of the integrand (6.2) can be very small depending on the location x and y. In this case, the integrand $k(x,y,z,\xi,\eta)$ behaves like it has a singularity at $(\xi,\eta) = (x,y)$ making it difficult to evaluate numerically. For instance, if $m = 0$ and $n = 0$, then $k(x,y,z,\xi,\eta)$ becomes

$$k(\xi,\eta,z,\xi,\eta) = \frac{\xi^m \eta^n}{z^{\ 4}}.$$

at $(x,y,z) = (\xi,\eta)$. An illustration of the possible ill-behavior is indicated in Figure 6.1 and 6.2 for different values of z as z gets close to 0. As we can see in these figures, a slight change in z value makes a dramatic difference in the value of $k(\xi,\eta,z,\xi,\eta)$.

6.2 Analytic Evaluation of $H_{0,0,4}$

First, we consider the evaluation of $H_{0,0}(x,y,z)$. We have by definition

$$\begin{aligned} &H_{0,0}(x,y,z) \\ &= \int\int_\Delta \frac{\xi^0 \eta^0}{((x-\xi)^2 + (y-\eta)^2 + z^2)^2} d\sigma \\ &= \int\int_\Delta \frac{1}{((x-\xi)^2 + (y-\eta)^2 + z^2)^2} d\sigma \\ &= \int_0^a \int_0^{\frac{b}{a}\xi} \frac{1}{((x-\xi)^2 + (y-\eta)^2 + z^2)^2} d\eta d\xi. \end{aligned} \tag{6.3}$$

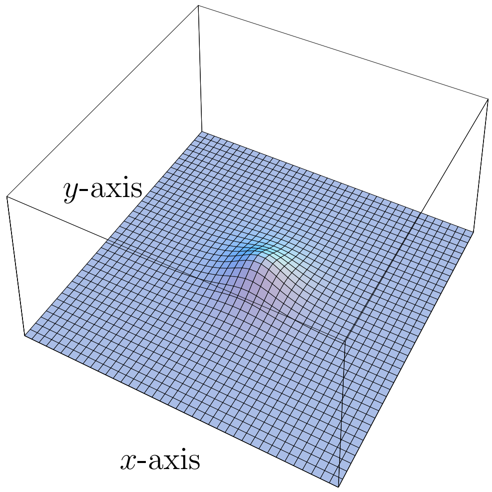

Figure 6.1: Plot of the integrand $k(x, y, z, \xi, \eta)$ for $(x, y, z) = (0, 0, 0.3)$.

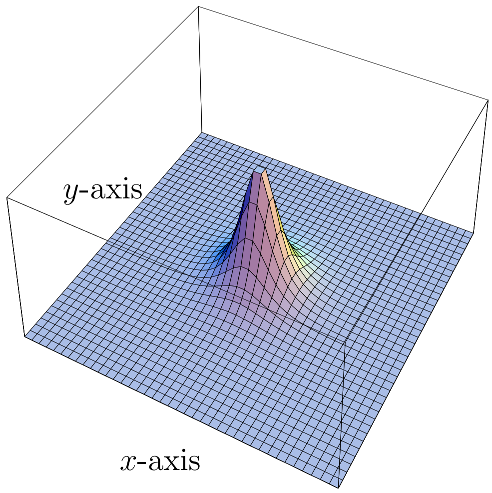

Figure 6.2: Plot of the integrand $k(x, y, z, \xi, \eta)$ for $(x, y, z) = (0, 0, 0.2)$.

In order to evaluate (6.3), we use the following integrations

$$\begin{aligned}
&\int \frac{1}{((x-\xi)^2+z^2+(y-\eta)^2)^2}d\eta \\
&= \frac{\eta-y}{2((x-\xi)^2+z^2)((x-\xi)^2+z^2+(\eta-y)^2)} \\
&+ \frac{\arctan(\frac{\eta-y}{\sqrt{(x-\xi)^2+z^2}})}{2((x-\xi)^2+z^2)^{\frac{3}{2}}},
\end{aligned}$$

then we have

$$\begin{aligned}
&H_{0,0}(x,y,z) \\
&= \int_0^a \int_0^{\frac{b}{a}\xi} \frac{1}{((x-\xi)^2+(y-\eta)^2+z^2)^2} d\eta d\xi \\
&= \int_0^a \left[\frac{\eta-y}{2\left((x-\xi)^2+z^2\right)\left((x-\xi)^2+z^2+(\eta-y)^2\right)}\right]_{\eta=0}^{\frac{b}{a}\xi} d\xi \\
&+ \int_0^a \left[\frac{\arctan(\frac{\eta-y}{\sqrt{((x-\xi)^2+z^2)}})}{2\left((x-\xi)^2+z^2\right)^{\frac{3}{2}}}\right]_{\eta=0}^{\frac{b}{a}\xi} d\xi.
\end{aligned}$$

Thus,

$$\begin{aligned}
&H_{0,0}(x,y,z) \\
&= \frac{1}{2}\int_0^a \frac{\frac{b}{a}\xi-y}{\left((x-\xi)^2+z^2\right)\left((x-\xi)^2+z^2+(\frac{b}{a}\xi-y)^2\right)}d\xi && (6.4)\\
&+ \frac{1}{2}\int_0^a \frac{y}{\left((x-\xi)^2+z^2\right)\left((x-\xi)^2+z^2+y^2\right)}d\xi && (6.5)\\
&+ \frac{1}{2}\int_0^a \frac{\arctan(\frac{\frac{b}{a}\xi-y}{\sqrt{((x-\xi)^2+z^2)}})}{\left((x-\xi)^2+z^2\right)^{\frac{3}{2}}}d\xi && (6.6)\\
&+ \frac{1}{2}\int_0^a \frac{\arctan(\frac{y}{\sqrt{((x-\xi)^2+z^2)}})}{\left((x-\xi)^2+z^2\right)^{\frac{3}{2}}}d\xi. && (6.7)
\end{aligned}$$

The integrations in (6.4), (6.5), (6.6) and (6.7) can be evaluated analytically as given in the followings. First, we can evaluate the integration (6.4) by

$$\begin{aligned}
&\int_0^a \frac{\frac{b}{a}\xi - y}{((x-\xi)^2+z^2)\,((x-\xi)^2+z^2+(\frac{b}{a}\xi-y)^2)}d\xi \\
&= \frac{a^2\delta}{\alpha\sqrt{\alpha+a^2z^2}}\arctan(\frac{\gamma}{\sqrt{\alpha+a^2z^2}}) - \frac{a\delta}{z\alpha}\arctan(\frac{x}{z}) \\
&+ \frac{ab}{2\alpha}(\log(\frac{x^2+z^2}{a^2\epsilon}) + \log(\frac{a^2(\epsilon-2\gamma+a^2+b^2)}{(x-a)^2+z^2})) \\
&- \frac{a\delta}{\alpha}(\frac{1}{z}\arctan(\frac{a-x}{z}) - \frac{a}{\sqrt{\alpha+a^2z^2}}\arctan(\frac{a^2+b^2-\gamma}{\sqrt{\alpha+a^2z^2}})).
\end{aligned} \tag{6.8}$$

Next, we can evaluate the integration (6.5) by

$$\begin{aligned}
&\int_0^a \frac{y}{((x-\xi)^2+z^2)\,((x-\xi)^2+z^2+y^2)}d\xi \\
&= \frac{1}{yz}(\arctan(\frac{a-x}{z}) + \arctan(\frac{x}{z})) \\
&- \frac{1}{y\sqrt{y^2+z^2}}(\arctan(\frac{a-x}{\sqrt{y^2+z^2}}) + \arctan(\frac{x}{\sqrt{y^2+z^2}})).
\end{aligned} \tag{6.9}$$

Third, we can evaluate the integration (6.6) by

$$\begin{aligned}
&\int_0^a \frac{\arctan(\frac{\frac{b}{a}\xi-y}{\sqrt{((x-\xi)^2+z^2)}})}{((x-\xi)^2+z^2)^{\frac{3}{2}}}d\xi \\
&= \frac{a\delta}{z\alpha}(\arctan(\frac{x}{z}) - \arctan(\frac{x-a}{z})) \\
&- \frac{x}{z^2\sqrt{x^2+z^2}}\arctan(\frac{y}{\sqrt{x^2+z^2}}) - \frac{x-a}{z^2\sqrt{\beta}}\arctan(\frac{b-y}{\sqrt{\beta}}) \\
&- \frac{\delta\sqrt{\alpha+(az)^2}}{z^2\alpha}(\arctan(\frac{\gamma}{\sqrt{\alpha+(az)^2}}) + \arctan(\frac{a^2+b^2-2\gamma}{\sqrt{\alpha+(az)^2}})) \\
&+ \frac{ab}{2\alpha}(\log(\frac{\beta}{x^2+z^2}) + \log(\frac{\epsilon}{\epsilon-2\gamma+a^2+b^2})
\end{aligned} \tag{6.10}$$

Finally, we can evaluate the integration (6.7) by

$$\int_0^a \frac{\arctan(\frac{y}{\sqrt{((x-\xi)^2+z^2)}})}{((x-\xi)^2+z^2)^{\frac{3}{2}}} d\xi$$

$$= -\frac{1}{yz}\arctan(\frac{x}{z}) + \frac{1}{yz}\arctan(\frac{x-a}{z}) \tag{6.11}$$

$$+ \frac{x}{z^2\sqrt{x^2+z^2}}\arctan(\frac{y}{\sqrt{x^2+z^2}})$$

$$- \frac{(x-a)}{z^2\sqrt{\beta}}\arctan(\frac{y}{\sqrt{\beta}})$$

$$+ \frac{\sqrt{y^2+z^2}}{yz^2}\arctan(\frac{x}{\sqrt{y^2+z^2}})$$

$$- \frac{\sqrt{y^2+z^2}}{yz^2}\arctan(\frac{x-a}{\sqrt{y^2+z^2}}).$$

Therefore,

$$H_{0,0}(x,y,z)$$

$$= (6.8) + (6.9) + (6.10) + (6.11)\,. \tag{6.12}$$

In (6.8), (6.9), (6.10), and (6.11), we have used the following abbreviated symbols

$$\alpha = (bx-ay)^2 + (bz)^2, \tag{6.13}$$

$$\beta = (x-a)^2 + z^2, \tag{6.14}$$

$$\gamma = (ax+by), \tag{6.15}$$

$$\delta = (ay-bx)\,, \tag{6.16}$$

$$\epsilon = x^2+y^2+z^2. \tag{6.17}$$

6.3 Analytic Evaluation of $H_{1,0,4}$ and $H_{0,1,4}$

Next, let's consider the analytic evaluation of $H_{1,0}(x,y,z)$. By definition, we have

$$
\begin{aligned}
& H_{1,0}(x,y,z) \\
&= \int\int_{\Delta} \frac{\xi^1 \eta^0}{((x-\xi)^2+(y-\eta)^2+z^2)^2} d\sigma \\
&= \int\int_{\Delta} \frac{\xi}{((x-\xi)^2+(y-\eta)^2+z^2)^2} d\sigma.
\end{aligned}
$$

Then,

$$
\begin{aligned}
& xH_{0,0}(x,y,z) - H_{1,0}(x,y,z) \\
&= \int\int_{\Delta} \frac{x}{((x-\xi)^2+(y-\eta)^2+z^2)^2} d\sigma \\
&- \int\int_{\Delta} \frac{\xi}{((x-\xi)^2+(y-\eta)^2+z^2)^2} d\sigma \\
&= \int_0^a \int_0^{\frac{b}{a}\xi} \frac{(x-\xi)^1}{((x-\xi)^2+(y-\eta)^2+z^2)^2} d\eta d\xi.
\end{aligned}
$$

Setting $u = x-\xi$ and $v = y-\eta$, we have

$$
\begin{aligned}
& xH_{0,0}(x,y,z) - H_{1,0}(x,y,z) \\
&= \int_x^{x-a} \int_y^{y-\frac{b}{a}(x-u)} \frac{u}{(u^2+v^2+z^2)^2} dv du \\
&= \int_x^{x-a} [\frac{uv}{2(u^2+z^2)(u^2+v^2+z^2)}]_{v=y}^{y-\frac{b}{a}(x-u)} du \\
&+ \int_x^{x-a} [\frac{u}{2(u^2+z^2)^{\frac{3}{2}}} \arctan(\frac{v}{\sqrt{u^2+z^2}})]_{v=y}^{y-\frac{b}{a}(x-u)} du
\end{aligned}
$$

Thus,

$$
\begin{aligned}
&xH_{0,0}(x,y,z) - H_{1,0}(x,y,z) \\
&= \int_x^{x-a} \frac{u\ (\frac{b}{a}(u-x)+y)}{2(u^2+(\frac{b}{a}(u-x)+y)^2+z^2)(u^2+z^2)} du && (6.18)\\
&- \int_x^{x-a} \frac{u\ y}{2(u^2+y^2+z^2)(u^2+z^2)} du && (6.19)\\
&+ \int_x^{x-a} \frac{u}{2(u^2+z^2)^{\frac{3}{2}}} \arctan(\frac{b(u-x)+ay}{a\sqrt{u^2+z^2}})\ du && (6.20)\\
&- \int_x^{x-a} \frac{u}{2(u^2+z^2)^{\frac{3}{2}}} \arctan(\frac{y}{\sqrt{u^2+z^2}})\ du. && (6.21)
\end{aligned}
$$

The integrations in (6.18), (6.19), (6.20) and (6.21) can be evaluated analytically using the indefinite integrations given in the following.

First, we can use the following indefinite integration to evaluate (6.18).

$$
\begin{aligned}
&\int \frac{u\ (\frac{b}{a}(u-x)+y)}{2(u^2+(\frac{b}{a}(u-x)+y)^2+z^2)(u^2+z^2)} du \\
&= \frac{abz}{2\alpha} \arctan\left(\frac{u}{z}\right) && (6.22)\\
&- \frac{a^2bz^2}{2\alpha\sqrt{\alpha+a^2z^2}} \arctan\left(\frac{a^2u+b^2(u-x)+aby}{a\sqrt{\alpha+a^2z^2}}\right) \\
&- \frac{a\,(bx-ay)}{4\alpha} \log\left(\frac{u^2+z^2}{b^2\,(u-x)^2+2ab\,(u-x)\,y+a^2\epsilon}\right).
\end{aligned}
$$

In here, the definitions of α and ϵ are the same as (6.13) and (6.17).

Second, we can use the following indefinite integration to evaluate (6.19).

$$
\begin{aligned}
&\int \frac{u\ y}{2(u^2+y^2+z^2)(u^2+z^2)} du \\
&= \frac{1}{4y} \log\left(\frac{u^2+z^2}{u^2+y^2+z^2}\right) && (6.23)
\end{aligned}
$$

Next, the following indefinite integration can be used to evaluate (6.20).

$$\begin{aligned}
&\int \frac{u}{2(u^2+z^2)^{\frac{3}{2}}} \arctan(\frac{b(u-x)+ay}{a\sqrt{u^2+z^2}})\ du \\
&= -\frac{abz}{2\alpha} \arctan\left(\frac{u}{z}\right) \\
&+ \frac{b\sqrt{\alpha+a^2z^2}}{2\alpha} \arctan\left(\frac{a^2u+b^2(u-x)+aby}{a\sqrt{\alpha+a^2z^2}}\right) \\
&+ \frac{a(bx-ay)}{4\alpha} \log\left(\frac{u^2+z^2}{b^2\left(u-x\right)^2+2ab\left(u-x\right)y+a^2\epsilon}\right) \\
&- \frac{1}{2\sqrt{u^2+z^2}} \arctan\left(\frac{b(u-x)+ay}{a\sqrt{u^2+z^2}}\right).
\end{aligned} \tag{6.24}$$

Finally, we can use

$$\begin{aligned}
&\int \frac{u}{2(u^2+z^2)^{\frac{3}{2}}} \arctan(\frac{y}{\sqrt{u^2+z^2}})\ du \\
&= -\frac{1}{2\sqrt{u^2+z^2}} \arctan\left(\frac{y}{\sqrt{u^2+z^2}}\right) + \frac{1}{4y}\log\left(1+\frac{y^2}{u^2+z^2}\right),
\end{aligned} \tag{6.25}$$

for the evaluation of (6.21).

Thus, we have

$$\begin{aligned}
& xH_{0,0}(x,y,z) - H_{1,0}(x,y,z) \\
&= \ [(6.22)]_{u=x}^{x-a} - [(6.23)]_{u=x}^{x-a} \\
&+ \ [(6.24)]_{u=x}^{x-a} - [(6.25)]_{u=x}^{x-a}
\end{aligned}$$

by (6.18), (6.19), (6.20), (6.21), (6.22), (6.23), (6.24), and (6.25). Therefore,

$$\begin{aligned}
& H_{1,0}(x,y,z) \\
&= \ xH_{0,0}(x,y,z) \\
&- [(6.22)]_{u=x}^{x-a} + [(6.23)]_{u=x}^{x-a} \\
&- \ [(6.24)]_{u=x}^{x-a} + [(6.25)]_{u=x}^{x-a}.
\end{aligned} \tag{6.26}$$

In order to find the evaluation of $H_{0,1}(x,y,z)$, we follow a similar scheme. By definition, we have

$$H_{0,1}(x,y,z) = \int\int_{\Delta} \frac{\xi}{((x-\xi)^2+(y-\eta)^2+z^2)^2} d\sigma.$$

To evaluate this integration, we evaluate the following integration first.

$$\begin{aligned} & yH_{0,0}(x,y,z) - H_{0,1}(x,y,z) && (6.27)\\ &= \int\int_{\Delta} \frac{y-\eta}{((x-\xi)^2+(y-\eta)^2+z^2)^2} d\sigma && (6.28)\\ &= \int_0^a \int_0^{\frac{b}{a}\xi} \frac{y-\eta}{((x-\xi)^2+(y-\eta)^2+z^2)^2} d\eta d\xi. \end{aligned}$$

Once we have the analytic evaluation of (6.28) , the analytic evaluation of $H_{0,1}(x,y,z)$ can be given by

$$H_{0,1}(x,y,z) = yH_{0,0}(x,y,z) - (6.28)\,.$$

In order to find the analytic integration of (6.28) , set $u = x-\xi$ and $v = y-\eta$. Then, we have

$$\begin{aligned} & yH_{0,0}(x,y,z) - H_{0,1}(x,y,z)\\ &= \int_x^{x-a} \int_y^{y-\frac{b}{a}(x-u)} \frac{v}{(u^2+v^2+z^2)^2} dv du\\ &= -\int_x^{x-a} \frac{a^2}{2(a^2(u^2+y^2+z^2)+b^2(u-x)^2+2aby(u-x))} du && (6.29)\\ &+ \int_x^{x-a} \frac{1}{2(u^2+y^2+z^2)} du && (6.30) \end{aligned}$$

Since the indefinite integration of (6.29) is given by

$$\begin{aligned} & -\int \frac{a^2}{2(a^2(u^2+y^2+z^2)+b^2(u-x)^2+2aby(u-x))} du\\ &= -\frac{a}{2\sqrt{\alpha}} \arctan\left(\frac{a^2u+b^2\,(u-x)+aby}{a\sqrt{\alpha}}\right), \end{aligned}$$

we have

$$
\begin{aligned}
&-\int_{x}^{x-a} \frac{a^2}{2(a^2(u^2+y^2+z^2)+b^2(u-x)^2+2aby(u-x))}du \\
&= \frac{a}{2\sqrt{\alpha+a^2z^2}}\arctan\left(\frac{ax+by}{\sqrt{\alpha+a^2z^2}}\right) \\
&- \frac{a}{2\sqrt{\alpha+a^2z^2}}\arctan\left(\frac{ax+by-a^2-b^2}{\sqrt{\alpha+a^2z^2}}\right).
\end{aligned}
\tag{6.31}
$$

And, since the indefinite integration of (6.30) is given by

$$
-\int \frac{1}{2(u^2+y^2+z^2)}du = -\frac{1}{2\sqrt{y^2+z^2}}\arctan\left(\frac{u}{\sqrt{y^2+z^2}}\right),
$$

we have

$$
\begin{aligned}
&-\int_{x}^{x-a} \frac{1}{2(u^2+y^2+z^2)}du \\
&= \frac{1}{2\sqrt{y^2+z^2}}\arctan\left(\frac{x}{\sqrt{y^2+z^2}}\right) \\
&- \frac{1}{2\sqrt{y^2+z^2}}\arctan\left(\frac{x-a}{\sqrt{y^2+z^2}}\right).
\end{aligned}
\tag{6.32}
$$

Thus, by (6.31) and (6.32) ,

$$
\begin{aligned}
&H_{0,1}(x,y,z) \qquad (6.33)\\
&= yH_{0,0}(x,y,z) \\
&- \frac{a}{2\sqrt{\alpha+a^2z^2}}\arctan\left(\frac{ax+by}{\sqrt{\alpha+a^2z^2}}\right) \\
&+ \frac{a}{2\sqrt{\alpha+a^2z^2}}\arctan\left(\frac{ax+by-a^2-b^2}{\sqrt{\alpha+a^2z^2}}\right) \\
&+ \frac{1}{2\sqrt{y^2+z^2}}\arctan\left(\frac{x}{\sqrt{y^2+z^2}}\right) \\
&- \frac{1}{2\sqrt{y^2+z^2}}\arctan\left(\frac{x-a}{\sqrt{y^2+z^2}}\right).
\end{aligned}
$$

6.4 Analytic Evaluation of $H_{1,1,4}$

In this section, we consider the analytic evaluation of $H_{1,1}(x,y,z)$. For that, we use the following identity.

$$\begin{aligned}
&\int\int_{\Delta} \frac{(x-\xi)(y-\eta)}{((x-\xi)^2+(y-\eta)^2+z^2)^2}d\sigma \qquad (6.34)\\
&=\int\int_{\Delta} \frac{xy}{((x-\xi)^2+(y-\eta)^2+z^2)^2}d\sigma\\
&-\int\int_{\Delta} \frac{x\eta}{((x-\xi)^2+(y-\eta)^2+z^2)^2}d\sigma\\
&-\int\int_{\Delta} \frac{y\xi}{((x-\xi)^2+(y-\eta)^2+z^2)^2}d\sigma\\
&+\int\int_{\Delta} \frac{\xi\eta}{((x-\xi)^2+(y-\eta)^2+z^2)^2}d\sigma\\
&= xyH_{0,0} - xH_{0,1} - yH_{1,0} + H_{1,1}.
\end{aligned}$$

Since we know the analytic evaluations of $H_{0,0}(x,y,z)$, $H_{1,0}(x,y,z)$ and $H_{0,1}(x,y,z)$ by (6.12), (6.26), and (6.33), it suffices to find the analytic evaluation of (6.34) to find the analytic evaluation of $H_{1,1}(x,y,z)$. Once we know the analytic evaluation of (6.34), the analytic evaluation of $H_{1,1}(x,y,z)$ can be found using the following identity.

$$\begin{aligned}
&H_{1,1}(x,y,z) \qquad (6.35)\\
&= (6.34) - xyH_{0,0}(x,y,z) + xH_{0,1}(x,y,z) + yH_{1,0}(x,y,z)
\end{aligned}$$

To evaluate

$$\begin{aligned}
&\int\int_{\Delta} \frac{(x-\xi)(y-\eta)}{((x-\xi)^2+(y-\eta)^2+z^2)^2}d\sigma\\
&=\int_0^a\int_0^{\frac{b}{a}\xi} \frac{(x-\xi)(y-\eta)}{((x-\xi)^2+(y-\eta)^2+z^2)^2}d\eta d\xi,
\end{aligned}$$

set $u = x - \xi$ and $v = y - \eta$. Then, we have

$$\int\int_{\Delta} \frac{(x-\xi)(y-\eta)}{((x-\xi)^2+(y-\eta)^2+z^2)^2} d\sigma \tag{6.36}$$
$$= \int_x^{x-a} \int_y^{y-\frac{b}{a}(x-u)} \frac{uv}{(u^2+v^2+z^2)^2} dvdu$$
$$= \int_x^{x-a} [-\frac{u}{2(u^2+v^2+z^2)}]_{v=y}^{y-\frac{b(x-u)}{a}} du$$
$$= -\int_x^{x-a} \frac{u}{2(u^2+(y-\frac{b(x-u)}{a})^2+z^2)} du \tag{6.37}$$
$$+ \int_x^{x-a} \frac{u}{2(u^2+y^2+z^2)} du \tag{6.38}$$

To evaluate (6.37) analytically, we use the following indefinite integration.

$$-\int \frac{u}{2(u^2+(y-\frac{b(x-u)}{a})^2+z^2)} du$$
$$= \frac{ab\,(ay-bx)}{2\,(a^2+b^2)\sqrt{\alpha+a^2z^2}} \arctan\left(\frac{a^2u+b^2\,(u-x)+aby}{a\sqrt{\alpha+a^2z^2}}\right)$$
$$- \frac{a^2}{4\,(a^2+b^2)} \log\left(b^2\,(u-x)^2+2ab\,(u-x)\,y+a^2\left(u^2+y^2+z^2\right)\right)$$

Thus, we have

$$-\int_x^{x-a} \frac{u}{2(u^2+(y-\frac{b(x-u)}{a})^2+z^2)} du$$
$$= \frac{ab\,(ay-bx)}{2\,(a^2+b^2)\sqrt{\alpha+a^2z^2}} \arctan\left(\frac{ax+by-(a^2+b^2)}{\sqrt{\alpha+a^2z^2}}\right) \tag{6.39}$$
$$- \frac{ab\,(ay-bx)}{2\,(a^2+b^2)\sqrt{\alpha+a^2z^2}} \arctan\left(\frac{ax+\ by}{\sqrt{\alpha+a^2z^2}}\right)$$
$$+ \frac{a^2}{4\,(a^2+b^2)} \log\left(\frac{(u^2+y^2+z^2)}{\left((a-x)^2\ +(b-y)^2\ +z^2\right)}\right).$$

To evaluate (6.38) analytically, we use the following indefinite integration.

$$-\int \frac{u}{2(u^2+y^2+z^2)} du$$
$$= -\frac{1}{4} \log\left(u^2+y^2+z^2\right).$$

Thus, we have

$$
\begin{aligned}
& -\int_x^{x-a} \frac{u}{2(u^2+y^2+z^2)} du \\
& = -\frac{1}{4}\log(\frac{(a-x)^2+y^2+z^2}{x^2+y^2+z^2}).
\end{aligned} \tag{6.40}
$$

By (6.39) and (6.40), we have

$$
\begin{aligned}
& \int\int_{\Delta} \frac{(x-\xi)(y-\eta)}{((x-\xi)^2+(y-\eta)^2+z^2)^2} d\sigma \\
& = \frac{ab(ay-bx)}{2(a^2+b^2)\sqrt{\alpha+a^2z^2}} \arctan(\frac{ax+by-(a^2+b^2)}{\sqrt{\alpha+a^2z^2}}) \\
& - \frac{ab(ay-bx)}{2(a^2+b^2)\sqrt{\alpha+a^2z^2}} \arctan(\frac{ax+by}{\sqrt{\alpha+a^2z^2}}) \\
& + \frac{a^2}{4(a^2+b^2)} \log(\frac{(x^2+y^2+z^2)}{(a-x)^2+(b-y)^2+z^2}) \\
& + \frac{1}{4}\log(\frac{(a-x)^2+y^2+z^2}{x^2+y^2+z^2}),
\end{aligned} \tag{6.41}
$$

where the definition of α follows that of (6.13).

Therefore, by (6.35) and (6.41), we have

$$
\begin{aligned}
& H_{1,1}(x,y,z) \\
& = xH_{0,1}(x,y,z) + yH_{1,0}(x,y,z) - xyH_{0,0}(x,y,z) \\
& + \frac{ab(ay-bx)}{2(a^2+b^2)\sqrt{\alpha+a^2z^2}} \arctan(\frac{ax+by-(a^2+b^2)}{\sqrt{\alpha+a^2z^2}}) \\
& - \frac{ab(ay-bx)}{2(a^2+b^2)\sqrt{\alpha+a^2z^2}} \arctan(\frac{ax+by}{\sqrt{\alpha+a^2z^2}}) \\
& + \frac{a^2}{4(a^2+b^2)} \log(\frac{(x^2+y^2+z^2)}{(a-x)^2+(b-y)^2+z^2}) \\
& + \frac{1}{4}\log(\frac{(a-x)^2+y^2+z^2}{x^2+y^2+z^2}).
\end{aligned} \tag{6.42}
$$

6.5 Analytic Evaluation of $H_{m,n}$ for General m and n

In general, it is not possible to find the analytic evaluation of $H_{m,n}(x,y,z)$ for all $m,n = 0,1,2,\ldots$, but we can find most of them. As a part of our effort to find the analytic evaluation of $H_{m,n}(x,y,z)$ for general $m,n \in N_0$, the set of non-negative integers, we prove the following lemma.

Lemma 6.1. *Suppose Δ is a rectangular triangle and ν the outward normal vector at a point on the boundary $\partial\Delta$ of the triangle. See Figure* 6.3. *Then, we have*

$$\int_{\partial\Delta} \frac{\xi^{m-1}\eta^n}{(x-\xi)^2+(y-\eta)^2+z^2}\cos(\nu,\xi)dl \tag{6.43}$$
$$= (m-1)H_{m-2,n,2}(x,y,z) + 2xH_{m-1,n}(x,y,z) - 2H_{m,n}(x,y,z),$$

and

$$\int_{\partial\Delta} \frac{\xi^{m}\eta^{n-1}}{(x-\xi)^2+(y-\eta)^2+z^2}\cos(\nu,\eta)dl \tag{6.44}$$
$$= (n-1)H_{m,n-2,2}(x,y,z) + 2yH_{m,n-1}(x,y,z) - 2H_{m,n}(x,y,z).$$

Proof. First, in order to prove (6.43) , we start with the following identity.

$$\begin{aligned}
&\frac{d}{d\xi}\frac{\xi^{m-1}\eta^n}{(x-\xi)^2+(y-\eta)^2+z^2} \\
&= \frac{(m-1)\xi^{m-2}\eta^n}{(x-\xi)^2+(y-\eta)^2+z^2} + \frac{2(x-\xi)\xi^{m-1}\eta^n}{((x-\xi)^2+(y-\eta)^2+z^2)^2}.
\end{aligned}$$

Then, we have

$$\int\int_{\Delta} \frac{d}{d\xi} \frac{\xi^{m-1}\eta^{n}}{(x-\xi)^2+(y-\eta)^2+z^2} d\sigma(\xi,\eta) \tag{6.45}$$

$$= (m-1)\int\int_{\Delta} \frac{\xi^{m-2}\eta^{n}}{(x-\xi)^2+(y-\eta)^2+z^2} d\sigma(\xi,\eta)$$

$$+ 2\int\int_{\Delta} \frac{(x-\xi)\xi^{m-1}\eta^{n}}{((x-\xi)^2+(y-\eta)^2+z^2)^2} d\sigma(\xi,\eta)$$

$$= (m-1)\int\int_{\Delta} \frac{\xi^{m-2}\eta^{n}}{(x-\xi)^2+(y-\eta)^2+z^2} d\sigma(\xi,\eta) \tag{6.46}$$

$$+ 2x\int\int_{\Delta} \frac{\xi^{m-1}\eta^{n}}{((x-\xi)^2+(y-\eta)^2+z^2)^2} d\sigma(\xi,\eta)$$

$$- 2\int\int_{\Delta} \frac{\xi^{m}\eta^{n}}{((x-\xi)^2+(y-\eta)^2+z^2)^2} d\sigma(\xi,\eta).$$

Applying Gauss's divergence theorem to (6.45), we have

$$\int\int_{\Delta} \frac{d}{d\xi} \frac{\xi^{m-1}\eta^{n}}{(x-\xi)^2+(y-\eta)^2+z^2} d\sigma(\xi,\eta) \tag{6.47}$$

$$= \int_{\partial\Delta} \frac{\xi^{m-1}\eta^{n}}{(x-\xi)^2+(y-\eta)^2+z^2} \nu_\xi dl$$

where $\nu = (\nu_\xi, \nu_\eta)$ is the normal vector at a point on $\partial\Delta$, the boundary of the triangle Δ. Thus, by combining (6.46) and (6.47), we can find

$$\int_{\partial\Delta} \frac{\xi^{m-1}\eta^{n}}{(x-\xi)^2+(y-\eta)^2+z^2} \nu_\xi dl$$

$$= (m-1)H_{m-2,n,2}(x,y,z) + 2xH_{m-1,n}(x,y,z) - 2H_{m,n}(x,y,z).$$

Similarly, in order to prove (6.44), we use the following identity.

$$\frac{d}{d\eta} \frac{\xi^{m}\eta^{n-1}}{(x-\xi)^2+(y-\eta)^2+z^2}$$

$$= \frac{(n-1)\xi^{m}\eta^{n-2}}{(x-\xi)^2+(y-\eta)^2+z^2} + \frac{2(y-\eta)\xi^{m}\eta^{n-1}}{((x-\xi)^2+(y-\eta)^2+z^2)^2}.$$

Thus, we have

$$
\begin{aligned}
&\int\int_{\Delta} \frac{d}{d\eta} \frac{\xi^m \eta^{n-1}}{(x-\xi)^2+(y-\eta)^2+z^2} d\sigma(\xi,\eta) \\
&= (n-1)\int\int_{\Delta} \frac{\xi^m \eta^{n-2}}{(x-\xi)^2+(y-\eta)^2+z^2} d\sigma(\xi,\eta) \\
&+ 2\int\int_{\Delta} \frac{(y-\eta)\xi^m \eta^{n-1}}{((x-\xi)^2+(y-\eta)^2+z^2)^2} d\sigma(\xi,\eta) \\
&= (n-1)\int\int_{\Delta} \frac{\xi^m \eta^{n-2}}{(x-\xi)^2+(y-\eta)^2+z^2} d\sigma(\xi,\eta) \\
&+ 2y\int\int_{\Delta} \frac{\xi^m \eta^{n-1}}{((x-\xi)^2+(y-\eta)^2+z^2)^2} d\sigma(\xi,\eta) \\
&- 2\int\int_{\Delta} \frac{\xi^m \eta^{n}}{((x-\xi)^2+(y-\eta)^2+z^2)^2} d\sigma(\xi,\eta).
\end{aligned} \tag{6.48}
$$

Using Gauss's divergence theorem once again, we have

$$
\begin{aligned}
&\int\int_{\Delta} \frac{d}{d\eta} \frac{\xi^m \eta^{n-1}}{(x-\xi)^2+(y-\eta)^2+z^2} d\sigma(\xi,\eta) \\
&= \int_{\partial\Delta} \frac{\xi^m \eta^{n-1}}{(x-\xi)^2+(y-\eta)^2+z^2} \nu_\eta dl,
\end{aligned} \tag{6.49}
$$

where $\nu = (\nu_\xi, \nu_\eta)$ is the normal vector at a point on $\partial\Delta$, the boundary of the triangle Δ. Therefore, by combining (6.48) and (6.49), we can prove

$$
\begin{aligned}
&\int_{\partial\Delta} \frac{\xi^m \eta^{n-1}}{(x-\xi)^2+(y-\eta)^2+z^2} \nu_\eta dl \\
&= (n-1)H_{m,n-2,2}(x,y,z) + 2yH_{m,n-1}(x,y,z) - 2H_{m,n}(x,y,z).
\end{aligned}
$$

□

By the above lemma, we have

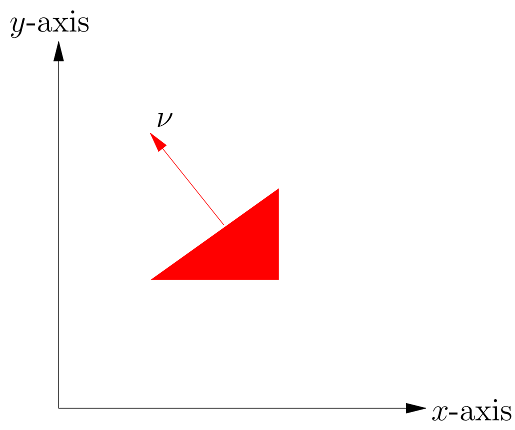

Figure 6.3: Normal vector on the boundary of the triangle Δ.

$$\begin{aligned} &H_{m,n}(x,y,z) \\ &= \frac{1}{2}\ (m-1)H_{m-2,n,2}(x,y,z) +\ xH_{m-1,n}(x,y,z) \\ &- \frac{1}{2}\int_{\partial\Delta} \frac{\xi^{m-1}\eta^n}{(x-\xi)^2+(y-\eta)^2+z^2}\nu_\xi dl \end{aligned} \tag{6.50}$$

and

$$\begin{aligned} &H_{m,n}(x,y,z) \\ &= \frac{1}{2}\ (n-1)H_{m,n-2,2}(x,y,z) +\ yH_{m,n-1}(x,y,z) \\ &- \frac{1}{2}\int_{\partial\Delta} \frac{\xi^{m}\eta^{n-1}}{(x-\xi)^2+(y-\eta)^2+z^2}\nu_\eta dl\ . \end{aligned} \tag{6.51}$$

for all $m, n \in N$. In general, the analytic evaluation of $H_{m,n}(x,y,z)$ for $m \geq 2$ or $n \geq 2$ can be simplified by using (6.50) and (6.51).

In order to show the use of these two formulas, we will find an analytic evaluation of $H_{2,0}(x,y,z)$ and $H_{0,2}(x,y,z)$. By use of (6.50) and (6.51) ,we have

$$\begin{aligned} &H_{2,0}(x,y,z) \\ &= \frac{1}{2}\ H_{0,0,2}(x,y,z) +\ xH_{1,0}(x,y,z) \\ &- \frac{1}{2}\int_{\partial\Delta} \frac{\xi^1}{(x-\xi)^2+(y-\eta)^2+z^2}\nu_\xi dl\ , \end{aligned} \tag{6.52}$$

and

$$\begin{aligned} &H_{0,2}(x,y,z) \\ &= \frac{1}{2}\ (n-1)H_{0,0,2}(x,y,z) +\ yH_{0,1}(x,y,z) \\ &- \frac{1}{2}\int_{\partial\Delta} \frac{\eta^1}{(x-\xi)^2+(y-\eta)^2+z^2}\nu_\eta dl\ . \end{aligned} \tag{6.53}$$

Thus, by (6.50) and (6.51) , we can evaluate both $H_{2,0}(x,y,z)$ and $H_{0,2}(x,y,z)$ analytically if we can find an analytic evaluation of the following integrations.

$$\int_{\partial\Delta} \frac{\xi}{(x-\xi)^2+(y-\eta)^2+z^2}\nu_\xi dl. \tag{6.54}$$

$$\int_{\partial\Delta} \frac{\eta}{(x-\xi)^2+(y-\eta)^2+z^2}\nu_\eta dl. \tag{6.55}$$

$$H_{0,0,2}(x,y,z) \tag{6.56}$$

The analytic evaluation of (6.54) can be simplified by using the assumption that the integration domain $\partial\Delta$ is the boundary of the rectangular triangle as given in Figure 5.1. Thanks to this assumption, we can assume that ν_ξ is constant along each edge of the triangle. That is,

$$\begin{aligned}
&\int_{\partial\Delta} \frac{\xi}{(x-\xi)^2+(y-\eta)^2+z^2}\nu_\xi dl \\
&= \nu_\xi \int_{e_d} \frac{\xi}{(x-\xi)^2+(y-\eta)^2+z^2} dl \\
&+ \nu_\xi \int_{e_v} \frac{\xi}{(x-\xi)^2+(y-\eta)^2+z^2} dl \\
&+ \nu_\xi \int_{e_h} \frac{\xi}{(x-\xi)^2+(y-\eta)^2+z^2} dl,
\end{aligned} \tag{6.57}$$

where e_h, e_v, and e_d are horizontal, vertical, and diagonal edge of the triangle Δ, respectively. This can be further simplified by using the facts that $\nu_\xi = 1$ on e_v and $\nu_\xi = 0$ on e_h. Thus, (6.57) becomes

$$\begin{aligned}
&\int_{\partial\Delta} \frac{\xi}{(x-\xi)^2+(y-\eta)^2+z^2}\nu_\xi dl \\
&= \nu_\xi \int_{e_d} \frac{\xi}{(x-\xi)^2+(y-\eta)^2+z^2} dl \qquad (6.58)\\
&+ \int_{e_v} \frac{\xi}{(x-\xi)^2+(y-\eta)^2+z^2} dl. \qquad (6.59)
\end{aligned}$$

The integrations in (6.58) and (6.59) can be evaluated analytically.

The analytic evaluation of (6.55) can be found using similar argument under the same assumption on the integration domain $\partial\Delta$. That is,

$$\begin{aligned}
&\int_{\partial\Delta} \frac{\eta}{(x-\xi)^2+(y-\eta)^2+z^2}\nu_\eta dl \\
&= \nu_\eta \int_{e_d} \frac{\eta}{(x-\xi)^2+(y-\eta)^2+z^2} dl \\
&+ \nu_\eta \int_{e_v} \frac{\eta}{(x-\xi)^2+(y-\eta)^2+z^2} dl \\
&+ \nu_\eta \int_{e_h} \frac{\eta}{(x-\xi)^2+(y-\eta)^2+z^2} dl.
\end{aligned}$$

Using the facts that $\nu_\eta = 0$ on e_v and $\nu_\eta = -1$ on e_h, we can further simplify this into

$$\int_{\partial\Delta} \frac{\eta}{(x-\xi)^2+(y-\eta)^2+z^2}\nu_\eta dl$$

$$= \nu_\eta \int_{e_d} \frac{\eta}{(x-\xi)^2+(y-\eta)^2+z^2} dl \tag{6.60}$$

$$- \int_{e_h} \frac{\eta}{(x-\xi)^2+(y-\eta)^2+z^2} dl. \tag{6.61}$$

The integrations in (6.60) and (6.61) can be evaluated analytically.

Next, we discuss the analytic evaluation of $H_{0,0,2}$. By definition, we have

$$H_{0,0,2}(x,y,z) = \int\int_\Delta \frac{1}{(x-\xi)^2+(y-\eta)^2+z^2} d\sigma(\xi,\eta)$$

Setting $u = \xi - x$ and $v = \eta - y$, we have

$$H_{0,0,2}(x,y,z) = \int\int_\Sigma \frac{1}{u^2+v^2+z^2} d\sigma(u,v) \tag{6.62}$$

The integration domain Σ is shown in Figure 6.4 which we can get after translating the original integration domain Δ by (x,y). Since there is no rotation involved, Σ always has the vertical and horizontal edges. In order to evaluate this integration analytically, we split the integration (6.62) into three parts as shown in Figure 6.5.

$$H_{0,0,2}(x,y,z)$$

$$= \int\int_\Sigma \frac{1}{u^2+v^2+z^2} d\sigma(u,v) \tag{6.63}$$

$$= sign(\Sigma_d) \int\int_{\Sigma_d} \frac{1}{u^2+v^2+z^2} d\sigma(u,v) \tag{6.64}$$

$$+ sign(\Sigma_h) \int\int_{\Sigma_h} \frac{1}{u^2+v^2+z^2} d\sigma(u,v) \tag{6.65}$$

$$+ sign(\Sigma_v) \int\int_{\Sigma_v} \frac{1}{u^2+v^2+z^2} d\sigma(u,v) \tag{6.66}$$

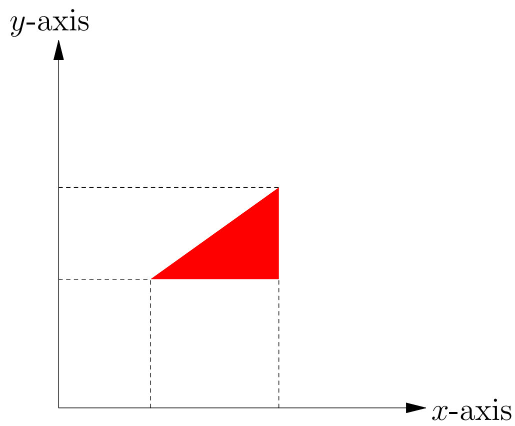

Figure 6.4: Translating Integral Domain

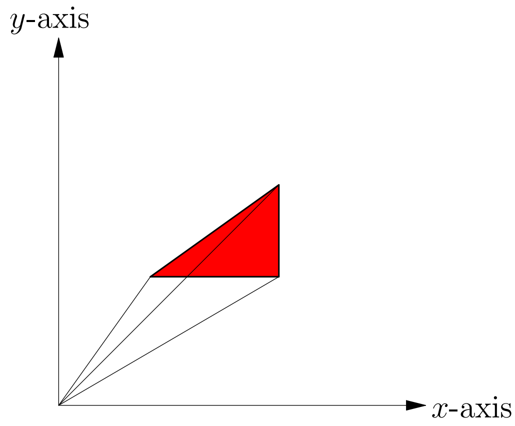

Figure 6.5: Splitting Integral Domain

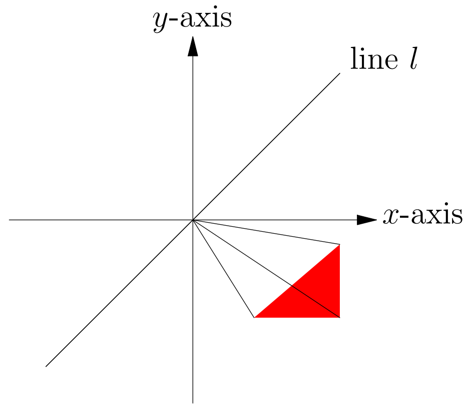

Figure 6.6: Partition of R^2 to decide the values of $sign(\sum_h)$, $sign(\sum_v)$,and $sign(\sum_d)$.

In here, Σ_d is the triangle formed by connecting $(0, 0)$ and the two vertices of the hypotenuse of the right triangle Σ. The triangles Σ_v and Σ_h are formed similarly by connecting $(0, 0)$ and the vertical and horizontal edges of the triangle Σ respectively. The values of $sign(\Sigma_h)$, $sign(\Sigma_v)$, and $sign(\Sigma_d)$ take on either $-1, 0$ or 1. They are determined so as to hold the equality in (6.63). Table (6.1) shows the algorithm to determine these values.

If we explain the symbols used in Table (6.1), $(0, \infty)_x$ and $(0, \infty)_y$ denote positive x-axis and positive y-axis, respectively. The line l which passes through $(0, 0)$ has the same the slope as the slope of the hypotenuse of the triangle Σ. We use the symbol l^- to denote the line l which lies in the third quadrant of R^2. For the determination of region A_1, B_1, A_3, and B_3, refer to Figure 6.6. The values of $sign(\Sigma_h)$, $sign(\Sigma_v)$, and $sign(\Sigma_d)$ changes only when certain event happens. For instance, the value of $sign(\Sigma_v)$ changes from -1 to 1 since the vertical edge of the triangle Σ crosses y-axis. Similarly, the values of $sign(\Sigma_h)$ and $sign(\Sigma_d)$ change from

Condition	$sign(\Sigma_h)$	$sign(\Sigma_v)$	$sign(\Sigma_d)$
$\Sigma \subset Q2$	-1	-1	1
$(0,\infty)_y \cap \Sigma \neq \emptyset$	-1	1	1
$\Sigma \subset A_1$	-1	1	1
$\Sigma \subset B_1$	-1	1	-1
$(0,\infty)_x \cap \Sigma \neq \emptyset$	1	1	-1
$\Sigma \subset Q4$	1	1	-1
$\Sigma \subset A_3$	1	-1	-1
$l^- \cap \Sigma \neq \emptyset$	1	-1	1
$\Sigma \subset B_3$	1	-1	1
$(0,0) \in \Sigma$	1	1	1

Table 6.1: The algorithm to determine the values of $sign(S_h), sign(S_v)$, and $sign(S_d)$

-1 to 1 when the horizontal edge of the triangle Σ crosses x-axis and the hypotenuse of the triangle Σ crosses the line l, respectively.

We first consider the integration over Σ_d in order to evaluate $H_{0,0,2}(x, y, z)$. Let's suppose $p(\theta)$ is a point on the hypotenuse whose angle is θ with respect to x axes and $v_1 = (x_1, y_1)$ and $v_2 = (x_2, y_2)$ are the two vertices of the hypotenuse of the right triangle Σ. The angle θ_1, and θ_2 are the angles which v_1 and v_2 make with respect to x axes respectively. Define $r(\theta)$ to be a distance from the origin to $p(\theta)$. See Figure 6.7. Then, by setting $u = r\cos(\theta)$ and $v = r\sin(\theta)$, we have

$$\begin{aligned}
&\int\int_{\Sigma_d} \frac{1}{u^2+v^2+z^2} d\sigma(u,v) \qquad (6.67)\\
&= \int_{\theta_1}^{\theta_2}\int_0^{r(\theta)} \frac{r}{r^2+z^2} dr d\theta\\
&= \frac{1}{2}\int_{\theta_1}^{\theta_2} [\log(r^2+z^2)]_{r=0}^{r(\theta)} d\theta\\
&= \int_{\theta_1}^{\theta_2} (\frac{1}{2}\log(r(\theta)^2+z^2) - \log(z)) d\theta\\
&= \frac{1}{2}\int_{\theta_1}^{\theta_2} \log(r(\theta)^2+z^2) d\theta - \log(z)(\theta_2-\theta_1). \qquad (6.68)
\end{aligned}$$

In order to find the analytic evaluation of (6.67), it suffices to find the analytic evaluation of

$$\frac{1}{2}\int_{\theta_1}^{\theta_2} \log(r(\theta)^2+z^2) d\theta. \qquad (6.69)$$

First, we define $s(\theta)$ as

$$s(\theta) = \frac{\|v_1 - p(\theta)\|}{\|v_1 - v_2\|}.$$

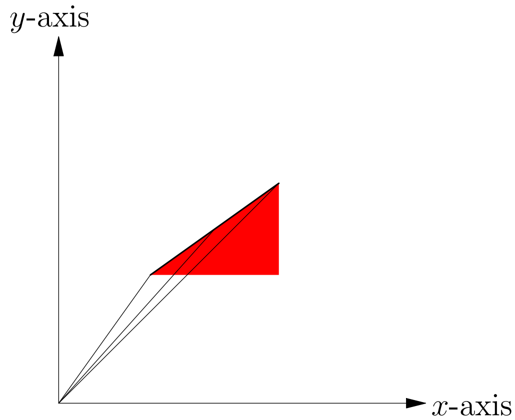

Figure 6.7: Illustration of $r(\theta)$

Then, we have

$$p(\theta) = (x_1 + s(\theta)(x_2 - x_1), y_1 + s(\theta)(y_2 - y_1)). \tag{6.70}$$

For all points $p(\theta)$ on the hypotenuse, the value of $s(\theta)$ is between 0 and 1. By (6.70), we have

$$\tan(\theta) = \frac{y_1 + s(\theta)(y_2 - y_1)}{x_1 + s(\theta)(x_2 - x_1)},$$

and

$$\theta = \arctan(\frac{y_1 + s(\theta)(y_2 - y_1)}{x_1 + s(\theta)(x_2 - x_1)}).$$

Thus,

$$d\theta = \frac{x_1 y_2 - x_2 y_1}{r(\theta)^2} ds \tag{6.71}$$

We can also derive the following relation between $r(\theta)$ and $s(\theta)$.

$$r(\theta)^2 = [(x_1 + s(\theta)(x_2 - x_1))^2 + (y_1 + s(\theta)(y_2 - y_1))^2] \tag{6.72}$$

By (6.72) and (6.71), the integration (6.69) becomes

$$
\begin{aligned}
&\frac{1}{2}\int_{\theta_1}^{\theta_2} \log(r(\theta)^2 + z^2)d\theta \\
&= \frac{1}{2}\int_{\theta_1}^{\theta_2} \log(\ (x_1 + s(\theta)(x_2 - x_1))^2 + (y_1 + s(\theta)(y_2 - y_1))^2 + z^2)d\theta \\
&= \frac{(x_1y_2 - x_2y_1)}{2}\int_0^1 \frac{\log(\ (x_1 + s(x_2 - x_1))^2 + (y_1 + s(y_2 - y_1))^2 + z^2)}{(x_1 + s(x_2 - x_1))^2 + (y_1 + s(y_2 - y_1))^2} ds \\
&= \frac{(x_1y_2 - x_2y_1)}{2}\int_0^1 \frac{\log(\ \alpha s^2 + \beta s + \gamma\ )}{\alpha s^2 + \beta s + \gamma} ds
\end{aligned} \tag{6.73}
$$

where

$$
\begin{aligned}
\alpha &= (x_2 - x_1)^2 + (y_2 - y_1)^2, \\
\beta &= 2\left(x_1(x_2 - x_1) + y_1(y_2 - y_1)\right), \\
\gamma &= x_1^2 + y_1^2 + z^2.
\end{aligned}
$$

The functional behavior of the integrand of (6.73) can be understood by considering the discriminant D and the minimum value of the quadratic equation $\alpha s^2 + \beta s + \gamma$. We first consider the discriminant D.

$$
\begin{aligned}
\frac{D}{4} &= (\frac{\beta}{2})^2 - \alpha\gamma \\
&= \langle v_1, v_2 - v_1\rangle^2 - \|v_1 - v_2\|^2 (\|v_1\|^2 + z^2) \\
&= (\ \langle v_1, v_2\rangle\ - \|v_1\|^2)^2 - \|v_1 - v_2\|^2 \|v_1\|^2 - \|v_1 - v_2\|^2 z^2 \\
&= (\ \langle v_1, v_2\rangle\ - \|v_1\|^2)^2 - \ \left(\|v_1\|^2 + \|v_2\|^2 - 2\langle v_1, v_2\rangle\right)\ \|v_1\|^2 \\
&- \|v_1 - v_2\|^2 z^2 \\
&= \ \langle v_1, v_2\rangle^2 - \|v_2\|^2 \|v_1\|^2\ - \|v_1 - v_2\|^2\ z^2
\end{aligned}
$$

That is,

$$\frac{D}{4} = (x_1x_2 + y_1y_2)^2 - (x_1^2 + y_1^2)(x_2^2 + y_2^2) - \|v_1 - v_2\|^2 \ z^2$$
$$= -(x_1y_2 - y_1x_2)^2 - \|v_1 - v_2\|^2 \ z^2. \tag{6.74}$$

Since $\|v_1 - v_2\|^2 \ z^2 > 0$, we have $\frac{D}{4} < 0$. Thus, we can say

$$\alpha s^2 + \beta s + \gamma > 0 \tag{6.75}$$

for all $s \in [0, 1]$ because $\alpha > 0$, $\gamma > 0$.

By setting

$$v_1 = (x_1, y_1)$$
$$= (r_1 \cos(\theta_1), r_1 \sin(\theta_1)),$$
$$v_2 = (x_2, y_2)$$
$$= (r_2 \cos(\theta_2), r_2 \sin(\theta_2)),$$

the minimum value of $\alpha s^2 + \beta s + \gamma$ is given by

$$\frac{4\alpha\gamma - \beta^2}{4\alpha} = \frac{(x_1y_2 - y_1x_2)^2}{\|v_1 - v_2\|^2} + \ z^2 \tag{6.76}$$
$$= \frac{(r_1r_2)^2(\cos(\theta_1)\sin(\theta_2) - \ \sin(\theta_1) \ \cos(\theta_2))^2}{\|v_1 - v_2\|^2} + \ z^2$$
$$= \frac{(r_1r_2)^2 \ \sin^2(\theta_2 \ - \theta_1)}{\|v_1 - v_2\|^2} + \ z^2 \geq \ z^2$$

By (6.76), the minimum of the quadratic equation $\alpha s^2 + \beta s + \gamma$ gets close to z^2 as the difference between angles of the vertices v_1 and v_2 gets small. Thus, we can say the integrand

$$\frac{\log(\ \alpha s^2 + \beta s + \gamma \ )}{\alpha s^2 + \beta s + \gamma} \tag{6.77}$$

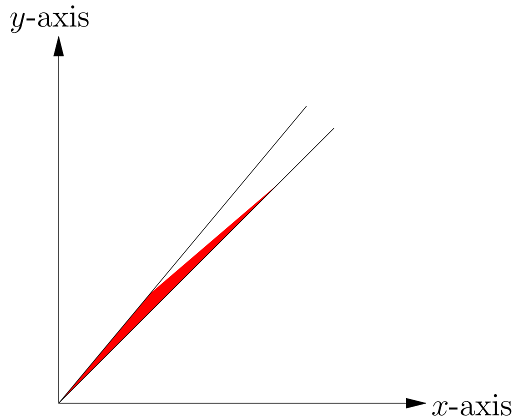

Figure 6.8: Triangle with low aspect ratio

in (6.73) is smooth by (6.75), but gets increasingly ill-behaved as the aspect ratio of the triangle Σ_d gets small since $\frac{\log(x)}{x} \to -\infty$ as x approaches to 0. See Figure 6.8 and 6.9.

In order to consider the analytic evaluation of the integration in (6.73), we use the complex number

$$\omega = \frac{-\beta + \sqrt{\beta^2 - 4\alpha\gamma}}{2\alpha}.$$

Since the discriminant $D < 0$ by (6.74) and α, β, and γ are all reals, we have

$$\alpha s^2 + \beta s + \gamma = \alpha(s - \omega)(s - \overline{\omega}).$$

Then, the integrand of (6.77) becomes

$$\begin{aligned} &\frac{\log(\ \alpha s^2 + \beta s + \gamma\ )}{\alpha s^2 + \beta s + \gamma} \\ &= \frac{\log(\alpha) + \log(s - \omega) + \log(s - \overline{\omega}.)}{\alpha(s - \omega)(s - \overline{\omega}).} \end{aligned}$$

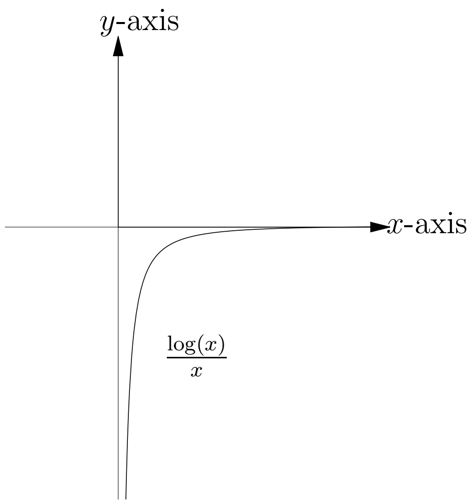

Figure 6.9: Plot of the function $\frac{\log(x)}{x}$

Thus,

$$\int_0^1 \frac{\log(\ \alpha s^2 + \beta s + \gamma\ )}{\alpha s^2 + \beta s + \gamma} ds$$
$$= \int_0^1 \frac{\log(\alpha) + \log(s - \omega) + \log(s - \overline{\omega}.)}{\alpha s^2 + \beta s + \gamma} ds$$
$$= \log(\alpha) \int_0^1 \frac{1}{\alpha s^2 + \beta s + \gamma} ds \tag{6.78}$$
$$+ \frac{1}{\alpha} \int_0^1 \frac{\log(s - \omega)}{(s - \omega)(s - \overline{\omega})} ds \tag{6.79}$$
$$+ \frac{1}{\alpha} \int_0^1 \frac{\log(s - \overline{\omega})}{(s - \omega)(s - \overline{\omega})} ds\ . \tag{6.80}$$

We can evaluate (6.78) analytically, since

$$\int \frac{1}{\alpha s^2 + \beta s + \gamma} ds$$
$$= \frac{2}{\sqrt{-\beta^2 + 4\alpha\gamma}} \arctan\left(\frac{2s\alpha + \beta}{\sqrt{-\beta^2 + 4\alpha\gamma}}\right). \tag{6.81}$$

We can also evaluate both (6.79) and (6.79) analytically, since

$$\begin{aligned}
&\int \frac{\log(s-\omega)}{(s-\omega)(s-\overline{\omega})}ds \\
&= \frac{\log^2(s-w)}{2(w-\overline{w})} - \frac{1}{w-\overline{w}}\log(s-w)\log\left(1+\frac{s-w}{w-\overline{w}}\right) \\
&+ \frac{1}{w-\overline{w}}\,\mathrm{polylog}\left(2,-\frac{s-w}{w-\overline{w}}\right) \\
&= \frac{\log^2(s-w)}{4i\,\mathrm{Im}\,(w)} - \frac{1}{2i\,\mathrm{Im}\,(w)}\log(s-w)\log\left(1+\frac{s-w}{2i\,\mathrm{Im}\,(w)}\right) \\
&+ \frac{1}{2i\,\mathrm{Im}\,(w)}\,\mathrm{polylog}\left(2,-\frac{s-w}{2i\,\mathrm{Im}\,(w)}\right),
\end{aligned} \tag{6.82}$$

and

$$\begin{aligned}
&\int \frac{\log(s-\overline{\omega})}{(s-\omega)(s-\overline{\omega})}ds \\
&= \frac{\log^2(s-\overline{w})}{2(\overline{w}-w)} - \frac{1}{\overline{w}-w}\log(s-\overline{w})\log\left(1+\frac{s-\overline{w}}{\overline{w}-w}\right) \\
&+ \frac{1}{\overline{w}-w}\,\mathrm{polylog}\left(2,-\frac{s-\overline{w}}{\overline{w}-w}\right) \\
&= \frac{\log^2(s-\overline{w})}{4i\,\mathrm{Im}\,(w)} + \frac{1}{2i\,\mathrm{Im}\,(w)}\log(s-\overline{w})\log\left(1-\frac{s-\overline{w}}{2i\,\mathrm{Im}\,(w)}\right) \\
&- \frac{1}{2i\,\mathrm{Im}\,(w)}\,\mathrm{polylog}\left(2,\frac{s-\overline{w}}{2i\,\mathrm{Im}\,(w)}\right).
\end{aligned} \tag{6.83}$$

In here, we used the function $\mathrm{polylog}(2,z)$ called dilogarithm.

The definition of dilogarithm is given by

$$\mathrm{polylog}(2,z) = \sum_{n=1}^{\infty}\frac{z^n}{n^2}.$$

The dilogarithm function is absolutely convergent in the unit disk and we can use the following functional relationship to evaluate the dilogarithm in the entire complex plane.

$$\text{polylog}(2, z) = -\frac{\pi}{6} - \frac{\log^2(-z)}{2} - \text{polylog}(2, \frac{1}{z}).$$

For more information about the dilogarithm function, refer to [22] and [33].

By combining (6.78) , (6.79) , (6.80) , (6.81), (6.82), and (6.83) , we now have the following analytic evaluation.

$$\begin{aligned}
&\int_0^1 \frac{\log(\ \alpha s^2 + \beta s + \gamma\ )}{\alpha s^2 + \beta s + \gamma} ds \\
&= \log(\alpha) \left[(6.81)\right]_{s=0}^1 + \frac{1}{\alpha} \left[(6.81)\right]_{s=0}^1 + \frac{1}{\alpha} \left[(6.81)\right]_{s=0}^1 .
\end{aligned} \tag{6.84}$$

Therefore, by (6.68) , (6.73) , and (6.84) , we can get

$$\begin{aligned}
&\int\int_{\Sigma_d} \frac{1}{u^2+v^2+z^2} d\sigma(u,v) \\
&= \frac{1}{2}\int_{\theta_1}^{\theta_2} \log(r(\theta)^2 + z^2) d\theta - \log(z)(\theta_2 - \theta_1) \\
&= \frac{(x_1y_2 - x_2y_1)}{2} \int_0^1 \frac{\log(\ \alpha s^2 + \beta s + \gamma\ )}{\alpha s^2 + \beta s + \gamma} ds - \log(z)(\theta_2 - \theta_1) \\
&= \frac{(x_1y_2 - x_2y_1)\log(\alpha)}{2} \left[(6.81)\right]_{s=0}^1 + \frac{(x_1y_2 - x_2y_1)}{2\alpha} \left[(6.81)\right]_{s=0}^1 \\
&+ \frac{(x_1y_2 - x_2y_1)}{2\alpha} \left[(6.81)\right]_{s=0}^1 - \log(z)(\theta_2 - \theta_1).
\end{aligned} \tag{6.85}$$

We can analytically evaluate the following integrations

$$\int\int_{\Sigma_h} \frac{1}{u^2+v^2+z^2} d\sigma(u,v),$$
$$\int\int_{\Sigma_v} \frac{1}{u^2+v^2+z^2} d\sigma(u,v),$$

in a similar fashion. In fact, the same algorithm (6.85) can be used to evaluate the above integrations analytically.

CHAPTER 7
NUMERICAL EXPERIMENTS

7.1 Numerical Tests for Sample Models

For our numerical experiments, we have chosen three different surface models. Using these models and properly chosen test solutions, we have tested timing, accuracy, and the effect of different subdivision schemes. We first introduce the models.

- Model 1. This first model is made of two planes, denoted by S_1 and S_2 as illustrated in Figure 7.1. The surfaces S_1 and S_2 joins with each other along a common edge at an angle $\theta = 26.5651°$. The dimensions of S_1 and S_2 are given by

$$S_1 = \{(x, y, 0) \mid 0 \le x \le 200,\ 0 \le y \le 100\},$$
$$S_1 = \left\{\left(x, y, \frac{y}{2}\right) \mid 0 \le x, y \le 200\right\}.$$

- Model 2. This model is made of two perpendicular surfaces, denoted by S_1 and S_2 as illustrated in Figure 7.2. This is like model 1, but with $\theta = 90°$. The dimensions of S_1 and S_2 are given by

$$S_1 = \{(x, y, 0) \mid 0 \le x \le 200,\ 0 \le y \le 100\},$$
$$S_2 = \{(x, 0, z) \mid 0 \le x, z \le 200\}.$$

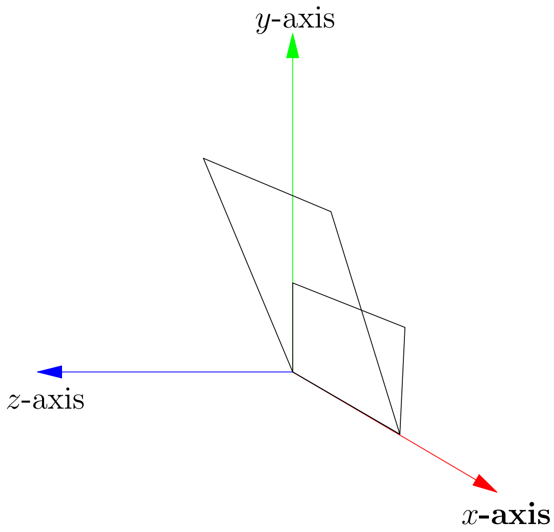

Figure 7.1: Two planes joining with angle $\theta = 26.5651°$.

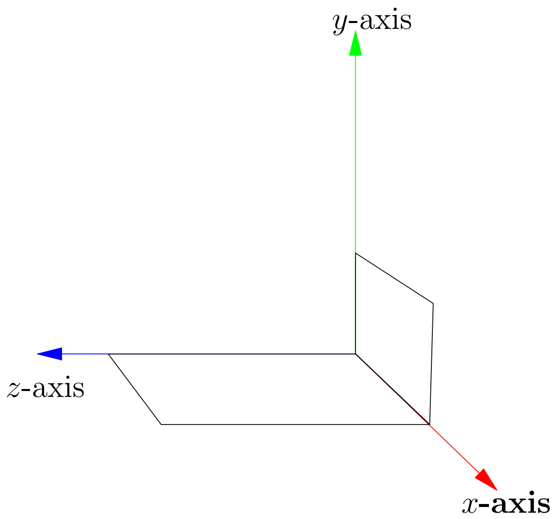

Figure 7.2: Two planes joining with angle $\theta = 90°$.

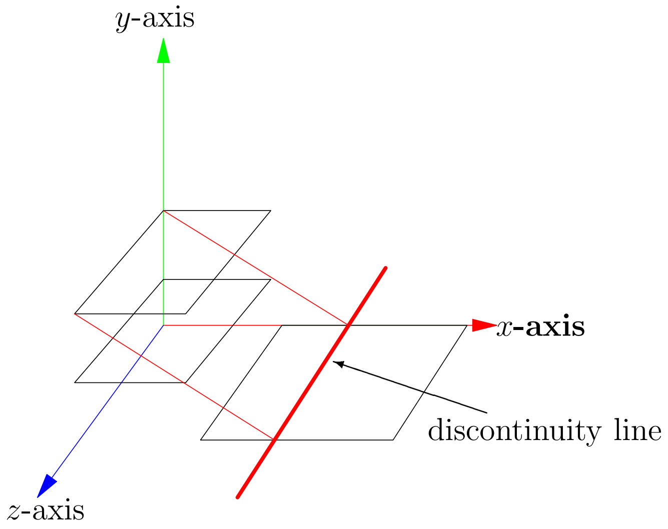

Figure 7.3: Four planes with discontinuity line.

- Model 3. This model is made of four surfaces, denoted by S_1, S_2, S_3, and S_4 as illustrated in Figure 7.3. The dimensions of S_1, S_2, S_3, and S_4 are given by

$$S_1 = \{(x, 240, z) \mid 0 \leq x \leq 120,\ 0 \leq z \leq 280\},$$

$$S_2 = \{(x, 120, z) \mid 0 \leq x \leq 120,\ 0 \leq z \leq 280\},$$

$$S_3 = \{(x, 120, z) \mid 0 \leq x \leq 120,\ 0 \leq z \leq 280\},$$

$$S_4 = \{(x, 0, z) \mid 120 \leq x \leq 400,\ 0 \leq z \leq 280\}.$$

The dimensions of the models are chosen to be compatible with computer graphics applications. That is why we use relatively high values like 120, 200, and the angle $\theta = 26.5651$. These numbers are easy to render in computer graphics.

In the future, we will consider more complicated models to study other aspects of solving the radiosity equation. Even if the surfaces S_2 and S_3 have the same dimension, we assume that the normal vector of S_2 is $(0, 0, 1)$, directed upward, and the normal vector of S_3 is $(0,0,-1)$, directed downward. In Figure 7.1, 7.2, and 7.3 illustrating these various models, the red axis represents x-axis, the green axis represents y-axis and the blue axis represents z-axis.

We applied both the *analytic integration method* developed in the previous chapter and a numerical integration scheme to evaluate

$$\int_{\Delta} \frac{\cos(\theta_p)\cos(\theta_q)}{\|p-q\|^2} dq, \tag{7.1}$$

with Δ an element of some kind. This integration is needed to setup the matrix of the centroid collocation method. The numerical method which we used for comparison to the analytic evaluation method is based on converting the integral to a new integral of the form

$$\int_{\sigma} g(s,t) d\sigma,$$

over the unit simplex $\sigma = \{(s,t) : 0 \leq s, t, s+t \leq 1\}$.

Among a number of well-known numerical approximations to such integrals, we use the following integration scheme.

$$\int_{\sigma} g(s,t) d\sigma \approx \sum_{j=1}^{7} w_j g(\rho_j).$$

In here, the weights w_j and nodes ρ_j taken from the formula T2:5-1 of Stroud [39]. This composite numerical integration scheme has degree of precision 5. In order to improve the accuracy of this method, we use the 7-point method over 4^n smaller triangles which we obtain by applying n levels of subdivisions to Δ. We refer to this scheme as the *7-point method with level n*.

n	Analytic	7-point			
	T_a	T_3	E_n	T_5	E_n
4	0.02	0	$4.9683E-6$	0.05	$9.4203E-10$
16	0.191	0.02	$3.8486E-6$	0.53	$4.7163E-10$
64	5.927	0.37	$1.9255E-6$	7.633	$2.3612E-10$

Table 7.1: Matrix setup error and timing comparison for model 1

n	Analytic	7-point			
	T_a	T_3	E_n	T_5	E_n
4	0.0	0.02	$4.4138E-4$	0.04	$6.8343E-8$
16	0.21	0.03	$1.1786E-4$	0.541	$3.5253E-8$
64	7.289	0.39	$5.8931E-5$	7.754	$1.7629E-8$

Table 7.2: Matrix setup error and timing comparison for model 2

We present matrix setup timing and error comparisons for models 1 and 2 in Tables 7.1 and 7.2, respectively. The number n is the size of elements which we use for the test and T_a, T_3, and T_5 are the time taken by the analytic integration method, the 7-point method with level 3 and the 7-point method with level 5, respectively, to evaluate the integration (7.1). The error E_n is the averaged sum of all the differences of the analytic evaluation and numerical evaluation of the integration (7.1) at the node points. By studying Tables 7.1 and 7.2, we observe that the analytic method is faster than the 7-point method with level 5, but is more expensive than the 7-point method with level 3. Even if 7-point method with level 3 is the better than the analytic method in terms of speed, it shows a significant error from the analytic evaluation method. The error becomes worse as the angle θ between the two surfaces becomes smaller.

In these tests, it should be noted that the analytic method is implemented in C++ using STL template classes, whereas the 7-point method is implemented in Fortran. It is a generally well-known fact that the C++ implementation with STL templates is slower than a Fortran implementation. Considering this, the analytic method shows relatively good performance over the 7-point method. The timings were done on Dell Inspiron 8100 Desktop with a 1.0GHz Pentium CPU and 256 MB RAM running Windows XP operating system. The Fortran programs which we used are part of BIEPACK [4].

Next, we use models 2 and 3 with properly chosen true solutions u to test the accuracy of the approximate solution u_n obtained using the analytic method to solve the radiosity equation. In order to setup the linear system needed in the centroid collocation method, we calculate the emissivity E using highly accurate numerical integration. The collocation procedure is applied to find the approximate solution u_n, which is then compared to the known true solution. The true solution which we will use for model 2 is given by

$$u(x,y,z) = \begin{cases} 0 & \text{otherwise} \\ z^\beta & y = 0 \end{cases} . \tag{7.2}$$

That is, $u(x,y,z) = 0$ on S_2 and $u(x,y,z) = z^\beta$ on S_1. This test solution is chosen since it is proven in [30] that the solution u has: the behavior

$$u(x,0,z) = O(z^\beta),\ \ z \to 0 \tag{7.3}$$

with $0 < \beta < 1$ at the common edge. If the solution u satisfies (7.3) , we can prove that

$$\|u - P_n u\|_\infty = O(h^\beta).$$

We use the solution (7.2) for model 2 with $\beta = 0.5$ and 0.9 to test the effect of an algebraic singularity along the common edge.

The test results for $\beta = 0.5$ are given in Table 7.3 and 7.4 for uniform meshing and simple adaptive meshing, respectively. In the case of uniform meshing, the expected rate of convergence is $O(h^{0.5})$ as explained in the above. Table 7.3 shows that the rate of convergence is getting close to $O(h^{0.5})$ as the number of elements n

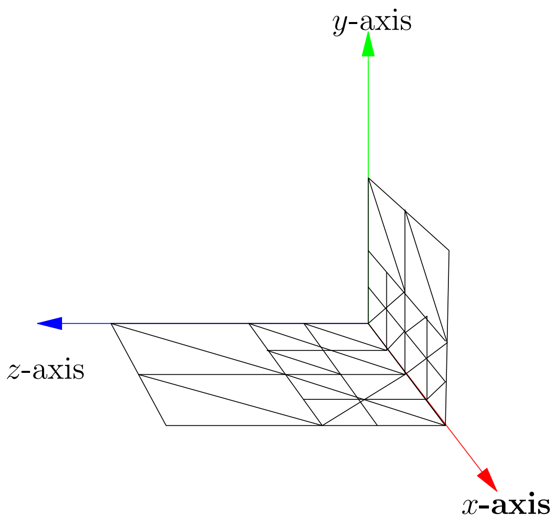

Figure 7.4: Two perpendicular planes with simple adaptive meshing.

	metric= $\|\cdot\|_1/n$		metric=$\|\cdot\|_\infty$	
n	E_n	*Ratio*	E_n	*Ratio*
4	0.5178890		1.1241126	
16	0.2097839	2.4687	1.0240879	1.0976
64	0.0845805	2.4802	0.7981865	1.2830
256	0.0332735	2.5419	0.5772808	1.3827

Table 7.3: Centroid collocation errors of u with $\beta = 0.5$ and uniform meshing on model 2.

	metric= $\|\cdot\|_1/n$		metric=$\|\cdot\|_\infty$	
n	E_n	*Ratio*	E_n	*Ratio*
4	0.5178890		1.1241126	
16	0.2097839	2.4687	1.0240879	1.0976
40	0.1479077	1.4183	0.8156686	1.2555
88	0.1235954	1.1967	0.6081240	1.3412
184	0.1099482	1.1241	0.4517210	1.3462

Table 7.4: Centroid collocation errors of u with $\beta = 0.5$ and adaptive meshing on model 2.

increases. The simple adaptive meshing was obtained by subdividing only the rectangular elements which share a common edge along the x-axis as illustrated in Figure 7.4. The triangular elements are obtained by splitting the rectangular elements into two triangles at the final stage. We observe that the rate of convergence is close to $O(n^{-1/2})$ even though we used our simple adaptive meshing scheme. We expect that more sophisticated meshing scheme can be employed to improve this rate of convergence. The subject of finding an optimal adaptive meshing scheme can be a subject of future study. Also note that the relative error is very small even though the errors given in the tables may look large.

The test results for $\beta = 0.9$ are given in Table 7.5 and 7.6 for uniform meshing and simple adaptive meshing, respectively. In the case of uniform meshing, the expected rate of convergence is $O(h^{0.9})$. The test results in Table 7.5 show that the

n	metric= $\|\cdot\|_1/n$		metric=$\|\cdot\|_\infty$	
	E_n	*Ratio*	E_n	*Ratio*
4	4.1403802		8.5621539	
16	1.3010115	3.1824	6.5596009	1.3052
64	0.4049425	3.2128	3.9413914	1.6642
256	0.1237672	3.2718	2.1854562	1.8038

Table 7.5: Centroid collocation errors of u with $\beta = 0.9$ and uniform meshing on model 2.

n	metric= $\|\cdot\|_1/n$		metric=$\|\cdot\|_\infty$	
	E_n	*Ratio*	E_n	*Ratio*
4	4.1403802		8.5621539	
16	1.3010115	3.1824	6.5596009	1.3052
40	0.8051290	1.6159	4.1577551	1.5776
88	0.6726532	1.1969	2.5196563	1.6501
184	0.6122515	1.0986	1.5860599	1.5886

Table 7.6: Centroid collocation errors of u with $\beta = 0.9$ and adaptive meshing on model 2.

rate of convergence is getting close to this theoretical expectation for $\beta = 0.9$ as we increase the number of elements n. The rate of convergence for the simple adaptive meshing is higher than $O(n^{-1/2})$. In cases for both $\beta = 0.5$ and $\beta = 0.9$, our numerical experiments show that adaptive meshing is superior to uniform meshing.

The true solution which we use for model 3 is given by

$$u(x, y, z) = \begin{cases} 0 & \text{otherwise} \\ e^{-\gamma(x-d)}(x-d)^{\beta} & x > d \text{ and } y = 0 \end{cases}, \tag{7.4}$$

where $d = 240$. The line $x = d$ on the xz-plane is the discontinuity line as defined in Chapter 2. To see the effect of a discontinuity in a derivative of u along this line, we solve the radiosity equation for u given by (7.4) with $\beta = 0.5$ and $\gamma = 0.02$.

We present the numerical testing result for both uniform meshing and discontinuity meshing. In general, meshing scheme should be applied to all the planes involved in the testing, but we subdivided only the bottom plane S_4. See Figure 7.5. This was done in order to increase the number of elements in the area of interest since our testing computer has a limited size of the core memory.

Tables 7.7 and 7.8 shows the testing results for uniform meshing and discontinuity meshing, respectively. Table 7.7 reveals that the rate of convergence with uniform meshing is higher than the theoretical expectation of $O(h^{1.5})$ as given in [5]. We expect the higher rate of convergence will settle down eventually as the number of elements increases. We can also observe that discontinuity meshing is not as good as the uniform meshing as far as the rate of convergence is concerned, even though the actual error of the discontinuity meshing is much smaller than that of the uniform

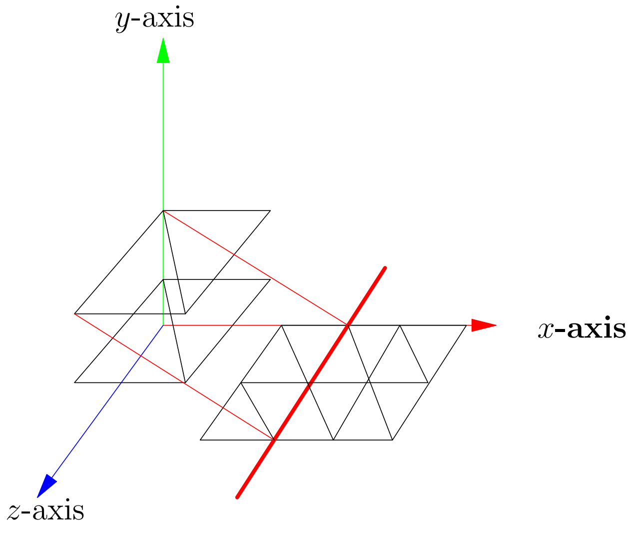

Figure 7.5: Four planes with discontinuity meshing on the bottom plane S_4.

meshing. This is consistent with what was proven for function $u \in D^r$.

7.2 Implementation

For approximately the past two decades, computer science has worked to replace Fortran with languages embodying better programming practices and better adapted to the needs of modern computing. Nonetheless, Fortran continues as the most popular language among researchers in numerical computing. In this thesis, we have moved from a Fortran-based approach in solving the radiosity equation to one based on C++ so that we can use more modern programming constructs.

One of the main benefits of Fortran is its simplicity. It is easy to use and easy to learn. Even if Fortran is getting more sophisticated as it gets updated to Fortran 90/2K, it is relatively easy to learn and use compared to other programming languages. Another benefit of Fortran is its efficiency. In general, it is common

n	$metric = \|\cdot\|_1 /n$		$metric = \|\cdot\|_\infty$	
	E_n	$Ratio$	E_n	$Ratio$
8	0.0175512		0.0733565	
14	0.0306716	0.57223	0.0882359	0.83136
38	0.0135118	2.26999	0.0649476	1.35857
134	0.0005834	23.2604	0.0044955	14.4472
518	0.0001868	3.12313	0.0012698	3.54032

Table 7.7: Centroid collocation errors of u with $\beta =$ 0.5 and uniform meshing on model 3.

n	$metric = \|\cdot\|_1 /n$		$metric = \|\cdot\|_\infty$	
	E_n	$Ratio$	E_n	$Ratio$
10	0.0024520		0.0080658	
22	0.0052996	0.46267	0.0193887	0.41600
70	0.0021476	2.46768	0.0119561	1.62166
262	0.0007409	2.89864	0.0050545	2.3654

Table 7.8: Centroid collocation errors of u with $\beta =$ 0.5 and discontinuity meshing on model 3.

knowledge that a Fortran implementation is faster than a C/C++ implementation even when they implement the same algorithms. Most importantly, Fortran has lots of excellent legacy code including the BLAS, LINPACK, LAPACK and BIEPACK which have been developed during last few decades.

Still, Fortran lacks the flexibility of C/C++. Especially, it is hard to do graphics programming in Fortran. The software package which I wrote was designed to best utilize both the simplicity and efficiency of Fortran and the flexibility of C/C++. It was designed so that it can be used as a testing package for future research of radiosity equation in numerical analysis. In addition to providing a visual user interface, it was designed according to the following.

- Be flexible with element types. It can take any type of element. The element can be either triangular or rectangular. They can be even mixed together allowing more flexibility for the programmer.

- Be flexible with the number of node points. The number of node points for each element is not fixed. For instance, element A can have three node points while element B has one node point.

- Have modularity. Numerical solution and geometric manipulation modules are decoupled so that programmers can focus on their own area of specialty.

- Have customizable subdivision schemes. The user can provide his/her own subdivision scheme.

In our implementation of the package, we have used a quad tree data structure because of its ease of use and well-known node traversal algorithms. But, there are other data structures which have been developed in the global illumination community for optimal visibility calculations. It is also possible to replace the quad tree structure of our package with such data structures without much difficulty, since element type is independent from the data structure which holds the elements.

One of the most popular ways of creating a triangulation is the Delaunay triangulation. But we use the triangulation based on the quad tree because most of the geometric shapes used in the global illumination are rectangular shaped. In order to triangulate all the surfaces, we first subdivide rectangular surface elements into quadrilateral elements honoring the preprocessed discontinuity information and then split each element into two triangular elements. In the process, we ensure the final triangular elements have proper aspect ratios.

7.3 Conclusions and Future Works

In this work we investigated several issues related to solving the radiosity equation using collocation methods. We defined the function space $D^{r+1}(S)$ and used it as a mathematical framework to understand visual events. We analyzed four basic models of visual events under this mathematical framework. These models are most frequently encountered in real applications. Still, there are cases of visual events which can't be covered by the four basic models. We believe our mathematical framework can be used to collect and classify all the cases of visual events which can happen in sophisticated real applications.

We also proved that the functions $u \in D^{r+1}(S)$ have the same rate of convergence as the functions $u \in C^{r+1}(S)$ as shown in the following inequality

$$\max_{(x,y)\in\Delta_{n,k}} |u(x,y) - P_n u(x,y)| \leq ch^{r+1} \max_{\substack{i,j\geq 0 \\ i+j=r+1}} \max_{(x,y)\in\Delta_{n,k}} \left|D^i D^j u(x,y)\right|,$$

for $u \in D^{r+1}(S)$. This result is a generalization of the standard results, but may not have a practical importance if the constant c is very large for the functions $u \in D^{r+1}(S)$ compared to the constant c for the functions $u \in C^{r+1}(S)$. Since we cannot readily determine these constants, it is not possible to prove or disprove the practicality of this result. However, we observed an adequate rate of convergence in one of our numerical experiments with $u \in D^{r+1}(S)$. Since the models which we used for our testing were quite small, this indicates that the convergence result actually has a practical importance.

We use numerical integration schemes when it is impossible to find the exact integrals or the analytic evaluation is so sophisticated that we could not gain much benefit out of the analytic evaluation. From our work, we have learned that the analytic evaluation of the integrals needed to solve the radiosity equation using collocation methods is worth the effort. It is faster and more accurate than well-known numerical schemes. We believe there is still some more work to be done to optimize the affine transforms used to transform triangles in R^3 to the standard triangles in R^2. This will improve the speed of our analytic integration scheme.

We have found the analytic evaluation of the integrals $H_{m,n,4}$ for m and n with $m + n \leq 2$, but we were not able to find the analytic evaluation of the integrals

$H_{m,n,4}(x, y, z)$ for all m, $n = 0, 1, 2, ...$ It is because of the difficulty in finding the analytic evaluation of $H_{m-2,n,2}(x, y, z)$ which are needed to evaluate $H_{m,n}(x, y, z)$ using the following equation.

$$\begin{aligned}
&H_{m,n}(x, y, z) \\
&= \frac{1}{2}\ (m-1)H_{m-2,n,2}(x, y, z) +\ xH_{m-1,n}(x, y, z) \\
&- \frac{1}{2}\int_{\partial\Delta} \frac{\xi^{m-1}\eta^n}{(x-\xi)^2 + (y-\eta)^2 + z^2}\nu_\xi dl.
\end{aligned}$$

As an example, we have not been able to evaluate $H_{0,2,2}(x, y, z)$ or $H_{2,0,2}(x, y, z)$ analytically. Since finding a proper change of variables to evaluate integrals analytically is somewhat an art, we leave the work to find a general scheme to evaluate $H_{m-2,n,2}(x, y, z)$ analytically for future work.

Finally, the software package was designed to embody better programming practices and better adapt to the needs of modern computing. It was implemented in C++. Using this package gave us a significant advantage during the time of numerical experiments. Quantifying the advantage of this software package under the principles of software engineering can be another subject of future work.

REFERENCES

[1] E. Angel. *Interactive Computer Graphics*, Prentice Hall, 2001.

[2] Kendall E. Atkinson, I. Graham, and I. Sloan. *Piecewise continuous collocation in integral equations*, SIAM Journal of Numerical Analysis, **20** (1983), pp.172-186.

[3] Kendall E. Atkinson. *The Numerical Solution of Integral Equations of the Second Kind*, Cambridge University Press, 1997.

[4] Kendall E. Atkinson. *User's Guide to a Boundary Element Package for Solving Integral Equations on Piecewise Smooth Surfaces (Release #2)*, Reports on Computational Mathematics #102, Dept of Mathematics, University of Iowa, 1998.

[5] Kendall E. Atkinson, David Chien, and Jaehoon Seol. *Numerical analysis of the radiosity equation using the collocation method*, Electronic Transactions on Numerical Analysis, **11** (2000), pp. 94-120.

[6] Kendall E. Atkinson and Weimin Han. *Theoretical Numerical Analysis: A Functional Analysis Framework*, Springer-Verlag, New York, 2001.

[7] Mark de Berg, M. Van Kreveld, M. Overmars, and O. Schwarzkopf. *Computational Geometry: Algorithms and Applications*, Springer-Verlag, New York, 2000.

[8] Per H. Christensen, Eric J. Stollnitz, Tony D. DeRose, and David H. Salesin. *Wavelet Radiance*, Proceedings of the Fifth Eurographics on Rendering, pp. 287-302.

[9] M. F. Cohen and J. R.Wallace. *Radiosity and Realistic Image Synthesis*, Academic Press Professional,1993.

[10] M. F. Cohen, and D. P. Greenberg. *The hemi-cube: A radiosity solution for complex environments*, Computer Graphics **19** (1985), pp. 31-40.

[11] Fredo Durand, George Drettakis and Claude Puech. *3D visibility made visibly simple: an introduction to the visibility skeleton*, Proceedings of the 24th Annual Conference on Computer Graphics & Interactive Techniques, 1997, pp. 89 - 100.

[12] J. D. Foley, A. Van Dam, S. K. Feiner, and J. F. Hughes. *Computer Graphics : Principles and Practice in C*, Addison Wesley Longman, Inc, 1995.

[13] A. Glassner. *An Introduction to Ray Tracing*, Academic Press, 1989.

[14] Z. Gigus and J. Malik. *Computing the aspect graph for line drawings of polyhedral objects*, IEEE Trans. Pattern Analysis and Machine Intelligence, **1** (1990), pp. 113-122.

[15] Z. Gigus, J. Canny, and R. Seidel. *Efficently computing and representing aspect graphs of polyhedral objects*, IEEE Trans. Pattern Analysis and Machine Intelligence, **13** (1991), pp. 542-551.

[16] C. M. Goral, K. E. Torrance, D. P. Greenberg, and B. Battaile. *Modelling the interaction of light between diffuse surfaces*, Computer Graphics(SIGGRAPH '84 Proceedings), **18** (1984) pp. 212-222.

[17] R. Hall. *Illumination and Color in Computer Generated Imagery*, Springer-Verlag, New York, 1989.

[18] P. Hanrahan and D. Saltzman. *A Rapid Hierarchical Radiosity Algorithm for Unoccluded Environments*, Photorealism in Computer Graphics, Springer-Verlag, New York, Eurographics Seminar series, 1992.

[19] O. Hansen. *The Radiosity Equation on Certain Spaces of Continuous Functions and its Numerical Solution*, Preprint 2, Habilitationschrift, Fachbereichs Mathematik, der Johannes Gutenberg-Universitt Mainz, 2001.

[20] F. Johnson. *A general panel method for the analysis and design of arbitrary configurations in incompressible flow*, NASA Tech. Rep. NASA-CR-3079, National Tech. Inform. Service, Springfield, VA.

[21] D. Lischinski, F. Rampieri, and D. P. Greenberg. *Discontinuity meshing for accurate radiosity*, IEEE Computer Graphics and Applications, **12** (1992), pp. 25-39.

[22] Yudell Luke. *The special functions and their approximations*, New York, Academic Press, 1969.

[23] B. T. Phong. *Illumination for computer generated pictures.* Communications of the ACM, **18** (1975), pp. 311-317.

[24] Michael F. Modest. *Radioative Heat Transfer*, McGraw-Hill, Inc, 1993.

[25] Ketan Mulmuley. *Computational Geometry: An introduction through randomized algorithms*, Prentice Hall, 1998.

[26] Y. Nievergelt and Y. Nievergelt. *Wavelets Made Easy*, Birkhauser Boston, 1999.

[27] T. Nishita and E. Nakamae. *Continuous tone representation of three dimensional objects taking account of shadows and interreflection*, Computer Graphics, **19** (1985), pp. 23-30.

[28] F. P. Preparata and M. I. Shamos. *Computational Geometry-An Introduction*, Sprinter Verlag, New York, 1985.

[29] J. O'Rourke. *Computational Geometry in C*, Cambridge University Press, 1994.

[30] A. Rathsfeld. *Edge asymptotics for the radiosity equation over polyhedral boundaries*, Math. Methods Appl. Sci. **22** (1999), pp 217-241

[31] D. F. Rogers. *Procedural Elements for Computer Graphics*, McGraw-Hill, New York, 1985.

[32] H. Samet. *The Analysis and Design of Spatial Data Structures*, Addison-Wesley series in computer science, 1990.

[33] P. Schröder and P. Harahan. *On the form factor between two polygons*, Computer Graphics(SIGGRAPH '93 Proceedings), **27** (1993), pp163-164.

[34] P. Schröder, S. Gortler, M. Cohen, and P. Hanrahan. *Wavelet projections for radiosity*, In Proceedings of Fourth Eurographics Workshop on Rendering, Eurographics (1993), pp. 105-114.

[35] C.Schwab and W. Wendland. *On numerical cubatures of singular surface integrals in boundary element methods*, Numerische Mathematik, **62** (1992), pp. 343-369.

[36] M. Sonka, R. Boyle, V. Hlavac, R. Boyle, and V. Hlavac. *Image Processing, Analysis, and Machine Vision*, Brooks Cole Publishing Company, 1999.

[37] J. Stoer and R. Bulirsch. *Introduction to Numerical Analysis*, Springer-Verlag, New York, 2001.

[38] G. Strang and T. Nguyen. *Wavelets and Filter Banks*, Wellesley-Cambridge Press, 2000

[39] A. Stroud. *Approximate Calculation of Multiple Integrals*, Prentice-Hall, New Jersey, 1964.

[40] S. J. Teller. *Computing the antipenumbra of an area light source*, Computer Graphics, **26** (1992).

[41] S. Upstill. *The RenderMan^{TM} Companion*, Addison-Wesley, Reading MA, 1989.

[42] Alan Watt and Mark Watt. *Advanced Animation and Rendering Techniques*, ACM Press, 1992.

[43] P. Wojtaszczyk. *A Mathematical Introduction to Wavelets*, Cambridge University Press, 1997.

[44] Harold R. Zatz. *Galerkin radiosity*, Proceedings of the 20th Annual Conference on Computer Graphics, (1993), pp. 213 - 220.